A THEORY FOR THE PROPELLER-RUDDER INTERACTION

S. Tsakonas, et al

Stevens Institute of Technology
Hoboken, New Jersey

August 1968

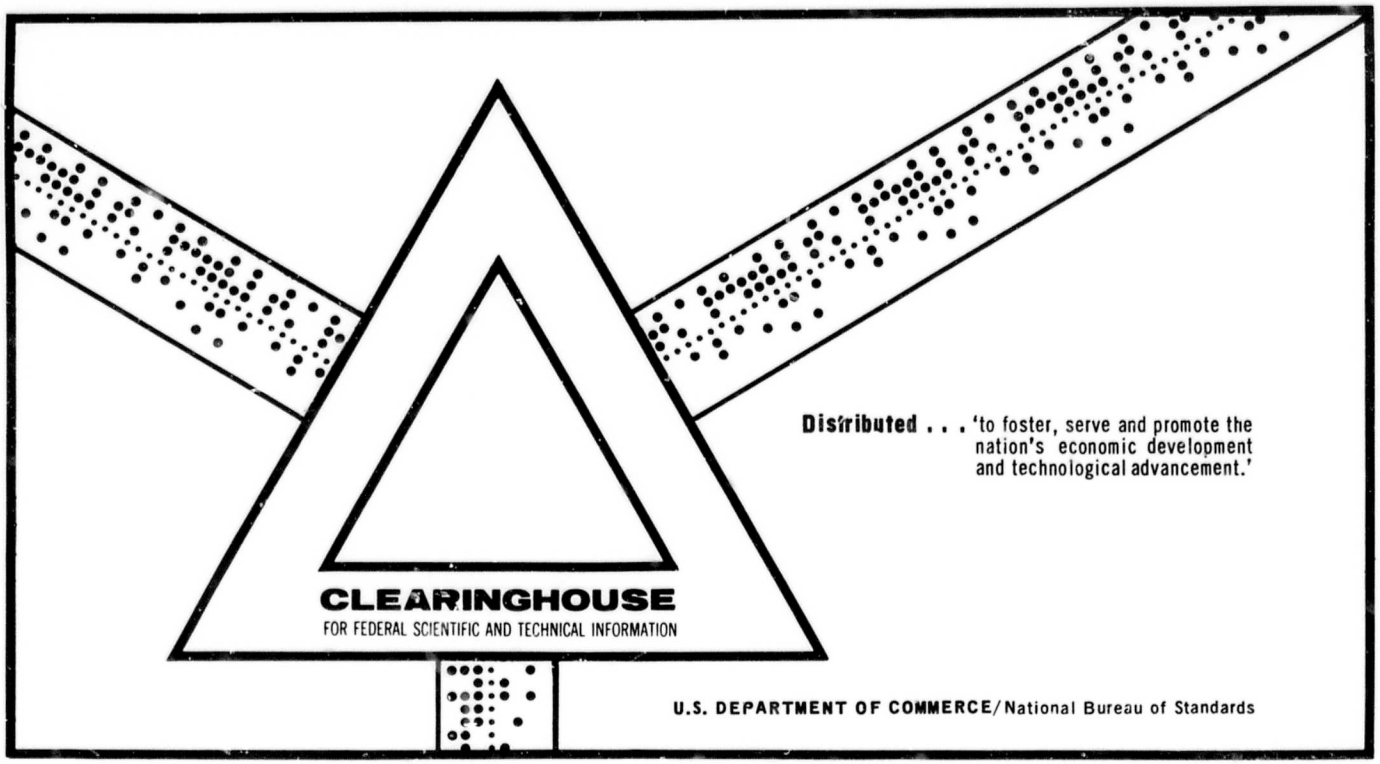

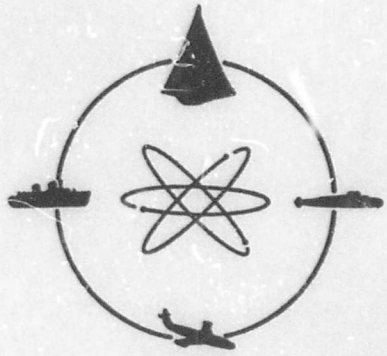

DAVIDSON LABORATORY

REPORT SIT-DL-68-1284

AUGUST 1968

A THEORY FOR THE PROPELLER-RUDDER INTERACTION

by

S. Tsakonas
W.R. Jacobs
M.R. Ali

This Research was Sponsored by the Department of Hydromechanics of the Naval Ship Research and Development Center under Contracts N600(167)61303X[illegible]6 and N00600-67-C-0725

STEVENS INSTITUTE OF TECHNOLOGY
CASTLE POINT STATION
HOBOKEN, NEW JERSEY

Report SIT-DL-68-1284

August 1968

A THEORY FOR THE PROPELLER-RUDDER INTERACTION

by

S. Tsakonas

W.R. Jacobs

M.R. Ali

This Research was Sponsored by the Department of Hydromechanics of the Naval Ship Research and Development Center under Contracts N600(167)61303XT06 and N00600-67-C-0725.

viii + 54 pages
6 tables
17 figures
7 appendices (19 pgs)

Approved

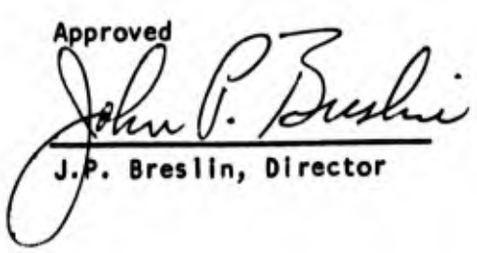

J.P. Breslin, Director

ABSTRACT

The propeller-rudder interaction problem is studied by means of the unsteady lifting-surface theory. Both surfaces of arbitrary geometry are immersed in a nonuniform flowfield (i.e., hull wake) of an ideal incompressible fluid. The boundary-value problem yields a pair of surface integral equations, the inversion of which is achieved by the so-called "generalized lift operator" technique, a new approach developed by the authors, in conjunction with the presently used "mode-collocation" method. The analysis demonstrates the mechanism of the interaction phenomenon by exhibiting the filtering effects of the propeller on the harmonic constituents of the wake which allow the rudder to be exposed only to the blade harmonic and multiples thereof. A numerical procedure adaptable to the CDC 6600 computer has been developed which furnishes information about 1) the steady and time-dependent pressure distribution on both lifting surfaces, and 2) the resultant hydrodynamic forces and moments. A limited number of calculations exhibits the importance of some parameters such as axial clearance, number of blades, and harmonic components of the hull wake.

KEY WORDS

Hydrodynamics
Unsteady Theory for Propeller-Rudder Interaction

TABLE OF CONTENTS

NOMENCLATURE

a	Ω/U
a_{ms} b_{ms}	coefficients defined in Equation (47)
B	defined in Equation (48)
C_R	semichord of rudder
$F( )$	function
$F_{x,y,z}$	propeller hydrodynamic forces
F_R	side force on rudder
$f( )$	function
$f^{(\bar{m},\bar{n})}( )$	function defined in Equation (42)
$I^{(\bar{m})}(x)$	defined in Equation (40)
$I_1^{(\bar{m})}(x)$	defined in Equation (43)
$I_m( )$	modified Bessel function of order m
l	index
$J_m( )$	Bessel function of order m
J	index
$K_m( )$	modified Bessel function of order m
K_{jl}	kernel of integral equation
$\bar{K}_{jl}$	kernel after θ_α- and φ_α- integrations
$K_{1,2}$	see Equations 30-32
k	variable of integration
k	positive numerical index
L'	loading, lb/ft^2

$L(r)$	spanwise loading distribution
$L^{(\bar{n})}(\rho)$	spanwise loading components (coefficients of Birnbaum distribution)
ℓ	integer multiple
M_R	moment about rudder stock
$\bar{m}$	order of lift operator
m_k	index of summation
N	number of blades
$\bar{n}$	order of chordwise mode
n	blade index
$\vec{n}$	normal to surface at loading point
$\vec{n}'$	normal to surface at control point
P	subscript index of propeller
p	perturbation pressure
p	index of summation
$Q_{x,y,z}$	propeller hydrodynamic moments
$Q_{m-1/2}(Z)$	Legendre spherical function of half odd-integer order
q	order of blade harmonic
R	subscript index of rudder
R,R'	Descartes distance
r	radial coordinate of control point
r	superscript index of control point
r_o	propeller radius
S	lifting surface
t	time, sec
U	uniform velocity

$V^{(q)}(r)$	Fourier coefficients of downwash velocity normal to propeller blade
W_P	downwash velocity distribution normal to propeller at control point
W_R	downwash velocity distribution normal to rudder at control point
X	see Equation (27)
x	longitudinal ordinate
x,r,φ	cylindrical coordinate system of control points on propeller or rudder
x,y,z	Cartesian coordinates of control points on rudder
x_o	distance between propeller plane and rudder stock (see Fig 1)
y	horizontal ordinate
Z	argument of Legendre function
z	vertical ordinate
z_o	$\lvert z - \zeta \rvert$
β	small radial length
δ	small length
$\delta(\ )$	Dirac delta function
ϵ_R	distance between rudder stock and rudder midchord (see Fig 1)
ζ	vertical ordinate on rudder
η	horizontal ordinate on rudder
Θ	see Equation (27)
$\Theta(\bar{n})$	chordwise modes
θ	angular coordinate of loading point
θ_o	angular position of propeller loading point with respect to midchord line

θ_α	angular chordwise location of loading point
θ_b	projected propeller semichord length, radians
$\bar{\theta}_n$	$\frac{2\pi}{N}$ (n-1), n=1,...N
$\bar{\theta}_o$	$\frac{2\pi}{N}$
$\theta_p(r)$	geometric pitch angle
$\Lambda^{(\bar{n})}(x)$	defined in Equation (40)
$\Lambda_1^{(\bar{n})}(x)$	defined in Equation (43)
λ_k	positive integer multiple
ξ	longitudinal ordinate of loading point
ξ,ρ,θ	cylindrical coordinate system of loading points on propeller or rudder
ξ,η,ζ	Cartesian coordinates of loading points on rudder
ρ	radial coordinate of loading point
ρ	superscript index of loading point
ρ_f	mass density of fluid
σ	angular measure of skewness
τ,τ'	variables of integration
Φ	velocity potential
$\Phi(\bar{m})$	generalized lift operator
φ	angular coordinate of control point
φ_o	angular position of propeller control point with respect to midchord line
φ_α	angular chordwise location of control point
Ψ	acceleration potential
Ω	angular velocity of propeller
ω	angular frequency of loading

INTRODUCTION

This study is an extension in scope of the series of theoretical investigations at Davidson Laboratory which have been concerned with adaptation of the lifting-surface theory to the marine propeller. The ultimate purpose of this series is to obtain adequate estimates of the vibratory loading on propeller blades in realistic flow conditions, information which is needed for the study of hull vibration, hydroelastic instability and material failure, as well as underwater acoustics.

The present investigation treats the problem of the unsteady hydrodynamic interference between a marine propeller and a rudder, when both lifting surfaces are located in the wake of a hull. The problem of propeller-rudder interaction is of considerable interest to the naval architect since it is immediately connected with the maneuvering of a ship and with its propulsive efficiency. Since the rudder is a steering device inducing the ship to assume its designated course, accurate knowledge of the rudder action is essential for a quick and proper response of the hull.

The previously developed method[1-6] which was used to evaluate the loading on propeller blades of known geometry rotating in a known wake and the method used to determine the loading on a finite aspect ratio hydrofoil operating in a known flow field or undergoing prescribed motions[7], are extended to this problem of propeller-rudder interaction. The fundamental difference between predicting the unsteady hydrodynamic loading on an isolated lifting surface and the loadings on two interfering surfaces is that a pair of simultaneous surface integral equations must be treated as contrasted with a single equation. New kernel functions are developed for the cross-coupling terms which indicate the effect of the mutual interference of the lifting surfaces. The "Generalized Lift Operator" technique, which was used successfully in predicting unsteady hydrodynamic forces of propellers and the lift on a foil is employed in conjunction with the collocation method for the solution of the pair of integral equations.

There has been very little theoretical treatment of the propeller-rudder interaction problem when propeller and rudder are in the spatially non-uniform flow in the wake of a hull. Isay[8] developed the integral equation describing the interaction problem in a uniform flow field through a combination of lifting line approach for the propeller and steady-state Weissinger method for the rudder. However, he abandoned this approach in favor of a simplified approximate theory where propeller loading is replaced by an optimal circulation distribution.

Sugai[9] used lifting-surface theory to evaluate the effect on the rudder of a propeller operating in uniform flow (no wake). He assumed there was no reciprocal effect of rudder on propeller. As was done in Ref. 1, he transformed the surface integral equation into a line integral equation by means of the Weissinger approximation in which the surface lift distribution is replaced by a line distribution along the $\frac{1}{4}$-chord line, with the control points along the 3/4-chord line. The line integral equation is then solved for the loading by the Glauert lift operator technique.

The interest of these and other theoretical investigators as well as experimental studies has been in the design of rudders and propeller-rudder configurations for increased propulsive efficiency based on uniform flow conditions.[10] Other experimental studies have measured rudder forces and moments behind a hull for single screw ships[11], but most have treated multiple-screw ships with the rudder on the centerline out of the propeller slip stream. Unfortunately, none of these has recorded the inflow field which is essential information input to the program for the theoretical approach.

The present investigation is more comprehensive than the other theoretical studies, treating realistic flow conditions and accurate geometry of lifting surfaces. It will provide fuller information on the propeller-rudder interaction and should clarify the question whether the rudder's influence on the propeller can be neglected, in respect to all steady and unsteady propeller hydrodynamic forces.

This research was sponsored by the Department of Hydromechanics of the Naval Ship Research and Development Center under Contracts N600(167)61303XT06 and N00600-67-C-0725.

STATEMENT OF THE PROBLEM

A propeller and a rudder of arbitrary geometry and zero thickness are immersed in the wake of a hull. Thus both surfaces are operating in a non-uniform inflow field which is assumed to be that of an ideal incompressible fluid. The propeller-rudder arrangement and the coordinate system are shown in Figures 1 and 2.

The fact that the induced velocities from each individual lifting surface should be equal to the given velocity distribution at that surface constitutes the basic relation of the interaction phenomenon. Through the application of the linearized unsteady lifting surface theory, the kinematic boundary conditions which exist on both lifting surfaces (propeller and rudder) are expressed as two simultaneous surface integral equations.

$$W_P(x_P, r_P, \varphi_P; t) = \int_{S_P}\int L'_P(\xi_P, \rho_P, \theta_P; t)\, K_{PP}(x_P, r_P, \varphi_P; \xi_P, \rho_P, \theta_P; t)\, d\, S_P + \int_{S_R}\int L'_R(\xi_R, 0, \zeta_R; t)\, K_{RP}(x_P, r_P, \varphi_P; \xi_R, 0, \zeta_R; t)\, d\, S_R \qquad (1)$$

$$W_R(x_R, 0, z_R; t) = \int_{S_P}\int L'_P(\xi_P, \rho_P, \theta_P; t)\, K_{PR}(x_R, 0, z_R; \xi_P, \rho_P, \theta_P; t)\, d\, S_P + \int_{S_R}\int L'_R(\xi_R, 0, \zeta_R; t)\, K_{RR}(x_R, 0, z_R; \xi_R, 0, \zeta_R)\, d\, S_R \qquad (2)$$

where x, r, φ and ξ, ρ, θ: cylindrical coordinates of control and loading points, respectively, associated with the propeller

x, y, z and ξ, η, ζ: Cartesian coordinates of the corresponding points associated with the rudder

t: time, sec.

S_P, S_R: propeller and rudder surfaces, respectively, ft^2

W_P, W_R: downwash velocity distributions normal to propeller and rudder, respectively, ft/sec

L'_P, L'_R: unknown loading on propeller blade and rudder, respectively, lb/ft^2

K_{ji} induced velocity on element i due to oscillatory load of unit amplitude located at element j, ft/lb sec

It may be more convenient to use cylindrical coordinates (x,r,φ) and (ξ,ρ,θ) for the rudder also. These are related to the Cartesian coordinates (x,y,z) and (ξ,η,ζ) in the following manner:

$$\begin{cases} y_R = \lim\limits_{\varphi_R \to \frac{0}{\pi}} (r_R \sin\varphi_R) \\ z_R = \lim\limits_{\varphi_R \to \frac{0}{\pi}} (r_R \cos\varphi_R) \end{cases} \qquad \begin{cases} \eta_R = \lim\limits_{\theta_R \to \frac{0}{\pi}} (\rho_R \sin\theta_R) \\ \zeta_R = \lim\limits_{\theta_R \to \frac{0}{\pi}} (\rho_R \cos\theta_R) \end{cases} \tag{3}$$

The second term on the right-hand side of Eq. (1) and the first term on the right-hand side of Eq. (2) represent the interference effect of the rudder on the propeller and of the propeller on the rudder, respectively. The remaining terms of Eq. (1) and (2) represent the contribution to downwash from the individual lifting surface. The kernel functions K_{PP}, K_{PR} and K_{RR} have high-order singularities with Hadamard finite contributions, whereas the cross-coupling term K_{RP} is not singular.

The oscillatory loading and the prescribed downwash velocity can be expressed as

$$L'_j(\xi,\rho,\theta;t) = \sum_{\lambda_k=0}^{\infty} L_j^{(\lambda_k)}(\xi,\rho,\theta) e^{i\lambda_k \Omega t}$$

$$W_j(x,r,\varphi;t) = \sum_{q=0}^{\infty} W_j^{q)}(x,r,\varphi) e^{iq\Omega t} \tag{4}$$

where Ω is angular velocity of the propeller, and λ_k and q are positive integers. Since in the linearized theory the principle of superposition

applies, the various flow disturbances can be treated separately and their effects are simply added. The flow disturbances considered are those due to hull wake, and to incidence angle and camber of propeller blades and rudder. Blade thickness and rudder thickness are not taken into account in this study.

The acceleration potential method was used in the earlier Davidson Laboratory papers[1-6] to derive the kernel K_{pp}, for the case where both control and loading points are on the propeller. The other kernels will be derived by the same method and, as before, expressed in separable form as the product of a function of the spanwise coordinates and a function of the chordwise coordinates.

The usual mode approach[6,7] will then be employed to reduce the surface integrals to line integrals. The procedure is to assume a form for the unknown chordwise distribution of loading and to leave the unknown spanwise distribution to be determined by the solution of the integral equations. In this case, $\bar{n}$ terms of the Birnbaum chordwise modes are taken as the chordwise distribution, since that series manifests the proper leading-edge singularity and fulfills the Kutta condition along the trailing edge.[12]

After the application of the "Generalized Lift Operator"[6,7] of $\bar{m}$ modes to both sides of equations (1) and (2), these are reduced to a set of line integral equations. The number $\bar{m}$ of the integral equations must be equal to the number $\bar{n}$ of the unknown chordwise modes. Thus the original integral equations after the chordwise integrations (θ and φ integrations) may be represented for a given frequency q as

$$\sum_{\bar{m}=1}^{\bar{n}} \bar{W}_P^{(q,\bar{m})}(x_P, r_P, \varphi_P) e^{iq\Omega t} =$$

$$\int_{\rho_P} \sum_{\lambda_1=0}^{\infty} \sum_{\bar{m}=1}^{\bar{n}} \sum_{\bar{n}=1}^{\bar{n}} L_P^{(\lambda_1,\bar{n})}(\rho_P) e^{i\lambda_1\Omega t} \bar{K}_{PP}^{(\bar{m},\bar{n})} d\rho_P$$

$$+ \int_{\zeta_R} \sum_{\lambda_2=0}^{\infty} \sum_{\bar{m}=1}^{\bar{n}} \sum_{\bar{n}=1}^{\bar{n}} L_R^{(\lambda_2,\bar{n})}(\zeta_R) e^{i\lambda_2\Omega t} \bar{K}_{RP}^{(\bar{m},\bar{n})} d\zeta_R \qquad (5)$$

$$\sum_{\bar{m}=1}^{\bar{n}} \bar{W}_R^{(q,\bar{m})}(x_R, r_R, \varphi_R) e^{iq\Omega t} =$$

$$\int_{\rho_P} \sum_{\lambda_3=0}^{\infty} \sum_{\bar{m}=1}^{\bar{n}} \sum_{\bar{n}=1}^{\bar{n}} L_P^{(\lambda_3,\bar{n})}(\rho_P) e^{i\lambda_3\Omega t} \bar{K}_{PR}^{(\bar{m},\bar{n})} d\rho_P$$

$$+ \int_{\zeta_R} \sum_{\lambda_4=0}^{\infty} \sum_{\bar{m}=1}^{\bar{n}} \sum_{\bar{n}=1}^{\bar{n}} L_R^{(\lambda_4,\bar{n})}(\zeta_R) e^{i\lambda_4\Omega t} \bar{K}_{RR}^{(\bar{m},\bar{n})} d\zeta_R \qquad (6)$$

where the superscripts $\bar{m}$ and $\bar{n}$ refer to the orders of the lift operator and the assumed chordwise mode, respectively, the bars over W and K indicate that the chordwise integrations (i.e., θ and φ integrations) have been performed, L_j is spanwise loading in lb/ft and λ_k an integer which will be determined in the course of development of the kernels.

Then the set of $\bar{m} = \bar{n}$ line integral equations is solved by the collocation method. In this method, the spans of propeller and rudder are divided into strips of small lengths. The spanwise loading is considered constant over each strip, hence only the kernel need be integrated over the span. With these simplifications, the integral equations (5) and (6) can be converted to a system of simultaneous algebraic equations.

On the left-hand side of Equation (1) or (5), the downwash distribution can be expressed in Fourier series as

$$W_P^{(q)}(x_P, r_P, \varphi_P) e^{iq\Omega t} = V^{(q)}(r_P) e^{iq(\Omega t - \varphi_{P0})} \qquad (7)$$

where $V^{(q)}(r_P)$ are Fourier coefficients of downwash velocity normal to the propeller blade and φ_{F_0} is initial angular position of the control point on the propeller blade. The downwash velocity is that due to hull wake, and in the steady-state case only, since the blades are considered rigid, that due to incidence angle and camber of the propeller blades in addition.

When the rudder is amidships, the normal component of the velocity (W_R) is zero. With rudder deflection there is a normal component of velocity due to incident flow angle which also, under the present assumptions, affects only the steady-state condition $q = 0$.

DEVELOPMENT OF THE KERNEL FUNCTIONS AND LOADING DISTRIBUTIONS

The Kernel K_{PP}

The kernel K_{PP} describes the self-induced velocity at a point on a propeller blade due to unit amplitude load at various locations on all the blades of the propeller. The linearized formulation of the unsteady lifting surface theory for a marine propeller alone, with its N blades lying on a helicoidal surface and operating in non-uniform flow of an incompressible, ideal fluid, was derived by means of the acceleration potential method in the earlier papers.[1-6] The following is an adaptation of the development of Ref. 6.

It is known that the pressure field generated by a lifting surface S is given by distributed doublets with axis parallel to the local normal, and with strength equal to the pressure jump across the surface S . Thus the pressure P at a point (x,r,φ) at time t will be given by

$$\psi(x,r,\varphi;t) = \frac{1}{4\pi\rho_f} \int_S\int \Delta P(\xi,\rho,\theta;t) \frac{\partial}{\partial n} \frac{1}{R'(x,r,\varphi;\xi,\rho,\theta)} dS \qquad (8)$$

(Note that, in this section, subscripts P of the coordinates of both control and loading points are omitted for simplicity.)

in Eq. (8) ψ is the acceleration potential function defined as $\psi = \frac{P}{\rho_f}$

ρ_f = fluid density

$\frac{\partial}{\partial n}$ = normal derivative on the surface S at the loading point (ξ,ρ,θ)

$\vec{n}$ = unit normal vector having positive axial component

$\Delta P(\xi,\rho,\theta;t)$ = pressure jump across the lifting surface, i.e. $\Delta P = P_+ - P_-$ (pressure difference between upper and lower surfaces)

$$R'(x,r,\varphi;\xi,\rho,\theta) = \left[(x-\xi)^2 + r^2 + \rho^2 - 2r\rho\cos(\theta-\varphi) \right]^{\frac{1}{2}}$$

= Descartes distance between the given control point and loading point.

For doublets with pulsating strength $\Delta P(\xi,\rho,\theta)e^{i\omega t}$ at point (ξ,ρ,θ) which rotates with angular velocity $-\Omega$, Eq. (8) yields

$$\psi(x,r,\varphi;t) = \frac{1}{4\pi\rho_f} \int_S\int \Delta P(\xi,\rho,\theta_o)e^{i\omega t} \frac{\partial}{\partial n} \frac{1}{R'(x,r,\varphi;\xi,\rho,\theta_o-\Omega t)} \, dS \qquad (9)$$

where ω = frequency

θ_o = initial angular position

When the relation between velocity potential Φ and acceleration potential ψ is utilized, viz.,

$$\Phi(x,r,\varphi;t) = -\frac{1}{U} \int_{-\infty}^{x} \psi(\tau',r,\varphi;\ t - \frac{x-\tau'}{U}) \, d\tau' \qquad (10)$$

and the lifting surface is identified as the helicoidal surface of an N-bladed propeller, where both control and loading points rotate with angular velocity $-\Omega$, then the expression for the velocity potential is given by

$$\Phi(x,r,\varphi_o;t) = -\sum_{n=1}^{N} \sum_{\lambda_1=0}^{\infty} \frac{e^{i\lambda_1\Omega t}}{4\pi\rho_f U} \cdot \int_S\int \Delta P^{(\lambda_1)}(\xi,\rho,\theta_o) \int_{-\infty}^{x} e^{i\lambda_1\left[a(\tau'-x)-\bar{\theta}_n\right]} \frac{\partial}{\partial n}\left(\frac{1}{R}\right) d\tau' dS \qquad (11)$$

where $a = \Omega/U$

$\lambda_1 = \omega/\Omega$ is order of harmonic

$\bar{\theta}_n = \frac{2\pi}{N}(n-1)$, $n = 1,2....N$

$$R = \left\{(\tau'-\xi)^2 + r^2 + \rho^2 - 2r\rho \cos\left[\theta_o-\varphi_o+\bar{\theta}_n-a(\tau'-x)\right]\right\}^{\frac{1}{2}}$$

φ_o = angular position of control point with respect to midchord line

The self-induced velocity at $(x,r,\varphi_o;t)$, the first integral of Eq. (5), will be given by

$$I_1 = \frac{\partial}{\partial n'}\Phi = -\sum_{n=1}^{N}\sum_{\lambda_1=o}^{\infty}\frac{e^{i\lambda_1\Omega t}}{4\pi\rho_f U} \cdot \int_S\int \Delta P^{(\lambda_1)}(\xi,\rho,\theta_o)\frac{\partial}{\partial n'}\int_{-\infty}^{x} e^{i\lambda_1\left[a(\tau'-x)-\bar{\theta}_n\right]}\frac{\partial}{\partial n}\left(\frac{1}{R}\right)d\tau' dS \quad (12)$$

where $\frac{\partial}{\partial n'}$, is the normal derivative on the helicoidal surface at (x,r,φ), the control point.

The directional derivatives normal to the helicoidal surface, which is given by $x = \varphi_o/a$ or $\xi = \theta_o/a$, are: at the control point

$$\frac{\partial}{\partial n'} = \frac{r}{\sqrt{1+a^2r^2}}\left(a\frac{\partial}{\partial x} - \frac{1}{r^2}\frac{\partial}{\partial \varphi_o}\right) \quad (13)$$

at the loading (doublet) point

$$\frac{\partial}{\partial n} = \frac{\rho}{\sqrt{1+a^2\rho^2}}\left(a\frac{\partial}{\partial \xi} - \frac{1}{\rho^2}\frac{\partial}{\partial \theta_o}\right) \quad (14)$$

The fact that the left-hand side of Eq. (1) is

$$W(x,r,\varphi_o;t) = \sum_{q=o}^{\infty} W^{(q)}(x,r,\varphi_o)e^{iq\Omega t} = \sum_{q=0}^{\infty} V_{(r)}^{(q)} e^{iq(\Omega t-\varphi_o)} \quad (15)$$

where the time dependence is of the form $e^{iq\Omega t}$, and that the time dependence of the first term of the right-hand side, which is equivalent to Eq. (12), is of the form $e^{i\lambda_1\Omega t}$, dictates that

$$\lambda_1 = q$$

hence

$$I_1 = \iint_{S_P} \sum_{q=0}^{\infty} L_P'^{(q)}(\rho,\theta_o) e^{iq\Omega t} K_{PP}(r,\varphi_o;\rho,\theta_o;q)\, dS_P \tag{16}$$

where

$$L_P'^{(q)}(\rho,\theta_o) \equiv \Delta p^{(\lambda_1)}(\rho,\theta_o),\ lb/ft^2$$

$$K_{PP} = -\frac{1}{4\pi\rho_f U} \lim_{\delta\to o} \sum_{n=1}^{N} e^{-iq\bar{\theta}_n} \frac{\partial}{\partial n'} \int_{-\infty}^{x} e^{iqa(\tau'-x)} \frac{\partial}{\partial n}\left(\frac{1}{R}\right) d\tau' \tag{17}$$

$$\delta = \frac{\varphi_o - \theta_o}{a} - (x - \xi)$$

and by $\delta\to 0$ is meant $x\to\varphi_o/a$ and $\xi\to\theta_o/a$. The limiting process is introduced to avoid the mathematical difficulty due to the high-order singularity of the kernel K_{PP}.

The surface integral (16) is equivalent to

$$I_1 = \int_{-\theta_b^\rho}^{\theta_b^\rho} \int_0 \left\{ \sum_{q=0}^{\infty} L_P'^{(q)}(\rho,\theta_o) e^{iq\Omega t} K_{PP} \right\} \frac{\sqrt{1+a^2\rho^2}}{a\rho} \rho d\rho d\theta_o \tag{18}$$

where θ_b^ρ is projected semichord length of the propeller blade at the loading point, in radians, and the factor $(\sqrt{1+a^2\rho^2}/a\rho)$ is the result of changing the integration over the actual propeller blade to integration over its projection in the propeller plane. With the transformation

$$\theta_o = \sigma^\rho - \theta_b^\rho \cos\theta_\alpha$$

(where θ_α is angular chordwise location of the loading point, and σ^ρ is angular position of the midchord line of the projected blade from the vertical through the hub, or skewness) and with

$$L_P^{(q)}(\rho,\theta_o) \equiv L_P'^{(q)}(\rho,\theta_o) \cdot \rho\theta_b^\rho, \text{ lb/ft}$$

the integral becomes

$$I_1 = \int_0^\pi \int_\rho \left\{ \sum_{q=0} L_P^{(q)}(\rho,\theta_\alpha) e^{iq\Omega t} K_{PP} \right\} \frac{\sqrt{1+a^2\rho^2}}{a\rho} \sin\theta_\alpha d\theta_\alpha d\rho \qquad (19)$$

where K_{PP} is given by (17).

By utilizing the expansion scheme for the inverse Descartes distance:

$$\frac{1}{R} = \frac{1}{\left[(\tau'-\xi)^2+r^2+\rho^2-2r\rho\cos\beta\right]^{\frac{1}{2}}}, \text{ where } \beta = \theta_o-\varphi_o+\bar{\theta}_n-a(\tau'-x)$$

$$= \frac{1}{\pi} \sum_{m_1=-\infty}^{\infty} e^{im_1\beta} \int_{-\infty}^{\infty} I_{m_1}(|k|\rho) K_{m_1}(|k|r) e^{i(\tau'-\xi)k}\, dk, \text{ for } \rho < r \qquad (20)$$

(for $\rho > r$, ρ and r are interchanged in $I_{m_1}(\ )$ and $K_{m_1}(\ )$ the modified Bessel functions of order m_1), the kernel (Eq. 17) was shown in Ref. 5 to be, for $\rho < r$:

$$K_{PP}(r,\varphi_o,\rho,\theta_o;q) = -\frac{N}{4\pi^2\rho_f U} \frac{\rho r}{\left[(1+a^2\rho^2)(1+a^2r^2)\right]^{\frac{1}{2}}}$$

$$\cdot \sum_{\substack{m_1=-\infty \\ m_1=q+\ell N}}^{\infty} \left\{ \pi e^{-iq(\varphi_o-\theta_o)} \left[a^2(m_1-q)+\frac{m_1}{r^2}\right]\left[a^2(m_1-q)+\frac{m_1}{\rho^2}\right] I_{m_1}(a|m_1-q|\rho) K_{m_1}(a|m_1-q|r) \right.$$

$$\left. - ia^2 e^{-im_1(\varphi_o-\theta_o)} \int_{-\infty}^{\infty} \frac{k^2 I_{m_1}(|k|\rho) K_{m_1}(|k|r) e^{i\frac{k}{a}(\varphi_o-\theta_o)}}{k-a(m_1-q)}\, dk \right.$$

$$
\left.
\begin{aligned}
&- iam_1\left(\frac{1}{r^2}+\frac{1}{\rho^2}\right)e^{-im_1(\varphi_o-\theta_o)}\int_{-\infty}^{\infty}\frac{kI_{m_1}(|k|\rho)K_{m_1}(|k|r)e^{i\frac{k}{a}(\varphi_o-\theta_o)}}{k-a(m_1-q)}\,dk \\
&-\frac{im_1^2}{r^2\rho^2}e^{-im_1(\varphi_o-\theta_o)}\int_{-\infty}^{\infty}\frac{I_{m_1}(|k|\rho)K_{m_1}(|k|r)e^{i\frac{k}{a}(\varphi_o-\theta_o)}}{k-a(m_1-q)}
\end{aligned}
\right\} \qquad (21)
$$

where the discrete values of $m_1 = q + \ell N$, $\ell = 0, \pm 1, \pm 2, \ldots$ are deduced from the fact that

$$
\sum_{n=1}^{N} e^{i(m_1-q)\bar{\theta}_n} = \sum_{n=1}^{N} e^{i(m_1-q)2\pi(n-1)/N} = \begin{cases} N \text{ for } (m_1-q) = \ell N \\ 0 \text{ for } (m_1-q) \neq \ell N \end{cases} \qquad (22)
$$

Since $\theta_o = \sigma^\rho - \theta_b^\rho \cos\theta_\alpha$ and $\varphi_o = \sigma^r - \theta_b^r \cos\varphi_\alpha$, where θ_α and φ_α are angular chordwise locations of loading and control points, in Eq. (21) the θ_α and φ_α chordwise dependence of the kernel function occur in exponential form

$$
e^{\pm i\nu\cos\theta_\alpha} \quad \text{and} \quad e^{\pm i\nu\cos\varphi_\alpha}
$$

as factors separated from each other and from the other coordinates. The kernel is now in separable form, which not only facilitates the θ_α chordwise loading integration, as will be seen later, but also permits use of the lift operator technique.

The φ_α exponential can be expanded in terms of the following orthogonal and complete set of functions, $\Phi(\bar{m})$

$$
1-\cos\varphi_\alpha,\ 1+2\cos\varphi_\alpha,\ \cos^2\varphi_\alpha,\ldots,\cos(\bar{m}-1)\varphi_\alpha,\ldots,\ 0 \le \varphi_\alpha \le \pi \qquad (23)
$$

in the form

$$e^{\pm i\nu\cos\varphi_\alpha} \equiv J_o(\nu) + 2\sum_{\lambda=1}^{\infty}(-1)^\lambda J_{2\lambda}(\nu)\cos 2\lambda\varphi_\alpha \mp 2i\sum_{\lambda=1}^{\infty}(-1)^\lambda J_{2\lambda-1}(\nu)\cos(2\lambda-1)\varphi_\alpha$$

where $J_n(\nu)$ are Bessel functions of the first kind. The orthogonality property of $\Phi(\bar{m})$ dictates operation on both sides of integral Eq. (1) by the following operators

$$\frac{1}{\pi}\int_o^\pi (1 - \cos\varphi_\alpha)\{\ \}\, d\varphi_\alpha \qquad \bar{m} = 1$$

$$\frac{1}{\pi}\int_o^\pi (1 + 2\cos\varphi_\alpha)\{\ \}\, d\varphi_\alpha \qquad \bar{m} = 2 \tag{24}$$

$$\frac{1}{\pi}\int_o^\pi \cos(\bar{m} - 1)\varphi_\alpha\{\ \}\, d\varphi_\alpha \qquad \bar{m} > 2\ .$$

which are termed "generalized lift operator" to conform with the well-known Glauert lift operator ($\bar{m} = 1$) introduced in steady airfoil theory. In this way the φ_α-dependence is eliminated from the kernel function and the chordwise θ_α-integration can now be analytically performed.

The unknown loading function $L_p^{(q)}(\rho,\theta_o)$ is now approximated in the chordwise direction by the Birnbaum mode shapes

$$L_p^{(q)}(\rho,\theta_o) = \frac{1}{\pi}\left\{L_p^{(q,1)}(\rho)\,\Theta(1) + \sum_{\bar{n}=2}^{\infty} L_p^{(q,\bar{n})}(\rho)\,\Theta(\bar{n})\right\} \tag{25}$$

where $L_p^{(q,\bar{n})}(\rho)$ are the spanwise loading components to be determined by the solution of integral Eqs. (5,6) and

$$\Theta(1) = \cot\frac{\theta_\alpha}{2}$$

$$\Theta(\bar{n}) = \sin(\bar{n} - 1)\theta_\alpha\ ,\ \bar{n} > 1$$

With Eqs. (24) and (25) the integral (19) becomes

$$I_1 = \sum_{q=o}^{\infty} e^{iq\Omega t} \int_{\rho} \sum_{\bar{m}=1}^{\bar{n}} \sum_{\bar{n}=1} L_p^{(q,\bar{n})} \bar{K}_{PP}^{(\bar{m},\bar{n})} \frac{\sqrt{1+a^2\rho^2}}{a\rho} d\rho \qquad (26)$$

where

$$\bar{K}_{PP} = \frac{1}{\pi^2} \int_0^{\pi} \int_0^{\pi} \Theta(\bar{n})\, \Phi(\bar{m}) K_{PP} \sin\theta_\alpha d\theta_\alpha d\varphi_\alpha \quad .$$

which is called the modified kernel function.

Equation (21) for K_{PP} was developed in Ref. 5 which treats the helicoidal wake exactly. When the helicoidal wake is approximated by a staircase function, the mathematics is simplified considerably. Since Ref. 5 shows that the results of both treatments are in satisfactory agreement, the staircase approximation[6] (see Figure 3) has been adopted in evaluating K_{PP}:

$$K_{PP} = -\frac{1}{4\pi\rho_f U a} \sum_{n=1}^{N} \lim_{\delta\to o} \sum_{p=o}^{\infty} \int_{\bar{\theta}_n+\theta_o-\varphi_o}^{\infty} e^{-iq(\Theta+\varphi_o-\theta_o)} \left[-\frac{\partial^2}{\partial X^2}\frac{1}{R}\right]_{X=p\frac{\theta_o}{a}+\delta} d\Theta \qquad (27)$$

where

$$R = \left[X^2+r^2+\rho^2-2r\rho\cos\Theta\right]^{\frac{1}{2}}$$

$$\bar{\theta}_o = 2\pi/N \quad \text{and} \quad p = 0,1\ldots.$$

In addition, in this approximation $\sqrt{Ha^2\rho^2}/a\rho \to 1$.

The kernel can be expressed in separable form by making use of the following expansion

$$\frac{1}{R} = \sum_{m_1=0}^{\infty} \epsilon_{m_1} \cos m_1\Theta \left[\frac{1}{\pi\sqrt{r\rho}} Q_{m_1-\frac{1}{2}}\left(\frac{X^2+r^2+\rho^2}{2r\rho}\right)\right] \qquad (28)$$

where

$$\epsilon_{m_1} = \begin{cases} 1, & m_1 = 0 \\ 2, & m_1 \neq 0 \end{cases}$$

and $Q_{m_1-\frac{1}{2}}(Z)$ is the Legendre function of second kind, of half-odd-integer order. Then

$$-\frac{\partial^2}{\partial X^2}\frac{1}{R} = -\frac{1}{\pi}\sum_{m_1=0}^{\infty}\epsilon_{m_1}\cos m_1\Theta\left[\frac{Q'_{m_1-\frac{1}{2}}(Z)}{(r\rho)^{3/2}} + \frac{X^2 Q''_{m_1-\frac{1}{2}}(Z)}{(r\rho)^{5/2}}\right] \tag{29}$$

where

$$Z = (X^2 + r^2 + \rho^2)/2r\rho$$

$$Q'_{m_1-\frac{1}{2}}(Z) = \partial Q_{m_1-\frac{1}{2}}(Z)/\partial Z$$

$$Q'_{m_1-\frac{1}{2}}(Z) = \partial^2 Q_{m_1-\frac{1}{2}}(Z)/\partial Z^2$$

Equation (27) can be reduced to the following form

$$K_{PP} = -\frac{1}{4\pi\rho_f U a r_o^2}(K_1 + K_2) \tag{30}$$

where

$$K_1 = -\frac{e^{-iq(\varphi_o-\theta_o)}}{\pi(r\rho)^{3/2}}\sum_{n=1}^{N}\sum_{m_1=0}^{\infty}\epsilon_{m_1}\left\{\lim_{\delta\to 0}\int_{\bar{\theta}_n+\theta_o-\varphi_o}^{\bar{\theta}_n+\bar{\theta}_o/2} e^{-iq\Theta}\cos m_1\Theta \cdot \left[Q'_{m_1-\frac{1}{2}}(Z) + \frac{X^2}{r\rho}\cdot Q''_{m_1-\frac{1}{2}}(Z)\right]_{X=\delta} d\Theta\right\} \tag{31}$$

$$K_2 = -\frac{e^{-iq(\varphi_o-\theta_o)}}{\pi(r\rho)^{3/2}} \sum_{p=1}^{\infty} \sum_{m_1=0}^{\infty} \epsilon_{m_1} \left\{ \lim_{\delta\to 0} \int_0^{2\pi} e^{-iq\Theta} \cos m_1\Theta \cdot \left[Q'_{m_1-\frac{1}{2}}(Z) + \frac{X^2}{r\rho} Q'_{m_1-\frac{1}{2}}(Z) \right]_{X=p\frac{\bar{\theta}_o}{a}+\delta} d\Theta \right\} \quad (32)$$

and r_o^2 appears in the denominator because now all dimensions of K_1 and K_2 are fractions of propeller radius r_o and $a = r_o\Omega/U$.

It is easily proved that the non-singular kernel K_2 is

$$K_2 = \sum_{p=1}^{\infty} \left[\frac{-2e^{-iq(\varphi_o-\theta_o)}}{(r\rho)^{3/2}} \right] \left[Q'_{q-\frac{1}{2}}(Z) + \frac{X^2}{r\rho} Q''_{q-\frac{1}{2}}(Z) \right]_{X=p\bar{\theta}_o/a} \quad (33)$$

Reference 6 shows that Eq. (33) can be approximated by

$$K_2 \approx -\frac{2e^{-iq(\varphi_o-\theta_o)}}{(r\rho)^{\frac{1}{2}}} \frac{a^2}{\bar{\theta}_o^2} \left[5.940 Q_{q-\frac{1}{2}}(Z_1) - 19.530 Q_{q-\frac{1}{2}}(Z_2) + 13.590 Q_{q-\frac{1}{2}}(Z_3) \right] \quad (34)$$

where

$$Z_1 = \left[\left(\frac{.678\bar{\theta}_o}{a}\right)^2 + r^2 + \rho^2 \right] / 2r\rho$$

$$Z_2 = \left[\left(\frac{1.16\bar{\theta}_o}{a}\right)^2 + r^2 + \rho^2 \right] / 2r\rho$$

$$Z_3 = \left[\left(\frac{1.30\bar{\theta}_o}{a}\right)^2 + r^2 + \rho^2 \right] / 2r\rho \quad (35)$$

When $\rho \neq r$, K_1 is also non-singular. It has been shown[6] to be equal to

$$K_1 = -\frac{1}{\pi(r\rho)^{3/2}} \sum_{m_1=0}^{\infty} \epsilon_{m_1} \sum_{n=1}^{N} f(m_1,q,n)\, Q'_{m_1-\frac{1}{2}}(Z) \tag{36}$$

where $Z = (r^2 + \rho^2)/2r\rho$ and $f(m_1, q, n)$ is a function of the chordwise coordinates, the result of the Θ-integration multiplied by $\exp\left[-iq(\varphi_o-\theta_o)\right]$.

When $\rho = r$, K_1 is given by

$$K_1 = -\frac{1}{\pi(r\rho)^{3/2}} \lim_{X\to 0} \sum_{m_1=0}^{\infty} \epsilon_{m_1} \sum_{n=1}^{N} f(m_1,q,n)\left[Q'_{m_1-\frac{1}{2}}(Z) + \frac{X^2}{r\rho} Q''_{m_1-\frac{1}{2}}(Z)\right] \tag{37}$$

where $Z = (X^2 + r^2 + \rho^2)/2r\rho$ approaches unity as $X \to 0$ when $\rho = r$. Equation (37) has a high-order singularity with Hadamard finite contribution which must be carefully evaluated.

Since the kernels are in the separable form, the ρ-integration and φ_α- and θ_α- integrations are independent of each other. With $\bar{K}_{pp}(\bar{m},\bar{n})$ used to designate the modified kernel after the chordwise integrations, the integral (26) becomes

$$I_1 = \sum_{q=0}^{\infty} e^{iq\Omega t} \int_{\rho} \sum_{\bar{m}=1}^{\bar{n}} \sum_{\bar{n}} L_p^{(q,\bar{n})}(\rho)\, \bar{K}_{pp}^{(\bar{m},\bar{n})}\, d\rho$$

$$= \sum_{q=0}^{\infty} -\frac{e^{iq\Omega t}}{4\pi\rho_f U a r_o} \int_{\rho} \sum_{\bar{m}=1}^{\bar{n}} \sum_{\bar{n}} L_p^{(q,\bar{n})}(\rho) \left[\bar{K}_1^{(\bar{m},\bar{n})} + \bar{K}_2^{(\bar{m},\bar{n})}\right] d\rho \tag{38}$$

where $d\rho$ is now nondimensionalized with respect to r_o.

In Eq. (38)

$$\bar{K}_2^{(\bar{m},\bar{n})} \approx e^{-iq(\sigma^r-\sigma^\rho)}\, I^{(\bar{m})}(q\theta_b^r)\, \Lambda^{(\bar{n})}(q\theta_b^\rho)\, F(r,\rho) \tag{39}$$

where

$F(r,\rho)$ is the factor of $\exp\left[-iq(\varphi_o-\theta_o)\right]$ in Eq. (34)

$$I^{(\bar{m})}(x) = \frac{1}{\pi}\int_0^{\pi} \Phi(\bar{m})\,\exp(ix\cos\varphi_\alpha)\,d\varphi_\alpha$$

$$\Lambda^{(\bar{n})}(x) = \frac{1}{\pi}\int_0^{\pi} \Theta(\bar{n})\,\exp(-ix\cos\theta_\alpha)\sin\theta_\alpha\,d\theta_\alpha \tag{40}$$

$$\bar{K}_1^{(\bar{m},\bar{n})}(\rho \neq r) = -\frac{1}{\pi(r\rho)^{3/2}}\sum_{m_1=0}^{\infty}\epsilon_{m_1}\sum_{n=1}^{N}\bar{f}^{(\bar{m},\bar{n})}(m_1,q,n)\,Q'_{m_1-\frac{1}{2}}(Z) \tag{41}$$

where $Z = (r^2+\rho^2)/2r\rho$. For $m_1 \neq q$

$$\sum_{n=1}^{N}\bar{f}^{(\bar{m},\bar{n})}(m_1,q,n) =$$

$$-\frac{iN}{2(m_1-q)}\left[e^{i(m_1-q)\bar{\theta}_o/2}\,e^{-iq(\sigma^r-\sigma^\rho)}\,I^{(\bar{m})}(q\theta_b^r)\,\Lambda^{(\bar{n})}(q\theta_b^\rho)\right.$$

$$\left.-e^{-im_1(\sigma^r-\sigma^\rho)}\,I^{(\bar{m})}(m_1\theta_b^r)\Lambda^{(\bar{n})}(m_1\theta_b^\rho)\right]$$

$$+\frac{iN}{2(m_1+q)}\left[e^{-i(m_1+q)\bar{\theta}_o/2}\,e^{-iq(\sigma^r-\sigma^\rho)}\,I^{(\bar{m})}(q\theta_b^r)\,\Lambda^{(\bar{n})}(q\theta_b^\rho)\right.$$

$$\left.-e^{im_1(\sigma^r-\sigma^\rho)}\,I^{(\bar{m})}(-m_1\theta_b^r)\,\Lambda^{(\bar{n})}(-m_1\theta_b^\rho)\right]$$

where $m_1 \mp q = \ell N$, ℓ integer, $m_1 \geq 0$, $q \geq 0$.

For $m_1 = q \neq 0$ and $2q = \ell N$

$$\sum_{n=1}^{N}\bar{f}^{(\bar{m},\bar{n})}(q,n) = \frac{N}{2}\,e^{-iq(\sigma^r-\sigma^\rho)}\left\{I^{(\bar{m})}(q\theta_b^r)\,\Lambda^{(\bar{n})}(q\theta_b^\rho)\left[\frac{\bar{\theta}_o}{2}+\sigma^r-\sigma^\rho+\frac{ie^{-iq\bar{\theta}_o}}{2q}\right]\right.$$

$$-I^{(\bar{m})}(-q\theta_b^r)\,\Lambda^{(\bar{n})}(-q\theta_b^\rho)\left[\frac{ie^{i2q(\sigma^r-\sigma^\rho)}}{2q}\right]$$

$$\left.-\theta_b^r\,I_1^{(\bar{m})}(q\theta_b^r)\Lambda^{(\bar{n})}(q\theta_b^\rho)+\theta_b^\rho\,I^{(\bar{m})}(q\theta_b^r)\Lambda_1^{(\bar{n})}(q\theta_b^\rho)\right\}$$

For $m_1 = q \neq 0,\ 2q \neq \ell N$

$$\sum_{n=1}^{N} \bar{f}^{(\bar{m},\bar{n})}(q,n) = \frac{N}{2} e^{-iq(\sigma^r-\sigma^\rho)}\Big\{ I^{(\bar{m})}(q\theta_b^r)\Lambda^{(\bar{n})}(q\theta_b^\rho)\Big[\frac{\bar{\theta}_o}{2} + \sigma^r - \sigma^\rho\Big] - \theta_b^r\, I_1^{(\bar{m})}(q\theta_b^r)\Lambda^{(\bar{n})}(q\theta_b^\rho) + \theta_b^\rho I^{(\bar{m})}(q\theta_b^r)\Lambda_1^{(\bar{n})}(q\theta_b^\rho)\Big\}$$

For $m_1 = q = 0$

$$\sum_{n=1}^{N} \bar{f}^{(\bar{m},\bar{n})}(o,n) = N\Big\{ I^{(\bar{m})}(0)\Lambda^{(\bar{n})}(0)\Big[\frac{\bar{\theta}_o}{2} + \sigma^r - \sigma^\rho\Big] - \theta_b^r\, I_1^{(m)}(0)\Lambda^{(\bar{n})}(0) + \theta_b^\rho\, I^{(\bar{m})}(0)\,\Lambda_1^{(\bar{n})}(0)\Big\} \tag{42}$$

The symbols $I_1^{(\bar{m})}(\ )$ and $\Lambda_1^{(\bar{n})}(\ )$ are defined as follows:

$$I_1^{(\bar{m})}(x) = \frac{1}{\pi}\int_o^{\pi} \Phi(\bar{m})\exp(ix\cos\varphi_\alpha)\cos\varphi_\alpha d\varphi_\alpha$$

$$\Lambda_1^{(\bar{n})}(x) = \frac{1}{\pi}\int_o^{\pi} \Theta(\bar{n})\exp(-ix\cos\theta_\alpha)\sin\theta_\alpha\cos\theta_\alpha d\theta_\alpha \tag{43}$$

The following relations can be easily proved:

$$\left.\begin{aligned} \Lambda^{(1)}(x) &= J_o(x) - iJ_1(x) \\ \Lambda^{(\bar{n})}(x) &= \frac{(-i)^{\bar{n}-2}}{2}\Big[J_{\bar{n}-2}(x) + J_{\bar{n}}(x)\Big],\quad \bar{n} > 1 \\ \Lambda_1^{(1)}(x) &= \frac{1}{2}\Big[J_o(x) - J_2(x)\Big] - iJ_1(x) \\ \Lambda_1^{(\bar{n})}(x) &= \frac{(-i)^{\bar{n}+1}}{4}\Big[J_{\bar{n}-3}(x) - J_{\bar{n}+1}(x)\Big],\quad \bar{n} > 1 \end{aligned}\right\} \tag{44}$$

$$\left.\begin{aligned} I^{(1)}(x) &= J_o(x) - iJ_1(x) \\ I^{(2)}(x) &= J_o(x) + 2iJ_1(x) \\ I^{(\bar{m})}(x) &= i^{\bar{m}-1} J_{\bar{m}-1}(x),\quad \bar{m} > 2 \end{aligned}\right\} \tag{45}$$
(Con't)

$$I_1^{(1)}(x) = -\tfrac{1}{2}\left[J_o(x) - J_2(x)\right] + i\, J_1(x)$$

$$I_1^{(2)}(x) = J_o(x) - J_2(x) + i\, J_1(x)$$

$$I_1^{(\bar{m})}(x) = \frac{i^{\bar{m}-2}}{2}\left[J_{\bar{m}-2}(x) - J_{\bar{m}}(x)\right], \quad \bar{m} > 2 \tag{45}$$

The values for (-x) are the complex conjugates of the foregoing expressions for (+x).

As mentioned earlier, the ρ-integration is done in strips, with the spanwise loading coefficient $L_\rho^{(q,\bar{n})}(\rho)$ assumed to be constant over each strip and evaluated by the collocation method. The kernel $\bar{K}_2^{(\bar{m},\bar{n})}$ can be integrated over each strip by any appropriate numerical method, as can $\bar{K}_1^{(\bar{m},\bar{n})}$ outside the strip in which the radial positions of control and loading points are close.

The integration of $\bar{K}_1^{(\bar{m},\bar{n})}$ over the narrow singular range $r_j-\beta < \rho_j < r_j+\beta$, β very small, can be done by expanding the Legendre function in a series valid near $Z = 1$. Such a series representation was given in Ref. 13 and used in Ref. 6 which showed that the integral can be given by

$$\int_{r_j-\beta}^{r_j+\beta} \bar{K}_1^{(\bar{m},\bar{n})}(r_j,\rho)\,d\rho \approx -\frac{1}{\pi r^5}\sum_{m_1=0}^{\infty}\epsilon_{m_1}\sum_{n=1}^{N}\bar{f}^{(\bar{m},\bar{n})}\cdot I_\rho \tag{46}$$

where

$$I_\rho = \frac{-4r^4 b_{m_1 o}}{\beta} + 2\beta r^2\sum_{s=1}^{\infty}\left(\frac{\beta^2}{2r^2}\right)^{s-1}\left\{\frac{s}{2s-1}\left[a_{m_1 s} + b_{m_1 s}\,\ell n\left(\frac{\beta^2}{2r^2}\right)\right] - \frac{1}{(2s-1)^2}\,b_{m_1 s}\right\}$$

$$a_{m_1 o} = \frac{5}{2}\,\ell n\ 2 - 2\sum_{j=1}^{m_1}\frac{1}{2j-1}(1-\delta_{m_1 o})$$

$$\delta_{m_1 o} = \begin{cases} 1, & m_1 = 0 \\ 0, & m_1 \neq 0 \end{cases}$$

$$b_{m_1 o} = -1/2$$

$$b_{m_1,p+1} = b_{m_1 p}\,\frac{m_1^2 - \frac{1}{4} - p(p+1)}{2(p+1)^2} \tag{47}$$

[Cont'd]

$$a_{m_1,p+1} = a_{m_1 p} \frac{\left[m_1^2 - \frac{1}{4} - p(p+1)\right]}{2(p+1)^2} - b_{m_1 p} \frac{\left[2(m^2 - \frac{1}{4}) + p + 1\right]}{2(p+1)^3} \tag{47}$$

It is to be noted that the staircase approximation of the helicoidal wake from the propeller blades, as defined in Eq. (27) and used in the subsequent development, viz.,

$$X = p \frac{\bar{\theta}_o}{a} + \delta$$

where

$$\bar{\theta}_o = \frac{2\pi}{N}$$

must be modified slightly in order to accommodate all propellers of practical interest with expanded area ratio EAR up to 1.3 . Thus, for general use, the upper limit of the Θ-integral of K_1 (Eq. 31) should be replaced by $\bar{\theta}_n + B$, and the staircase function in the representation of K_2 (Eq.32) should be replaced by

$$X = \frac{1}{a}\left[B - \frac{\bar{\theta}_o}{2} + p\bar{\theta}_o\right] + \delta \tag{48}$$

where

$$B = \bar{\theta}_o/2 \qquad \text{if} \quad (\theta_b^r + \theta_b^\rho) \leq \bar{\theta}_o/2$$

and

$$B = \theta_b^r + \theta_b^\rho \qquad \text{if} \quad (\theta_b^r + \theta_b^\rho) > \bar{\theta}_o/2$$

In the latter case, the arguments (35) of the Legendre functions of Eq. (34) will be changed to

$$Z_1 = \left[\left(\frac{B - \bar{\theta}_o/2 + .678\bar{\theta}_o}{a}\right)^2 + r^2 + \rho^2\right]/2r\rho$$

$$Z_2 = \left[\left(\frac{B - \bar{\theta}_o/2 + 1.16\bar{\theta}_o}{a}\right)^2 + r^2 + \rho^2\right]/2r\rho \tag{49}$$

$$Z_3 = \left[\left(\frac{B - \bar{\theta}_o/2 + 1.30\bar{\theta}_o}{a}\right)^2 + r^2 + \rho^2\right]/2r\rho$$

The Kernel K_{RP}

When the control point is on the propeller and the loading point is on the rudder, the pressure field is generated by the lifting surface S_R of the rudder and is given by distributed doublets with axis parallel to the local normal and with strength equal to the pressure jump across the surface.

The pressure at a point x_P, r_P, φ_P at time t will be given by (cf. Eq. 8)

$$\psi(x_P, r_P, \varphi_P; t) = \frac{1}{4\pi\rho_f} \iint_{S_R} \sum_{\lambda_2=0}^{\infty} L_R'^{(\lambda_2)}(\xi_R, \rho_R, \theta_R) e^{i\lambda_2\Omega t} \frac{\partial}{\partial n_R}\left(\frac{1}{R'}\right)\Big|_{\theta_R=0}^{\pi} dS_R \quad (50)$$

Here R' is expressed in cylindrical coordinates

$$R' = \left[(x_P-\xi_R)^2 + r_P^2 + \rho_R^2 - 2r_P\rho_R\cos(\theta_R - \varphi_P)\right]^{-\frac{1}{2}} \quad (51)$$

provided that $\theta_R = 0$ when $\zeta_R > 0$, and $\theta_R = \pi$ when $\zeta_R < 0$.

$$\frac{\partial}{\partial n_R} = \pm \frac{1}{\rho_R}\frac{\partial}{\partial \theta_R} \quad (52)$$

is the normal derivative on the surface S_R at the loading point. (The positive sign is taken when $\theta_R = 0$, the negative when $\theta_R = \pi$.)

$$\sum_{\lambda_2=0}^{\infty} L_R'^{(\lambda_2)}(\xi_R, \rho_R, \theta_R) e^{i\lambda_2\Omega t} \equiv \Delta p(\xi_R, \rho_R, \theta_R; t) \quad (53)$$

represents the sinusoidal pressure jump with frequency $\lambda_2\Omega$, where Ω is the angular velocity of the propeller and λ_2 is a positive integer.

The velocity potential is then from Eq. (10)

$$\Phi(x_P, r_P, \varphi_P; t) = \frac{1}{4\pi\rho_f U} \iint_{S_R} \sum_{\lambda_2=0}^{\infty} L_R'^{(\lambda_2)}(\xi_R, \rho_R, \theta_R) e^{i\lambda_2\Omega t} \int_{-\infty}^{x_P} e^{i\lambda_2 a(\tau'-x_P)} \frac{\partial}{\partial n_R}\left(\frac{1}{R}\right) d\tau' dS_R \quad (54)$$

where

$$R = \left\{(\tau'-\xi_R)^2 + r_P^2 + \rho_R^2 - 2r_P\rho_R\cos(\theta_R-\varphi_{P_o} + \Omega t)\right\}^{\frac{1}{2}} \tag{55}$$

and the substitution $\varphi_p = \varphi_{po} - \Omega t$ has been made since the control point is rotating with angular velocity $-\Omega$.

The induced velocity at a point on the propeller due to a pulsating load on the rudder will be given by

$$I_2 = \frac{-1}{4\pi\rho_f U}\iint_{S_R}\sum_{\lambda_2=0}^{\infty} L_R'^{(\lambda_2)}(\xi_R,\rho_R,\theta_R)e^{i\lambda_2\Omega t}\frac{\partial}{\partial n'}\int_{-\infty}^{x_P} e^{i\lambda_2 a(\tau'-x_P)}\frac{\partial}{\partial n_R}\left(\frac{1}{R}\right)d\tau' dS_R \tag{56}$$

where $\frac{\partial}{\partial n'}$ is the normal derivative on the helicoidal surface at the control point (given by Eq. 13).

The second surface integral of Eq. (1) can then be written, after putting $\tau' = \tau + \xi_R$, as

$$I_2 = \iint_{S_R}\sum_{\lambda_2=0}^{\infty} L_R'^{(\lambda_2)}(\xi_R,\rho_R,\theta_R)e^{i\lambda_2\Omega t}K_{RP}(x_P,r_P,\varphi_{P_o};\xi_R,\rho_R,\theta_R;\lambda_2)dS_R$$

$$= \int_{-c_R}^{c_R}\int_{\zeta_R}\sum_{\lambda_2=0}^{\infty} L_R'^{(\lambda_2)}(\xi_R,\rho_R,\theta_R)e^{i\lambda_2\Omega t}\,K_{RP}d\xi_R' d\zeta_R \tag{57}$$

where

$$K_{RP} = -\frac{1}{4\pi\rho_f U}\lim_{\delta_{RP}\to 0}\left\{\frac{r_P}{\sqrt{1+a^2r_P^2}}\left(a\frac{\partial}{\partial x_P} - \frac{1}{r_P^2}\frac{\partial}{\partial\varphi_{Po}}\right)\left(\pm\frac{1}{\rho_R}\frac{\partial}{\partial\theta_R}\right)\right.$$

$$\left.\cdot\int_{-\infty}^{x_P-\xi_R}\frac{e^{i\lambda_2 a(\tau-x_P+\xi_R)}}{R}\,d\tau\right|_{\theta_R=\begin{cases}0\\ \pi\end{cases}} \tag{58}$$

$$R = \left\{\tau^2 + r_P^2 + \rho_R^2 - 2r_P\rho_R\cos(\theta_R - \varphi_{Po} + \Omega t)\right\}^{\frac{1}{2}}$$

$$\delta_{RP} = x_P - \varphi_{Po}/a$$

$$\varphi_{Po} = \sigma^r - \theta_b^r \cos\varphi_\alpha \tag{59}$$

$$\xi_R = x_o + \epsilon_R^\rho + \xi_R' \quad \text{and} \quad \xi_R' = -c_R^\rho \cos\theta_\alpha$$

c_R^ρ = semichord of rudder at loading point

Since $d\xi_R' = c_R^\rho \sin\theta_\alpha d\theta_\alpha$, (57) becomes

$$I_2 = \int_0^\pi \int_{\zeta_R} \sum_{\lambda_2=0}^{\infty} L_R^{(\lambda_2)}(\xi_R, \rho_R, \theta_R) e^{i\lambda_2\Omega t} K_{RP} \sin\theta_\alpha d\theta_\alpha d\zeta_R \tag{60}$$

where $L_R^{(\lambda_2)} = c_R^\rho L_R'^{(\lambda_2)}$, lb/ft. (The superscripts ρ and r refer to the values at the loading point and the control point, respectively.

The kernel K_{RP} (Eq. 58) is expressed in separable form by utilizing the expansion scheme

$$\frac{1}{R} = \frac{1}{\pi} \sum_{m=-\infty}^{\infty} e^{im(\theta_R - \varphi_{Po} + \Omega t)} \int_{-\infty}^{\infty} I_m(|k|\rho) K_m(|k|r) e^{i\tau k} dk \tag{61}$$

(for $\rho < r$). The indicated τ-integration can now be performed, yielding

$$\int_{-\infty}^{x_P - \xi_R} e^{i(\lambda_2 a + k)\tau} d\tau = \pi\delta(k + a\lambda_2) - \frac{ie^{i(k+a\lambda_2)(x_P - \xi_R)}}{k + a\lambda_2}$$

where $\delta(\,)$ is the Dirac delta function. After the derivatives with respect to x_P, φ_{Po} and θ_R are taken, the kernel function becomes, for $\rho_R < r_P$,

$$K_{RP} = -\frac{1}{4\pi^2\rho_f U r_o^2}\left[\frac{r_P}{\sqrt{1+a^2 r_P^2}} \lim_{\delta_{RP}\to 0} \sum_{m_2=-\infty}^{\infty} \begin{cases} +1 & \text{for } \zeta_R > 0 \\ (-1)^{m_2+1} & \text{for } \zeta_R < 0 \end{cases}\right.$$

$$\left. \cdot \frac{m_2}{\rho_R} e^{im_2(\Omega t - \varphi_{Po})} \left\{\left[a^2\lambda_2 - \frac{m_2}{r_P^2}\right]\pi I_{m_2}(a\lambda_2\rho_R) K_{m_2}(a\lambda_2 r_P) e^{-ia\lambda_2(x_P - \xi_R)}\right.\right. \tag{62}$$

[Cont'd]

$$+ ia \int_{-\infty}^{\infty} k \frac{I_{m_2}(|k|\rho_R) K_{m_2}(|k|r_P) e^{ik(x_P - \xi_R)}\, dk}{k + a\lambda_2} \qquad (62)$$

$$+ i \frac{m_2}{r_P} \int_{-\infty}^{\infty} \frac{I_{m_2}(|k|\rho_R) K_{m_2}(|k|r_P) e^{ik(x_P - \xi_R)}\, dk}{k + a\lambda_2} \Big\} \Big]$$

where all the dimensional quantities within the square brackets are non-dimensionalized with respect to propeller radius r_o. When $\rho_R > r_P$, ρ_R and r_P are interchanged in the modified Bessel functions.

The time-dependent factor in the second integral of Eq. (1), as can be seen from Eq. (60) and Eq. (62), is of the form $\exp\left[i(\lambda_2 + m_2)\Omega t \right]$ whereas on the left-hand side of Eq. (1) it is of the form $\exp(iq\Omega t)$ (see Eq. 15). The equality of time-dependent expressions requires that

$$\lambda_2 + m_2 = q$$

or

$$m_2 = q - \lambda_2$$

Since $\lambda_2 \geq 0$, m_2 cannot be larger than q. Therefore, the m_2-series ranges from $-\infty$ to q and the double series over λ_2 and m_2 can be reduced to a single infinite series.

The expansion scheme has introduced a Cauchy-type singularity in the k-integration. There are no other singularities. Appendix A proves that $1/R$ is non-singular since $x_P - \xi_R < 0$.

After the limit is taken and the transformations (59) are made, the chordwise integrations over θ_α and φ_α are performed by following the procedure of the preceding section for $\bar{K}_{PP}^{(\bar{m},\bar{n})}$. With $\Phi(\bar{m})$ and $\Theta(\bar{n})$ as defined in (24,25), Eq. (60) becomes

$$I_2 = \frac{1}{\pi^2} \int_0^{\pi} \int_0^{\pi} r_o \int_{\zeta_R} \sum_{\lambda_2=0}^{\infty} \sum_{\bar{m}=1}^{\bar{n}} \sum_{\bar{n}} L_R^{(\lambda_2,\bar{n})} e^{i\lambda_2 \Omega t} K_{RP}^{\Theta}(\bar{n}) \Phi(\bar{m}) \sin\theta_\alpha d\theta_\alpha d\varphi_\alpha d\zeta_R$$

$$= r_o \int_{\zeta_R} \sum_{\lambda_2=0}^{\infty} \sum_{\bar{m}=1}^{\bar{n}} \sum_{\bar{n}} L_R^{(\lambda_2,\bar{n})} e^{iq\Omega t} \bar{K}_{RP}^{(\bar{m},\bar{n})} d\zeta_R \qquad (63)$$

where ζ_R is nondimensionalized with respect to r_o and, for $\rho_R < r_P$,

the kernel function is

$$\bar{K}_{RP}^{(\bar{m},\bar{n})}(m_2 = q-\lambda_2) = -\frac{1}{4\pi^2 \rho_f U r_o^2} e^{-i m_2 \sigma^r} \frac{r_P}{\sqrt{1+a^2 r_P^2}} \begin{cases} (+1) & \text{for } \zeta_R > 0 \\ (-1)^{m_2+1} & \text{for } \zeta_R < 0 \end{cases} \frac{m_2}{\rho_R}$$

$$\cdot \left\{ e^{ia(q-m_2)(x_o+\epsilon_R^\rho-\sigma^r/a)} \left[a^2(q-m_2) - \frac{m_2}{r_P^2} \right] \pi \, I_{m_2}(a|q-m_2|\rho_R) K_{m_2}(a|q-m_2|r_P) I^{(\bar{m})}(q\theta_b^r) \right.$$

$$\cdot \Lambda^{(\bar{n})}(a(q-m_2)C_R^\rho)$$

$$+ia \int_{-\infty}^{\infty} \frac{k I_{m_2}(|k|\rho_R) K_{m_2}(|k|r_P) e^{-ik(x_o+\epsilon_R^\rho-\sigma^r/a)} I^{(\bar{m})}((m_2-\frac{k}{a})\theta_b^r) \Lambda^{(\bar{n})}(-kC_R^\rho) dk}{k + a(q-m_2)}$$

$$\left. +i \frac{m_2}{r_P^2} \int_{-\infty}^{\infty} \frac{I_{m_2}(|k|\rho_R) K_{m_2}(|k|r_P) e^{-ik(x_o+\epsilon_R^\rho-\sigma^r/a)} I^{(\bar{m})}((m_2-\frac{k}{a})\theta_b^r) \Lambda^{(\bar{n})}(-kC_R^\rho) dk}{k + a(q-m_2)} \right\}$$

(64)

evaluated at $m_2 = q - \lambda_2$. (For $\rho_R \geq r_P$, ρ_R and r_P are interchanged in the modified Bessel functions.) $I^{\bar{m}}(x)$ and $\Lambda^{(\bar{n})}(x)$ are given by (44) and (45).

It should be noted that when $m_2 = 0$, $\bar{K}_{RP}^{(\bar{m},\bar{n})} = 0$, even when q or k are also zero since

$$\lim_{\substack{m\to 0 \\ x\to 0}} m I_m(x) K_m(x) = \lim_{\substack{m\to 0 \\ x\to 0}} \left[-m x^m \log x \right] = 0$$

The first k-integral may be simplified for the numerical solution by substituting

$$\frac{k}{k+a(q-m_2)} = 1 - \frac{a(q-m_2)}{k+a(q-m_2)}$$

the second term of which can be combined with the second k-integral. The k-integrations are done by Simpson's rule. Appendix B evaluates the integrand of Eq. (64) at $k = a(m_3 - q)$. The amplitudes of unknown loading for the different values of λ_3 are assumed constant over a small radial strip. The corresponding kernel is integrated over the elemental strip by a convenient numerical method.

The Kernel K_{PR}

When the control points are on the rudder and the loading points are on the propeller, the induced velocity due to a pulsating load of all frequencies

$$\sum_{\lambda_3=0}^{\infty} L_P'^{(\lambda_3)}(\xi_P, \rho_P, \theta_{Po}) e^{i\lambda_3 \Omega t}$$

will be

$$I_3 = -\sum_{n=1}^{N} \frac{1}{4\pi\rho_f U} \iint_{S_P} \sum_{\lambda_3=0}^{\infty} L_P'^{(\lambda_3)}(\xi_P, \rho_P, \theta_{Po}) e^{i\lambda_3 \Omega t} \frac{\partial}{\partial n_R'} \int_{-\infty}^{x_R} e^{i\lambda_3 \left[a(\tau' - x_R) - \bar{\theta}_n \right]} \frac{\partial}{\partial n} \left(\frac{1}{R} \right) d\tau' dS_P \tag{65}$$

where

$$\frac{\partial}{\partial n_R'} = \pm \frac{1}{r_R} \left. \frac{\partial}{\partial \varphi_R} \right|_{\varphi_R = \begin{cases} 0 \\ \pi \end{cases}}$$

is the normal derivative at the control point and $\partial/\partial n$ is given by Eq. (14). The Descartes distance R is, in this case,

$$R = \left\{ (\tau' - \xi_P)^2 + r_R^2 + \rho_P^2 - 2 r_R \rho_P \cos\left[\theta_{Po} - \varphi_R - \Omega t + \bar{\theta}_n - a(\tau' - x_R) \right] \right\}^{\frac{1}{2}} \tag{66}$$

The first surface integral of Eq. (2) can be written as

$$I_3 = \iint_{S_P} \sum_{\lambda_3=0}^{\infty} L'^{(\lambda_3)}(\rho_P, \theta_{Po}) e^{i\lambda_3 \Omega t} K_{PR}(x_R, r_R, \varphi_R; \xi_P, \rho_P, \theta_{Po}; \lambda_3) dS_P$$

$$= \int_0^{\pi} \int_{\rho_P} \sum_{\lambda_3=0}^{\infty} L_P^{(\lambda_3)}(\rho_P, \theta_{Po}) e^{i\lambda_3 \Omega t} K_{PR} \frac{\sqrt{1 + a^2 \rho_P^2}}{a \rho_P} \sin\theta_\alpha d\theta_\alpha d\rho_P \tag{67}$$

where

$$L_P(\rho_P,\theta_{Po}) \equiv L'_P(\rho_P,\theta_{Po})\cdot\rho\theta_b^{\rho} \ , \ \text{lb/ft}$$

which is approximated by Eq. (25). The kernel K_{PR} is

$$K_{PR} = -\frac{1}{4\pi\rho_f U}\sum_{n=1}^{N}\lim_{\delta_{PR}\to 0}\left[\pm\frac{1}{r_R}\frac{\partial}{\partial\varphi_R}\right]_{\varphi_R=\frac{0}{\pi}}\frac{\rho_P}{\sqrt{1+a^2\rho_P^2}}\left(a\frac{\partial}{\partial\xi_P}-\frac{1}{\rho_P^2}\frac{\partial}{\partial\theta_{Po}}\right)$$

$$\cdot\int_{-\infty}^{x_R-\xi_P}\frac{e^{i\lambda_3\left[a(\tau-x_R+\xi_P)-\bar{\theta}_n\right]}}{R}\,d\tau \qquad (68)$$

where $\delta_{PR} = \xi_P - \theta_{Po}/a$ and τ has been substituted for $(\tau'-\xi_P)$. The reciprocal Descartes distance can be expanded as before

$$\frac{1}{R}=\frac{1}{\pi}\sum_{m_3=-\infty}^{\infty}e^{im_3\left[\bar{\theta}_n+\theta_{Po}-\varphi_R-\Omega t-a(\tau-x_R+\xi_P)\right]}\int_{-\infty}^{\infty}I_{m_3}(|k|\rho_P)K_{m_3}(|k|r_R)e^{i\tau k}dk \qquad (69)$$

for $\rho_P < r_R$.

On substituting (69) into Eq. (65), it is easily seen by the same reasoning used in the case of the kernel function K_{RP} that

$$\lambda_3 - m_3 = q \qquad (70)$$

Because of this, tne double series in λ_3 and m_3 can be reduced to a single infinite series in m_3 or λ_3. With the following

$$\int_{-\infty}^{x_R-\xi_P}e^{i(qa+k)\tau}d\tau=\pi\delta(k+aq) - \frac{ie^{i(k+aq)(x_R-\xi_P)}}{k+aq}$$

and

$$\sum_{n=1}^{N}e^{-iq\bar{\theta}_n} = \begin{cases}N & \text{for q=a multiple of N}\\ 0 & \text{for all other values of q}\end{cases}$$

the kernel becomes

$$K_{PR} = -\frac{N}{4\pi^2\rho_f U}\lim_{\delta_{PR}\to 0}\left[\pm\frac{1}{r_R}\frac{\partial}{\partial\varphi_R}\right]_{\varphi_R=\begin{cases}0\\ \pi\end{cases}}\frac{\rho_P}{\sqrt{1+a^2\rho_P^2}}\left(a\frac{\partial}{\partial\xi_P}-\frac{1}{\rho_P^2}\frac{\partial}{\partial\theta_{Po}}\right)$$

$$\cdot\sum_{m_3=-q}^{\infty} e^{-im_3(\Omega t+\varphi_R-\theta_{Po})}\left\{\pi e^{-iaq(x_R-\xi_P)} I_{m_3}(aq\rho_P)K_{m_3}(aqr_R)\right.$$

$$\left.-i\int_{-\infty}^{\infty}\frac{I_{m_3}(|k|\rho_P)K_{m_3}(|k|r_R)e^{ik(x_R-\xi_P)}dk}{k+aq}\right\} \qquad (71)$$

where q is a multiple of number of blades, $q = \ell N$.

After the derivatives with respect to φ_R, θ_{Po} and ξ_P are taken, Eq. (71) becomes, for $\rho_P < r_R$,

$$K_{PR} = \frac{N}{4\pi^2\rho_f U}\frac{\rho_P}{r_R\sqrt{1+a^2\rho_P^2}}\lim_{\delta_{PR}\to 0}\sum_{\substack{m_3=-q\\ m_3=\lambda_3-q}}^{\infty}\left\{\begin{matrix}(-1) & \text{for } z_R>0)\\ (-1)^{m_3} & \text{for } z_R<0)\end{matrix}\right\}_{m_3} e^{-im_3(\Omega t-\theta_{Po})}$$

$$\cdot\left\{\pi\left[a^2 q-\frac{m_3}{\rho_P^2}\right]e^{-iaq(x_R-\xi_P)} I_{m_3}(aq\rho_P)\, K_{m_3}(aqr_R)\right.$$

$$+ia\int_{-\infty}^{\infty}\frac{k I_{m_3}(|k|\rho_P)K_{m_3}(|k|r_R)^{ik(x_R-\xi_P)}dk}{k+aq}$$

$$\left.+i\frac{m_3}{\rho_P^2}\int_{-\infty}^{\infty}\frac{I_{m_3}(|k|\rho_P)K_{m_3}(|k|r_R)e^{ik(x_R-\xi_P)}dk}{k+aq}\right\} \qquad (72)$$

where

$$\begin{aligned}\theta_{Po} &= \sigma^\rho - \theta_b^\rho\cos\theta_\alpha\\ x_R &= x_o + \varepsilon_R^r - C_R^r\cos\varphi_\alpha\\ \delta_{PR} &= \xi_P - \theta_{Po}/a\\ C_R^r &= \text{semichord of rudder at control point}\end{aligned} \qquad (73)$$

If $\rho_P > r_R$, ρ_P and r_R are interchanged in the modified Bessel functions.

This is the case when $r_R = z_R = 0$ and $\rho_P > 0$, in which case there is no singularity.

The expansion scheme has again introduced a Cauchy-type singularity in the k-integration. In addition, examination of the original kernel (Eq. 68), before the expansion of 1/R, reveals a singularity when $\rho_P = r_R$ and $\tau = 0$, which can occur since $x_R - \xi_P > 0$. Appendix C demonstrates that this singularity is also present in the infinite m_3-series of Eq. (72) and that it is a high-order singularity.

After substitution of (73) in (72), application of the lift operators and introduction of the Birnbaum distribution, the θ_α- and φ_α-integrations are performed. Equation (67) then becomes

$$I_3 = \frac{1}{\pi^2}\int_0^\pi\int_0^\pi r_o\int_{\rho_P}^{\infty}\sum_{\lambda_3=0}^{\infty}\sum_{\bar{m}=1}^{\bar{n}}\sum_{\bar{n}} L_P^{(\lambda_3,\bar{n})}(\rho_P)e^{i\lambda_3\Omega t}K_{PR}(m_3=\lambda_3-q)\frac{\sqrt{1+a^2\rho_P^2}}{a\rho_P}$$

$$\cdot\Theta(\bar{n})\Phi(\bar{m})\sin\theta_\alpha d\theta_\alpha d\varphi_\alpha d\rho_P$$

$$= r_o\int_{\rho_R}^{\infty}\sum_{\lambda_3=0}^{\infty}\sum_{\bar{m}=1}^{\bar{n}}\sum_{\bar{n}} L_P^{(\lambda_3,\bar{n})}(\rho_P)e^{iq\Omega t}\bar{K}_{PR}^{(\bar{m},\bar{n})}(m_3=\lambda_3-q)\,d\rho_P \qquad (74)$$

where $\Phi(\bar{m})$ and $\Theta(\bar{n})$ are given by (24) and (25), and ρ_P is a fraction of r_o. The modified kernel function becomes

$$\bar{K}_{PR}^{(\bar{m},\bar{n})}(m_3=\lambda_3-q) = \frac{N}{4\pi^2\rho_f U r_o^2}\,\frac{1}{ar_R}\begin{cases}(-1) & \text{for } z_R>0\\ (-1)^{m_3} & \text{for } z_R<0\end{cases} m_3 e^{im_3\sigma^\rho}$$

$$\cdot\left\{\pi\left[a^2q-\frac{m_3}{\rho_P^2}\right]e^{-iaq(x_o+\epsilon_R^r-\sigma^\rho/a)}I_{m_3}(aq\rho_P)K_{m_3}(aqr_R)I^{(\bar{m})}(aqC_R^r)\Lambda^{(\bar{n})}((m_3+q)\theta_b^\rho)\right.$$

$$+ia\int_{-\infty}^{\infty}\frac{kI_{m_3}(|k|\rho_P)K_{m_3}(|k|r_R)e^{ik(x_o+\epsilon_R^r-\sigma^\rho/a)}}{k+aq}I^{(\bar{m})}(-kC_R^r)\Lambda^{(\bar{n})}((m_3-\tfrac{k}{a})\theta_b^\rho)\,dk$$

$$\left.+i\frac{m_3}{\rho_P^2}\int_{-\infty}^{\infty}\frac{I_{m_3}(|k|\rho_P)K_{m_3}(|k|r_R)e^{ik(x_o+\epsilon_R^r-\sigma^\rho/a)}}{k+aq}I^{(\bar{m})}(-kC_R^r)\Lambda^{(\bar{n})}((m_3-\tfrac{k}{a})\theta_b^\rho)\,dk\right\} \qquad (75)$$

for $\rho_P < r_R$, evaluated at $m_B = \lambda_3 - q$, with q a multiple of N. All dimensions within the brace are fractions of propeller radius r_o and $a = r_o\Omega/U$. Again, the first k-integral may be simplified for the numerical solution, by substituting

$$\frac{k}{k+aq} = 1 - \frac{aq}{k+aq} \tag{76}$$

Appendix D evaluates the integrands of Eq. (75) at $k = -aq$. The integration with respect to k is performed by Simpson's method.

The loading amplitude for harmonic λ_3 is assumed constant over each elemental strip into which the propeller radius is divided, and the kernel evaluated at $m_B = \lambda_3 - q$ is integrated over the strip by any appropriate numerical method. In the region where ρ_P approaches r_R, a numerical scheme is used which avoids the point $\rho_P = r_R$. This is justified by the fact that although the infinite m_B-series of Eq. (72) has a high-order singularity, each term does not and only a discrete number of these terms are used.

The Kernel K_{RR}

When both control and loading points are on the rudder, as in the second surface integral of Eq. (2), I_4, the self-induced velocity is (cf. Ref. 7 for the case of a finite foil)

$$\begin{aligned} I_4 &= \iint_{S_R} \sum_{\lambda_4=0}^{\infty} L_R'^{(\lambda_4)}(\xi_R,0,\zeta_R) e^{i\lambda_4\Omega t} K_{RR}(x_R,0,z_R;\xi_R,0,\zeta_R;\lambda_4)\, dS_R \\ &= \int_{-C_R}^{C_R}\int_{\zeta_R} \sum_{\lambda_4=0}^{\infty} L_R'^{(\lambda_4)}(\xi_R,0,\zeta_R) e^{i\lambda_4\Omega t} K_{RR}\, d\xi_R' d\zeta_R \\ &= \int_0^{\pi}\int_{\zeta_R} \sum_{\lambda_4=0}^{\infty} L_R^{(\lambda_4)}(\xi_R,0,\zeta_R) e^{i\lambda_4\Omega t} K_{RR} \sin\theta_\alpha\, d\theta_\alpha\, d\zeta_R \end{aligned} \tag{77}$$

where

$$\xi_R = x_o + \epsilon_R^\rho + \xi_R'$$

$$\xi_R' = -C_R^\rho \cos\theta_\alpha$$

$$x_R = x_o + \epsilon_R^r - C_R^r \cos\varphi_\alpha$$

$$L_R = C_R^\rho L_R'$$

and the kernel K_{RR} is, in Cartesian coordinates,

$$K_{RR} = -\frac{1}{4\pi\rho_f U} \lim_{\delta_{RR}\to 0} \left(-\frac{\partial^2}{\partial y_R^2}\right) \int_{-\infty}^{x_R} \frac{e^{i\lambda_4 a(\tau'-x_R)}}{R} d\tau' \tag{78}$$

where

$$R = \left[(\tau'-\xi_R)^2 + r_R^2\right]^{\frac{1}{2}}$$

$$r_R^2 = (y_R-\eta_R)^2 + (z_R-\zeta_R)^2$$

$$\delta_{RR} = y_R - \eta_R$$

(The subscripts will be omitted in the following discussion.)

The reciprocal of the Descartes distance R can be expressed as

$$\frac{1}{R} = \frac{1}{\pi} \int_{-\infty}^{\infty} K_o(|k|r) e^{ik(\tau'-\xi)} dk \tag{79}$$

where $K_o(\ )$ is the modified Bessel function of order zero. It is clear from Eqs. (2), (77), (78) and (79) that if the time-dependent expressions of the left- and right-hand sides of Eq. (2) are equated

$$\lambda_4 = q \tag{80}$$

Then the kernel can be written as

$$K_{RR} = -\frac{1}{4\pi^2\rho_f U} \lim_{\delta\to 0} \left(-\frac{\partial^2}{\partial y^2}\right) \int_{-\infty}^{x} e^{iqa(\tau'-x)} d\tau' \int_{-\infty}^{\infty} K_o(|k|r) e^{ik(\tau'-\xi)} dk \tag{81}$$

The τ'-integration involves

$$\int_{-\infty}^{x} e^{i(qa+k)\tau'} d\tau' = \pi\delta(k+qa) - \frac{ie^{i(k+qa)x}}{k+qa} \tag{82}$$

The k-integration then becomes

$$I_k = \int_{-\infty}^{\infty} K_o(|k|r)e^{-i\xi k}\left\{\pi\delta(k+qa) - \frac{ie^{i(k+qa)x}}{k+qa}\right\} dk$$

$$= \pi K_o(qar)e^{iqa\xi} - ie^{iqax}\int_{-\infty}^{\infty} \frac{K_o(|k|r)e^{ik(x-\xi)}}{k+qa} dk \tag{83}$$

which has an integrable Cauchy-type singularity. After the y-derivatives and the limit are taken, with

$$\frac{\partial^2 I_k}{\partial y^2} = \frac{\partial^2 r}{\partial y^2}\frac{\partial I_k}{\partial r} + \left(\frac{\partial r}{\partial y}\right)^2 \frac{\partial^2 I_k}{\partial r^2}$$

and

$$\lim_{(y-\eta)\to 0} \left(-\frac{\partial^2 I_k}{\partial y^2}\right) = \frac{-1}{r}\frac{\partial I_k}{\partial r}$$

K_{RR} becomes

$$K_{RR} = -\frac{1}{4\pi\rho_f U z_o^2}\left\{qaz_o K_1(qaz_o)e^{-iqa(x-\xi)}\right.$$

$$\left. - \frac{iz_o}{\pi}\int_{-\infty}^{\infty} \frac{|k| K_1(|k|z_o)e^{ik(x-\xi)}}{k+aq} dk\right\} \tag{84}$$

where $z_o = |z - \zeta|$.

When $z_o = 0$, the terms within the brace of (84) reduce to

$$\left\{e^{-iqa(x-\xi)} - \frac{i}{\pi}\int_{-\infty}^{\infty} \frac{e^{ik(x-\xi)}}{k+aq} dk\right\} = e^{-iqa(x-\xi)}\left[1 + \operatorname{sgn}(x-\xi)\right]$$

$$= e^{-iqa(x-\xi)}\begin{cases} 2 \text{ when } (x-\xi) > 0 \\ 0 \text{ when } (x-\xi) < 0 \end{cases} \tag{85}$$

Therefore, the kernel K_{RR} has a high-order singularity when $z \to \zeta$ and $(x-\xi) > 0$. Equation (85) demonstrates the well-known step behavior of the kernel function as $x = x-\xi \to 0^{\pm}$,

When $q = 0$, the kernel is

$$K_{RR}(q=0) = -\frac{1}{4\pi\rho_f U z_o^2}\left\{1 - \frac{iz_o}{\pi}\int_{-\infty}^{\infty} \frac{|k| K_1(|k| z_o) e^{ik(x-\xi)}}{k}\, dk\right\}$$

$$= -\frac{1}{4\pi\rho_f U z_o^2}\left\{1 + \frac{2z_o}{\pi}\int_0^{\infty} K_1(|k| z_o)\sin k x_o\, dk\right\} \tag{86}$$

If the Birnbaum mode shapes are used for the chordwise rudder loading distribution and the generalized lift operators are applied to Eq.(2), the second integral of that equation becomes

$$I_4 = \int_{\zeta_R} \sum_{q=0}^{\infty} e^{iq\Omega t} r_o \sum_{\bar{m}=1}^{\bar{n}} \sum_{\bar{n}} L_R^{(q,\bar{n})}(\zeta) \bar{K}_{RR}^{(\bar{m},\bar{n})}\, d\zeta_R \tag{87}$$

where

$$\bar{K}_{RR}^{(\bar{m},\bar{n})} = \frac{1}{\pi^2}\int_0^{\pi}\int_0^{\pi} \Theta(\bar{n})\, \Phi(\bar{m}) K_{RR} \sin\theta_\alpha\, d\theta_\alpha\, d\varphi_\alpha$$

$\Phi(\bar{m})$ and $\Theta(\bar{n})$ are as given by Eqs. (24) and (25) and ζ_R is nondimensionalized with respect to r_o.

For $q \neq 0$, and with z_o, C, ϵ_R and $1/a$ non-dimensionalized with respect to r_o,

$$\bar{K}_{RR}^{(\bar{m},\bar{n})} = -\frac{1}{4\pi\rho_f U r_o^2 z_o^2}\left\{qaz_o K_1(qaz_o) I^{(\bar{m})}(qaC^r)\Lambda^{(\bar{n})}(qaC^\rho) e^{-iqa(\epsilon_R^r - \epsilon_R^\rho)}\right.$$

$$\left. - \frac{i}{\pi}\int_{-\infty}^{\infty} \frac{|k| z_o K_1(|k| z_o) I^{(\bar{m})}(-kC^r)\Lambda^{(\bar{n})}(-kC^\rho) e^{ik(\epsilon_R^r - \epsilon_R^\rho)}}{k+qa}\, dk\right\} \tag{88}$$

and for $q = 0$,

$$\bar{K}_{RR}^{(\bar{m},\bar{n})}(q=0) = -\frac{1}{4\pi\rho_f U r_o^2 z_o^2}\left\{ I^{(\bar{m})}(0)\Lambda^{(\bar{n})}(0) - \frac{i}{\pi}\int_{-\infty}^{\infty} \frac{|k|}{k} z_o K_1(|k|z_o) I^{(\bar{m})}(-kc^r)\,\Lambda^{(\bar{n})}(-kc^\rho) \cdot e^{ik(\epsilon_R^r - \epsilon_R^\rho)}\, dk \right\} \qquad (89)$$

where $I^{(\bar{m})}(x)$ and $\Lambda^{(\bar{n})}(x)$ are defined in Eqs. (44) and (45).

Appendix E describes the treatment of the singular k-integral. The k-integration is again done by Simpson's rule.

The integration of $\bar{K}_{RR}^{(\bar{m},\bar{n})}$ over all elements of the rudder span except that which includes $z = \zeta$ is performed by the tangential method. In the region where $z_o = |z-\zeta| \to 0$, the integral has a high-order singularity. Its finite part is obtained by using a polynomial approximation of the modified Bessel function valid in a narrow range about $z_o = 0$, and a three-point Gaussian quadrature for the immediately adjacent ranges (see Appendix F).

The linearized unsteady lifting surface theory requires the rudder to be amidships (i.e., rudder angle $\delta = 0$) in which case the downwash distribution normal to the rudder $W_R^{(q,\bar{m})} = 0$, and hence from Eq. (2)

$$I_3 = -I_4 \quad .$$

Therefore, the time-dependent expressions of I_3 and I_4 must be equal, which dictates that

$$\lambda_4 = \lambda_3 - m_3 = q = \ell N \quad .$$

Thus, the rudder loading must be at blade frequency and multiples of blade frequency.

On the other hand, a non-zero rudder angle will affect the steady-state propeller-rudder interaction. In such case the rudder angle of attack gives rise to a resulting normal velocity $W_R^{(0,\bar{m})} \neq 0$.

SOLUTION OF THE PAIR OF INTEGRAL EQUATIONS

Direct Solution

On summarizing the results obtained in the preceding sections, one can write Eqs. (1) and (2), or equivalently, Eqs. (5) and (6) for given q (order of shaft frequency, or order of wake harmonic) and given $\bar{m}$ (order of lift operator) as follows.

Equation (1) or (5) is written as

$$\bar{W}_P^{(q,\bar{m})} = \sum_{m_1=0}^{\infty} \int_{\rho_P} L_P^{(q,\bar{n})} \bar{K}_{PP}^{(m_1,\bar{m},\bar{n})} d\rho_P$$

$$+ \sum_{\lambda_2=0}^{\infty} \int_{\zeta_R} L_R^{(\lambda_2,n)} \bar{K}_{RP}^{(m_2,\bar{m},\bar{n})} d\zeta_R \qquad (90)$$

where $m_1 = q + \ell_1 N$, $\ell_1 = 0, \pm 1, \pm 2, \ldots$

$m_2 = q - \lambda_2$

(It will be shown below that $\lambda_2 = \ell_2 N$, $\ell_2 = 0,1,2,\ldots$)

Equation (2) or (6), in the unsteady case, can be written as

$$0 = \sum_{\lambda_3=0}^{\infty} \int_{\rho_P} L_P^{(\lambda_3,\bar{n})} \bar{K}_{PR}^{(m_3,\bar{m},\bar{n})} d\rho_P$$

$$+ \int_{\zeta_R} L_R^{(\lambda_4,\bar{n})} \bar{K}_{RR}^{(1,\bar{m},\bar{n})} d\zeta_R \qquad (91)$$

where $\lambda_3 - m_3 = \ell N$, ℓ any non-zero integer.

It is shown in Appendix G that Eq. (91) is equivalent to

$$\sum_{\lambda_3=0}^{\infty} \int_{\rho_P} \left\{ L_P^{(\lambda_3,\bar{n})} \bar{K}_{PR}^{(\lambda_3-\ell_2 N,\bar{m},\bar{n})} + \text{conjugate} \left[L_P^{(\lambda_3,\bar{n})} K_{PR}^{(\lambda_3+\ell_2 N,\bar{m},\bar{n})} \right] \right\} d\rho_P$$

$$= - \int_{\zeta_R} L_R^{(\lambda_4=\ell_2 N)} \bar{K}_{RR}^{(1,\bar{m},\bar{n})} d\zeta_R \qquad (91)$$

where $\ell_2 = +1, +2, \ldots\ldots$ Since $\lambda_4 = \ell_2 N$, λ_2 in Eq. (90) is limited to multiples of blade number only.

In the steady state case, $\lambda_4 = \lambda_3 - m_B = 0$, Eq. (2) or (6) can be written

$$\bar{W}_R^{(0,\bar{m})} = \sum_{\lambda_3=0}^{\infty} \int_{\rho_P} L_P^{(\lambda_3,\bar{n})} \bar{K}_{PR}^{(\lambda_3,\bar{m},\bar{n})} \, d\rho_P + \int_{\zeta_R} L_R^{(0,\bar{n})} \bar{K}_{RR}^{(1,\bar{m},\bar{n})} \, d\zeta_R \tag{92}$$

where $\bar{W}_R^{(0,\bar{m})}$ is the normal velocity component, equal to $U\delta\, I^{(\bar{m})}(0)$, δ is rudder angle and $I^{(\bar{m})}(0) = 1$ for $\bar{m} = 1, 2$ and zero otherwise.

It is seen that the propeller loading is affected by all harmonics of the inflow field (hull wake), whereas the rudder loading occurs only at blade frequency and multiples thereof. The propeller is exposed to all harmonic constituents of the wake, but through the mechanism of its cyclic motion, it acts as a filter so that those harmonics not at blade frequencies do not act on the rudder. It appears that this filtering mechanism will affect the loading of any appendage located in the neighborhood of an operating propeller. In a study at Davidson Laboratory of the propeller-duct interaction[14] (at present in the computational stage), it is seen that the duct responds only to components at blade frequency and multiples of blade frequency although the propeller is influenced by all harmonic components of the inflow field.

It should be remarked that the resultant integral equations for the propeller and rudder loadings are frequency coupled. A large number of frequency components of the loadings of both lifting surfaces participate in the interaction problem even at one given frequency of the inflow. For instance, if a three-bladed propeller is considered and propeller loading is evaluated up to blade-frequency-plus-one (i.e., $q = 0,1,2,3,4$) and the rudder loading is evaluated at $\lambda_3 = 0, 3$ only, it is seen that seven unknown loadings are present in the set of integral equations. If, in addition, each loading is expressed in terms of $\bar{n} = 3$ Birnbaum modes, the unknowns are increased to $7 \times 3 = 21$. There are available two equations. The required 21 can be achieved through the concept of lift operator. However, the lift operator approach in conjunction with the collocation method brings the total of simultaneous algebraic equations to an extremely

high number. Although this direct approach is feasible, it is impractical.

An iterative procedure is therefore suggested which is on the one hand physically plausible, and on the other, computationally advantageous.

The Iteration Procedure

It is assumed initially that the effect of rudder on propeller is small and, hence, that the second term of Eq. (90) can be neglected.

The first approximation of propeller loading $L_{P0}^{(q,\bar{n})}$ at any frequency $q = 0,1,2 \ldots , N, N+1, \ldots$ is evaluated from Eq. (90) by the numerical method of References 6 and 7. The substitution of these loadings into Eq. (91) reduces the latter to an integral equation with unknown $L_{R1}^{(\lambda_3 N,\bar{n})}$ which can be solved for each $\lambda_3 = 0,1,2 \ldots$

Upon substituting the loadings $L_{R1}^{(0,\bar{n})}$, $L_{R1}^{(N,\bar{n})}$, $L_{R1}^{(2N,\bar{n})}$ ... into Eq. (90), the second approximation of the propeller loading $L_{P1}^{(q,\bar{n})}$ will be obtained for arbitrary q . If L_{P1} values are different from L_{P0} , a new iteration is started with L_{P1} as input into Eq. (91), and so on. When the rudder is not amidships (i.e., $\delta \neq 0$), the solution $L_R^{(0,\bar{n})}$ from Eq. (92) is used in the iteration for the steady-state value.

The procedure is illustrated below for a three-bladed propeller (curtailing the infinite series, i.e., $\lambda_3 = 0,3$ and λ_3 and $q = 0,1,2,3,4$)

0-Iteration

$$L_{P0}^{(0,\bar{n})} = \bar{W}_P^{(0,\bar{m})}\left[\bar{K}_{PP}^{(\bar{m},\bar{n})}(q=0)\right]^{-1}$$

$$L_{P0}^{(1,\bar{n})} = \bar{W}_P^{(1,\bar{m})}\left[\bar{K}_{PP}^{(\bar{m},\bar{n})}(q=1)\right]^{-1}$$

$$L_{P0}^{(2,\bar{n})} = \bar{W}_P^{(2,\bar{m})}\left[\bar{K}_{PP}^{(\bar{m},\bar{n})}(q=2)\right]^{-1}$$

$$L_{P0}^{(3,\bar{n})} = \bar{W}_P^{(3,\bar{m})}\left[\bar{K}_{PP}^{(\bar{m},\bar{n})}(q=3)\right]^{-1}$$

$$L_{P0}^{(4,\bar{n})} = \bar{W}_P^{(4,\bar{m})}\left[\bar{K}_{PP}^{(\bar{m},\bar{n})}(q=4)\right]^{-1}$$

$$L_{R1}^{(0,\bar{n})} = \left\{\bar{U\delta} - L_{P0}^{(0,\bar{n})}\bar{K}_{PR}^{(0,\bar{m},\bar{n})} - L_{P0}^{(1,\bar{n})}\bar{K}_{PR}^{(1,\bar{m},\bar{n})} - L_{P0}^{(2,\bar{n})}\bar{K}_{PR}^{(2,\bar{m},\bar{n})} - L_{P0}^{(3,\bar{n})}\bar{K}_{PR}^{(3,\bar{m},\bar{n})} - L_{P0}^{(4,\bar{n})}\bar{K}_{PR}^{(4,\bar{m},\bar{n})}\right\}\left[\bar{K}_{RR}(q=0)\right]^{-1}$$

$$L_{R1}^{(3,\bar{n})} = -\left\{L_{P0}^{(0,\bar{n})}\bar{K}_{PR}^{(-3,\bar{m},\bar{n})} + L_{P0}^{(1,\bar{n})}\bar{K}_{PR}^{(-2,\bar{m},\bar{n})} + L_{P0}^{(2,\bar{n})}\bar{K}_{PR}^{(-1,\bar{m},\bar{n})} + L_{P0}^{(3,\bar{n})}\bar{K}_{PR}^{(0,\bar{m},\bar{n})} + L_{P0}^{(4,\bar{n})}\bar{K}_{PR}^{(1,\bar{m},\bar{n})}\right\}\left[\bar{K}_{RR}(q=3)\right]^{-1}$$

$$\text{-conj.}\left\{L_{P0}^{(o,\bar{n})}\bar{K}_{PR}^{(3,\bar{m},\bar{n})} + L_{P0}^{(1,\bar{n})}\bar{K}_{PR}^{(4,\bar{m},\bar{n})} + \text{--} + L_{P0}^{(4,\bar{n})}\bar{K}_{PR}^{(7,\bar{m},\bar{n})}\right\}\left[\bar{K}_{RR}^{(q=3)}\right]^{-1}$$

where

$$\bar{K}_{PP}^{(\bar{m},\bar{n})} = \sum_{m_1=0}^{\infty} \bar{K}_{PP}^{(m_1,\bar{m},\bar{n})}$$

$$m_1 = q + \ell_1 N \qquad \ell_1 = 0, \pm 1, \pm 2, \ldots$$

$$\bar{U\delta} = U\delta\, I^{(\bar{m})}(0)$$

1-Iteration

$$L_{P1}^{(0,\bar{n})} = \left\{\bar{W}_P^{(0,\bar{m})} - L_{R1}^{(0,\bar{n})}\bar{K}_{RP}^{(0,\bar{m},\bar{n})} - L_{R1}^{(3,\bar{n})}\bar{K}_{RP}^{(-3,\bar{m},\bar{n})}\right\}\left[\bar{K}_{PP}^{(\bar{m},\bar{n})}(q=0,)\right]^{-1}$$

$$L_{P1}^{(1,\bar{n})} = \left\{\bar{W}_P^{(1,\bar{m})} - L_{R1}^{(0,\bar{n})}\bar{K}_{RP}^{(1,\bar{m},\bar{n})} - L_{R1}^{(3,\bar{n})}\bar{K}_{RP}^{(-2,\bar{m},\bar{n})}\right\}\left[\bar{K}_{PP}^{(\bar{m},\bar{n})}(q=1)\right]^{-1}$$

$$L_{P1}^{(2,\bar{n})} = \left\{\bar{W}_P^{(2,m)} - L_{R1}^{(0,\bar{n})}\bar{K}_{RP}^{(2,\bar{m},\bar{n})} - L_{R1}^{(3,\bar{n})}\bar{K}_{RP}^{(-1,\bar{m},\bar{n})}\right\}\left[\bar{K}_{PP}^{(\bar{m},\bar{n})}(q=2)\right]^{-1}$$

$$L_{P1}^{(3,\bar{n})} = \left\{\bar{W}_P^{(3,\bar{m})} - L_{R1}^{(0,\bar{n})}\bar{K}_{RP}^{(3,\bar{m},\bar{n})} - L_{R1}^{(3,\bar{n})}\bar{K}_{RP}^{(0,\bar{m},\bar{n})}\right\}\left[\bar{K}_{PP}^{(\bar{m},\bar{n})}(q=3)\right]^{-1}$$

$$L_{P1}^{(4,\bar{n})} = \left\{\bar{W}_P^{(4,\bar{m})} - L_{R1}^{(0,\bar{n})}\bar{K}_{RP}^{(4,\bar{m},\bar{n})} - L_{R1}^{(3,\bar{n})}\bar{K}_{RP}^{(1,\bar{m},\bar{n})}\right\}\left[\bar{K}_{PP}^{(\bar{m},\bar{n})}(q=4)\right]^{-1}$$

$$L_{R2}^{(0,\bar{n})} = \left\{\overline{U\delta} - L_{P1}^{(0,\bar{n})}\bar{K}_{PR}^{(0,\bar{m},\bar{n})} - L_{P1}^{(1,\bar{n})}\bar{K}_{PR}^{(1,\bar{m},\bar{n})} - L_{P1}^{(2,\bar{n})}\bar{K}_{PR}^{(2,\bar{m},\bar{n})} - L_{P1}^{(3,\bar{n})}\bar{K}_{PR}^{(3,\bar{m},\bar{n})} - L_{P1}^{(4,\bar{n})}\bar{K}_{PR}^{(4,\bar{m},\bar{n})}\right\}\left[\bar{K}_{RR}(q=0)\right]^{-1}$$

$$L_{R2}^{(3,\bar{n})} = -\left\{L_{P1}^{(0,\bar{n})}\bar{K}_{PR}^{(-3,\bar{m},\bar{n})} + L_{P1}^{(1,\bar{n})}\bar{K}_{PR}^{(-2,\bar{m},\bar{n})} + L_{P1}^{(2,\bar{n})}\bar{K}_{PR}^{(-1,\bar{m},\bar{n})} + L_{P1}^{(3,\bar{n})}\bar{K}_{PR}^{(0,\bar{m},\bar{n})} + L_{P1}^{(4,\bar{n})}\bar{K}_{PR}^{(1,\bar{m},\bar{n})}\right\}\left[\bar{K}_{RR}(q=3)\right]^{-1}$$

$$-\text{conj.}\left\{L_{Pl}^{(o,\bar{n})}\bar{K}_{PR}^{(3,\bar{m},\bar{n})}+L_{Pl}^{(1,\bar{n})}\bar{K}_{PR}^{(4,\bar{m},\bar{n})}+\cdots+L_{Pl}^{(4,\bar{n})}\bar{K}_{PR}^{(7,\bar{m},\bar{n})}\right\}\left[\bar{K}_{RR}^{(q=3)}\right]^{-1}$$

The final values of $L_P^{(q,\bar{n})}$ and $L_R^{(q,\bar{n})}$ are used to determine the spanwise loading distributions, which follow from Eq. (25).

$$L_P^{(q)}(r) = \int_o^\pi L_P^{(q)}(r,\theta_o)\sin\theta_\alpha d\theta_\alpha$$

$$= \frac{1}{\pi}\int_o^\pi L_P^{(q,1)}(r)(1+\cos\theta_\alpha)d\theta_\alpha + \frac{1}{\pi}\sum_{\bar{n}=2}^{\infty}\int_o^\pi L_P^{(q,\bar{n})}(r)\sin(\bar{n}-1)\theta_\alpha\sin\theta_\alpha d\theta_\alpha$$

$$= L_P^{(q,1)}(r) + \frac{1}{2}L_P^{(q,2)}(r) \qquad (93)$$

and similarly

$$L_R^{(q)}(z) = \frac{1}{\pi}\int_o^\pi L_R^{(q,1)}(z)(1+\cos\theta_\alpha)d\theta_\alpha$$

$$+\frac{1}{\pi}\sum_{\bar{n}=2}^{\infty}\int_o^\pi L_R^{(q,\bar{n})}(z)\sin(\bar{n}-1)\theta_\alpha\sin\theta_\alpha d\theta_\alpha$$

$$= L_R^{(q,1)}(z) + \frac{1}{2}L_R^{(q,2)}(z) \qquad (94)$$

HYDRODYNAMIC FORCES AND MOMENTS

Propeller-Generated Forces and Moments

The principal components of the propeller-induced forces and moments are shown in Figure 4 and listed below:

Forces: F_x = thrust (x-direction)

F_y and F_z = horizontal and vertical components, respectively, of the bearing forces

Moments: Q_x = torque about the x-axis

Q_y and Q_z = bending moments about the y- and z-axis, respectively

The elementary forces and moments of the various components can be determined by resolving the loading force $L_p^{(q)}(r)$ acting on an elementary radial strip, normal to the strip, and taking the corresponding moments about any axis. The forces acting on a strip at radius r of the N-bladed propeller will be given by (cf. Ref. 15)

$$\Delta F_x = \sum_{n=1}^{N} L_p^{(q)}(r)\, e^{iq(\Omega t+\bar{\theta}_n)} \cos\theta_p(r)\, \Delta r$$

$$\Delta F_y = \sum_{n=1}^{N} L_p^{(q)}(r)\, e^{iq(\Omega t+\bar{\theta}_n)} \sin\theta_p(r)\cos(\Omega t+\bar{\theta}_n)\, \Delta r$$

$$\Delta F_z = \sum_{n=1}^{N} L_p^{(q)}(r)\, e^{iq(\Omega t+\bar{\theta}_n)} \sin\theta_p(r)\sin(\Omega t+\bar{\theta}_n)\, \Delta r$$

where $\theta_p(r)$ is the geometric pitch angle. Since

$$\sum_{n=1}^{N} e^{iq\bar{\theta}_n} = \begin{cases} N & \text{when } q = \ell N\ ,\ \ell = 0,1,2,\ \ldots \\ 0 & \text{when } q \neq \ell N \end{cases}$$

and

$$\sum_{n=1}^{N} e^{i(q\pm 1)\bar{\theta}_n} = \begin{cases} N & \text{when } q = \ell N \mp 1 \\ 0 & \text{when } q \neq \ell N \mp 1 \end{cases}$$

the total forces at frequency ℓN acting on the N-bladed propeller will

be given by

$$F_x = \mathrm{Re}\left\{Nr_o e^{i\ell N\Omega t}\int_0^1 L_P^{(\ell N)}(r)\cos\theta_p(r)dr\right\} \tag{95}$$

$$F_y = \mathrm{Re}\left\{\frac{Nr_o}{2} e^{i\ell N\Omega t}\int_0^1\left[L_P^{(\ell N-1)}(r)+L_P^{(\ell N+1)}(r)\right]\sin\theta_p(r)dr\right\} \tag{96}$$

$$F_z = \mathrm{Re}\left\{\frac{Nr_o}{2i} e^{i\ell N\Omega t}\int_0^1\left[L_P^{(\ell N-1)}(r)-L_P^{(\ell N+1)}(r)\right]\sin\theta_p(r)dr\right\} \tag{97}$$

(with the sign convention adopted in the present investigation).

The moments are determined by

$$Q_x = -\mathrm{Re}\left\{Nr_o^2 e^{i\ell N\Omega t}\int_0^1 L_P^{(\ell N)}(r)\sin\theta_p(r)rdr\right\} \tag{98}$$

$$Q_y = \mathrm{Re}\left\{\frac{Nr_o^2}{2} e^{i\ell N\Omega t}\int_0^1\left[L_P^{(\ell N-1)}(r)+L_P^{(\ell N+1)}(r)\right]\cos\theta_p(r)rdr\right\} \tag{99}$$

$$Q_z = \mathrm{Re}\left\{\frac{Nr_o^2}{2i} e^{i\ell N\Omega t}\int_0^1\left[L_P^{(\ell N-1)}(r)-L_P^{(\ell N+1)}(r)\right]\cos\theta_p(r)rdr\right\} \tag{100}$$

It may be observed from the foregoing that the propeller-generated transverse forces and bending moments are evaluated from propeller loadings associated with wake harmonics at frequencies adjacent to blade frequency, i.e., at $q = \ell N \pm 1$, whereas the thrust and torque are determined by the loading at blade frequency. The steady-state thrust and torque are determined at zero frequency; the corresponding mean transverse forces and bending moments are determined at shaft frequency.

Rudder Forces and Moments

The side force on the rudder at any frequency $q = \ell N$ is simply

$$F_R = r_o\int_z L_R^{(q)}(z)dz \tag{101}$$

where $L_R^{(q)}(z)$ is given by Eq. (94).

The moment about the rudder stock is obtained from

$$M_R = \frac{r_o^2}{\pi} \int_z \int_0^{\pi} \left\{ L_R^{(q,1)}(z)\,(1+\cos\theta_\alpha) + \sum_{\bar{n}=2} L_R^{(q,\bar{n})}(z) \sin(\bar{n}-1)\theta_\alpha \sin\theta_\alpha \right\} \left[\epsilon_R - C_R \cos\theta_\alpha \right] \cdot d\theta_\alpha dz$$

where $\left[\epsilon_R - C_R \cos\theta_\alpha \right]$ is the moment arm. Then

$$M_R = r_o^2 \int_z \epsilon_R \left[L_R^{(q,1)}(z) + \frac{1}{2} L_R^{(q,2)}(z) \right] dz$$

$$- \frac{r_o^2}{\pi} \int_z C_R \int_0^{\pi} \left\{ L_R^{(q,1)}(z)\,(1+\cos\theta_\alpha)\cos\theta_\alpha + \sum_{\bar{n}=2} L_R^{(q,\bar{n})}(z) \sin(\bar{n}-1)\theta_\alpha \sin\theta_\alpha \cos\theta_\alpha \right\} \cdot d\theta_\alpha dz$$

With

$$\frac{1}{\pi} \int_0^{\pi} (1 + \cos\theta_\alpha)\cos\theta_\alpha d\theta_\alpha = 1/2$$

and

$$\frac{1}{\pi} \int_0^{\pi} \sin(\bar{n}-1)\theta_\alpha \sin\theta_\alpha \cos\theta_\alpha d\theta_\alpha$$

$$= \frac{1}{2\pi} \int_0^{\pi} \sin(\bar{n}-1)\theta_\alpha \sin 2\theta_\alpha d\theta_\alpha$$

$$= \begin{cases} 0 & \text{for } (\bar{n}-1) \neq 2 \\ \frac{1}{4} & \text{for } (\bar{n}-1) = 2 \end{cases}$$

the moment becomes

$$M_R = r_o^2 \int_z \left\{ \epsilon_R \left[L_R^{(q,1)}(z) + \frac{1}{2} L_R^{(q,2)}(z) \right] - C_R \left[\frac{1}{2} L_R^{(q,1)}(z) + \frac{1}{4} L_R^{(q,3)}(z) \right] \right\} dz \qquad (102)$$

(Note that ϵ_R, C_R and z are fractions of r_o .)

NUMERICAL RESULTS

A numerical procedure has been developed and adapted to a high-speed digital computer which yields a numerical solution of the propeller-rudder interaction problem. The solution evaluates (a) the steady and time-dependent pressure distributions on both lifting surfaces, propeller and rudder, and (b) the steady and time-dependent hydrodynamic forces and moments on the propeller (three forces and three moments) and on the rudder (side force and rudder-stock moment).

The expressions for the kernel functions given by Eqs. (39),(41), (46),(64),(75), and (88) and the pair of integral Equations (90) and (91) or (92) constitute the desired working forms. The computer program prepares all the necessary information for the application and execution of the suggested iteration procedure.

It is a lengthy program, the duration depending on the number of propeller blades, on the number of selected chordwise modes and on the harmonic constituents of the hull wake. In fact, the latter influences the decision as to a proper truncation of the harmonic series of the loading functions on both lifting surfaces.

The information required as input to the program is divided into two main categories: the geometry of both lifting surfaces including their relative positions, and the velocity survey of the inflow field. The geometrical information is readily available, in the form of detailed drawings, from which measurements can be taken, if not of more accurate tabulated data. Unfortunately, detailed wake surveys (wake in the absence of propeller and rudder) are scarce.

Primarily to test the developed program and to find out the number of iterations necessary to attain a stable solution and also to obtain an estimate of the time required for computation, a numerical example was worked out for a 3-bladed propeller and a thin rectangular rudder, both immersed in an inflow field defined by an available wake survey for a

surface ship. This is an artificial case, i.e., the combination of ship, rudder and propeller is not an actual one. A 3-bladed propeller was chosen for this pilot example to cut down on computer time. For this reason also, the number of chordwise modes was limited to five. It had become apparent in preliminary calculations that this number was the minimum which could fairly represent the loadings on both lifting surfaces.

The propeller was the NSRDC propeller 4118 (see Refs. 15 and 16) with the following particulars,

number of blades, $N = 3$

propeller radius, $r_o = 0.5$ ft.

expanded area ratio, $EAR = 0.6$

pitch-diameter ratio, $P/D = 1.077$

design advance ratio, $J = \frac{U}{nD} = 0.831$ where $U = 12.465$ f.p.s.

The particulars for the thin rectangular rudder were, with reference to the propeller-rudder arrangement shown in Fig. 1,

$C_R = 0.562\ r_o$

$b_u = 1.025\ r_o$

$b_\ell = .975\ r_o$

$\epsilon_R = .337\ r_o$

$x_o = .35\ r_o$

rudder angle, $\delta = -0.1$ radian (to starboard). The wake survey was that measured in the propeller plane behind the Mod V hull of NSRDC Model 4423-2 (for details see Ref. 17) with high third and fourth harmonics of the wake components. The 3-blade propeller thus is assumed to operate in the wake of a ship which requires a propeller of at least 4 blades.

Although this artificial example was attempted primarily to test the numerical procedure, certain conclusions of a general type can be drawn about trends. Results of the calculations are exhibited graphically in Figs. 5 to 10.

Figures 5 to 7 present the values of all hydrodynamic forces and moments in terms of iteration number. Attention is called to the fact that "zero iteration" identifies the condition where the propeller loading is determined in the absence of the rudder and the rudder loading is determined in the presence of the propeller. It is seen that four iterations are sufficient to bring all hydrodynamic forces and moments, steady and unsteady, to their final values.

The calculations indicate that the presence of a thin rudder has negligible effect on the mean thrust and torque, which confirms the conclusion of Ref. 18. In contrast the rudder has a large effect on the steady propeller transverse forces and bending moments. The presence of the rudder also has considerable effect on the propeller vibratory forces and moments. It will be seen later that the percentage variation up or down depends on the particular case as well as on rudder angle.

In Fig. 7 the mean rudder side force coefficient in the presence of the propeller is seen to be 0.29 at angle of attack δ = -0.1 radian. This compares with a value of 0.296 obtained from aerodynamic theory for a wing of the same aspect ratio 1.78, without propeller. On the other hand, the vibratory rudder force and moment, which should be zero in the absence of a propeller, are shown to be relatively large. Figures 8 and 9 show the spanwise distributions (amplitude and phases) of the mean rudder lift and rudder stock moment at δ = - 0.1 radian. Figure 10 shows the real and imaginary parts of the corresponding spanwise distributions of the vibratory force and moment.

After the success of the developed program in attaining a stable solution for the pilot example after only a few iterations, it was decided to apply the procedure to the actual case of the Mod V hull with its designed 4-blade propeller and rudder of aspect ratio 1.72, for three values of axial clearance between propeller and rudder, the designed clearance to the smallest possible clearance. Calculations have been made for a range of rudder angles from 0.3 radian to port to 0.3 radian to starboard. The theoretical development assumes, of course, that the ship is steering a straight course. There is a lag between the time when the rudder is first

thrown over and the time when it reaches its maximum angle, at which point the stern of the ship begins to swing. The calculated results for the various rudder angles therefore apply to the time interval before the rudder reaches its maximum and approximate the initial conditions of steering and turning.

The propeller is NSRDC No. 3376 with the following particulars:

$N = 4$

$r_o = 11$ ft

EAR = 0.499

P/D = 1.10

J = 0.726

U = 28.29 ft/sec

The particulars of the rudder, which again is assumed to have negligible thickness, are:

$C_R = .682\ r_o$

$b_u = 1.318\ r_o$

$b_\ell = 1.023\ r_o$

$\epsilon_R = .273\ r_o$

$x_o = \begin{cases} 0.8356\ r_o \text{ (design)} \\ 0.72\ r_o \text{ and} \\ 0.56\ r_o \end{cases}$

Tables I-VI show the amplitudes of the hydrodynamic forces and moments at the various iterations. When $x_o = 0.8356\ r_o$, stable values are reached in all cases after the third iteration. In the case of the smallest axial clearance, $x_o = 0.56\ r_o$, four iterations are required.

The calculations for the propeller hydrodynamic forces and moments show that the presence of the rudder has no effect on the mean thrust and torque and very little on the vibratory thrust and torque. The propeller transverse forces and bending moments, both steady and unsteady, show the

effects of rudder angle ($\delta \neq 0$). In the unsteady case these effects are more pronounced for $\tilde{F}_y$ and $\tilde{Q}_y$ than for $\tilde{F}_z$ and $\tilde{Q}_z$.

Figures 11-13 present the final values of the amplitudes and phases of mean and blade frequency propeller bearing forces and bending moments as functions of rudder angle δ. It is seen that when the rudder is on the centerline ($\delta = 0$) there is no effect of axial clearance x_o, but when $\delta \neq 0$ the generated forces and moments are larger for the smaller clearance.

Figure 14 shows the variation with rudder angle of mean rudder side force and rudder stock moment, as evaluated in the presence of the propeller by the present lifting surface theory, and without a propeller by the aerodynamic lifting line theory and by the semi-empirical formulas of Whicker and Fehlner[15]. (The calculated amplitudes are approximately the same for negative δ, with phases out by 180^o.) It is seen that, in contrast to the case of the 3-blade propeller behind the Mod V hull with small axial clearance between propeller and rudder, with the 4-blade propeller the rudder forces show a propeller effect and the effect is somewhat larger for smaller axial clearance.

Figure 15 presents the spanwise distributions of the mean rudder side force for the various rudder angles. The curves are similar in form to those derived from measurements in Ref. 11, which shows an asymmetrical distribution with respect to the propeller axis. In fact, for a rudder angle to port the distribution bulges above the axis, whereas for a rudder angle to starboard the bulge is in the lower section.

Figure 16 is a graph of the calculated amplitudes and phases of the blade-frequency rudder force and rudder stock moment versus rudder angle. The calculations show that in the unsteady case the axial clearance has a great effect, not only when the rudder is thrown over but also for $\delta = 0$, which was not the case for the steady rudder force and moment nor for all propeller forces and moments. As can be seen in the section on the iteration procedure, the rudder loadings (and hence forces and moments) depend on the products of propeller loading coefficients $L_P^{(m_3+q)}$ and the kernel functions $\bar{K}_{PR}^{(m_3)}$ defined by Eq. (75), which shows that $\bar{K}_{PR}^{(m_3)}$ varies

approximately as exp $(-iaq\ x_o)$. Here m_3 is the frequency of the space function and q is the shaft frequency. When $\delta = 0$ and $q = 0$, there is little influence of axial clearance x_o, either indirectly through the effect of rudder loading on propeller loading or directly through the kernel function. On the other hand, at blade frequency, $q = N$, there is a variation with axial clearance x_o which is oscillatory in nature, the period of the oscillation depending on number of blades N and inverse advance ratio $a = \pi/J$. Sugai[9] in his theoretical treatment implies this oscillation in the propeller-induced rudder force as a function of spacing distance, and the experimental data of Ref. (20) not only shows the oscillation but also that the wave length of oscillation is smaller for lower J. Lewis, in his experimental study[21], has also observed that the rudder is subjected to a periodic force depending on its position relative to the propeller (i.e. x_o), with period approximately equal to pitch divided by the number of blades.

Figure 17 presents the real and imaginary spanwise distributions of blade-frequency rudder force and moment for one axial clearance. The curves are for one rudder angle only; for the other rudder angles the curves are the same in form and only slightly different in magnitude. Comparison between the spanwise distributions in this case with 4-blade propeller and those shown in Fig. 10 for the case of a 3-blade propeller indicate why the integrated vibratory rudder force is so much smaller in the 4-blade case. In contrast to the distributions of Fig. 10, those in Fig. 17 above the propeller axis are opposite in sign to the distributions below the propeller axis and almost the same in magnitude. The explanation for this difference between the cases with 3- and 4-blade propellers can be found in an examination of the kernel function $\bar{K}_{PR}^{(-N,\bar{m},\bar{n})}$ which is the factor of $L_p^{(o,n)}$, the largest propeller loading contributor to the blade frequency rudder force (see under Iteration Procedure). In Eq. (75) it is seen that $\bar{K}_{PR}^{(-N,\bar{m},\bar{n})}$ has the factor (-1) for the rudder span above the propeller axis and $(-1)^{-N}$ below the propeller axis. When N is odd upper and lower distributions have the same sign, and when N is even opposite signs.

Another comparison of the two cases (3- and 4-blade propellers) for $\delta = -0.1$ yields the observation that the amplitudes of the mean K coefficients, which depend on the zero wake harmonic for thrust and torque and on the first wake harmonic for bearing forces and bending moments,

are only slightly different in both cases. The vibratory thrust and torque depend on the blade wake harmonic, and since the third and fourth harmonics of the wake are not too different in strength the blade frequency thrust and torque coefficients for 3- and 4-blade propellers are not far apart. On the other hand the coefficients of bearing force and bending moment depend on the (N-1) and(N+1) wake harmonics, in the 3-blade case on the second and fourth and in the 4-blade case on the third and fifth, and since the second wake harmonic for a hull symmetrical about the centerline is strong and the fifth is weak, the coefficients are larger for the 3-blade case than for the 4-blade.

Thus, although the number of calculations is limited, the results exhibit the importance of such parameters as axial clearance, number of blades and harmonic components of hull wake.

CONCLUSIONS

The problem of the unsteady hydrodynamic interference between a marine propeller and a rudder, when both thin lifting surfaces are located in the wake of a hull, has been studied theoretically and a numerical procedure adaptable to high-speed digital computer (CDC6600) has been developed for its solution. The theory demonstrates the filtering effect of the propeller on the harmonic constituents of the wake, an effect which results in a flow to the rudder of blade frequency and integer multiples of blade frequency. The numerical solution furnishes information about

a) the steady and time-dependent pressure distributions on both lifting surfaces,

b) the steady and unsteady components of all hydrodynamic forces and moments on both interacti..g surfaces.

The numerical solution provides means for a systematic study of the effects of all parameters, such as number of blades, geometry of both lifting surfaces, axial clearance and wake constituents. From the small number of calculations performed it is seen that the mean thrust and torque

are not affected by the presence of the rudder, in contrast to the corresponding vibratory components and to the steady and unsteady transverse forces and moments. The axial clearance plays an important role in evaluating both steady and unsteady hydrodynamic forces and moments on both lifting surfaces. The experimental evidence of Ref. 21 indicates that very large reductions in transverse forces can be achieved by placing the rudder at its optimum location. A small deviation from this rudder clearance gives rise to a sizable increase in the vibratory level of the side force.

The limited number of calculations have demonstrated the inadequacy of the currently used method, based on a modification of low aspect ratio aerodynamic theory, for evaluating steady-state rudder lateral force and rudder stock moment. Furthermore, the failure of semi-empirical methods to take cognizance of the vibratory components of lateral force and rudder stock moment can easily lead to erroneous conclusions and disastrous consequences. There are cases where the lateral force is smaller than estimated by the modified low aspect ratio theory, but the shape of the pressure distribution is such as to introduce a large rudder bending moment which cannot be predicted by that theory. There are cases where the unsteady rudder stock moment is of the same order or larger than the steady-state moment, and neglect of this time-dependent component will foster false conclusions.

The present study provides a clearer understanding of the nature of the interaction effects and more information of practical interest for the design of hull-propeller-rudder configurations than do the currently used methods. For greater precision in estimating the magnitudes of the interaction effects it is suggested that this study be complemented by a study of the effects of thickness of both lifting surfaces. It is imperative to exploit further the concept of optimum rudder location by studying a variety of propeller-rudder configurations under different wake conditions.

ACKNOWLEDGMENT

The authors wish to acknowledge their indebtedness to Dr. John Breslin and Dr. Charles Henry for their valuable discussions which clarified certain aspects of the present study, in particular for Dr. Breslin's contribution in discovering the additional terms (designated as conjugate terms in the text) for the vibratory loading distribution on the rudder.

REFERENCES

1. SHIOIRI, J. and TSAKONAS, S., "Three-Dimensional Approach to the Gust Problem for a Screw Propeller," DL Report 940, Stevens Institute of Technology, March 1963; J. Ship Research Vol. 7, No. 4, April 1964, pp. 29-53.

2. TSAKONAS, S., ENG, K.S., and JACOBS, W.R., CONFIDENTIAL DL Report 987, Stevens Institute of Technology, December 1963.

3. TSAKONAS, S. and JACOBS, W.R., "Unsteady Lifting Surface Theory for a Marine Propeller of Low Pitch Angle with Chordwise Loading Distribution." DL Report 994, Stevens Institute of Technology, January 1964; J. Ship Research Vol. 9, No. 2, September 1965, pp. 79-101.

4. TSAKONAS, S., CHEN, C.Y. and JACOBS, W.R., CONFIDENTIAL DL Report 1055, Stevens Institute of Technology, February 1965.

5. TSAKONAS, S., CHEN, C.Y. and JACOBS, W.R., "Exact Treatment of the Helicoidal Wake in the Propeller Lifting-Surface Theory." DL Report 1117, Stevens Institute of Technology, August 1966; J. Ship Research Vol. 11, No. 3, September 1967, pp. 154-170.

6. TSAKONAS, S., JACOBS, W.R. and RANK, P., "Unsteady Propeller Lifting Surface Theory with Finite Number of Chordwise Modes." DL Report 1133, Stevens Institute of Technology, December 1966; J. Ship Research, Vol. 12, No. 1, March 1968, pp. 14-46.

7. JACOBS, W.R. and TSAKONAS, S., "Generalized Lift Operator Technique for the Solution of the Downwash Integral Equation." DL Report 1308, Stevens Institute of Technology, August 1968, published as "A New Procedure for the Solution of Lifting Surface Problems," J. Hydronautics Vol. 3, No. 1, January 1969, pp. 20-28.

8. ISAY, W.H., "On the Interaction Between Ship Rudder and Screw Propeller," Schiffstechnik, Vol. 12, No. 62, May 1965, pp. 65-76.

9. SUGAI, K., "On Vibratory Forces Induced on the Rudder Behind a Propeller," Ship Research Institute, Tokyo; presented at Spring Meeting of S.N.A. in Japan, May 1964.

10. LINDGREN, H., editor, "The Influence of Propeller Clearance and Rudder upon the Propulsive Characteristics." Swedish State Shipbuilding Experimental Tank (SSPA), Göteborg, Report No. 33, 1955.

11. LÖTVEIT, M., "A Study of Rudder Action with Special Reference to Single-Screw Ships." North-East Coast Institute of Engineers and Shipbuilders, Vol. 73, 1959, p. 87ff.

12. LANDAHL, M., "Pressure-Loading Functions for Oscillating Wings with Control Surfaces." AIAA Journal, Vol. 6, No. 2, February 1968.

13. SLUYTER, M.M., "A Computational Program and Extended Tabulation of Legendre Functions of Second Kind and Half Order." THERM Report TAR-TR601, 1960.

14. TSAKONAS, S., JACOBS, W.R. and ALI, M.R., "A Theory for the Propeller-Duct Interaction." DL Report 1309, Stevens Institute of Technology (in preparation).

15. TSAKONAS, S., BRESLIN, J.P. and MILLER, M., "Correlation and Application of an Unsteady Flow Theory for Propeller Forces." Transactions of SNAME Vol. 75, 1967.

16. TSAKONAS, S. and JACOBS, W.R., "Propeller Loading Distributions," DL Report 1319, Stevens Institute of Technology, August 1968.

17. HADLER, J.B. and CHENG, H.M., "Analysis of Experimental Wake Data in Way of Propeller Plane of Single and Twin-Screw Ship Models." Transactions of SNAME Vol. 73, 1965.

18. BRUNNSTEIN, K., "Wechselwirkung zwischen Schiffsnachstrom, Schrauben-propeller und Schiffsruder," Bericht Nr. 210, Institut für Schiffbau der Universität Hamburg, 1968.

19. WHICKER, L.F. and FEHLNER, L.F., "Free-Stream Characteristics of a Family of Low-Aspect-Ratio, All-Movable Control Surfaces for Application to Ship Design," Report 933, David Taylor Model Basin, December 1958.

20. LEHMAN, A.F. and ROMANDETTO, R., "An Experimental Study of the Unsteady Forces Induced on a Rudder due to a Propeller Acting in a Wake," Report No. 68-58, Oceanics, Inc., December 1968.

21. LEWIS, F.M., "Propeller Vibration Forces in Single-Screw Ships," Presented at Annual Meeting of SNAME, November 12-14, 1969.

Table I

Variation of Mean Force and Moment Coefficients
With Iteration Number for a Range of Rudder Angles
(4-Blade Propeller and Rudder behind Mod V Hull)
$x_o = 0.8356\ r_o$

Amplitudes	Rudder Angle (rad)	Iteration Number 0	1	2	3	4	5
$\bar{K}_T$	-0.3	.3738	.3737	→			
	0	.3738	.3737	→			
	0.3	.3738	.3737	→			
$\bar{K}_Q$	-0.3	.0648	→				
	0	.0648	→				
	0.3	.0648	→				
$\bar{K}_{F_{y,z}}$	-0.3	.00227	.00386	.00380	.00379	→	
	0	.00227	.00220	→			
	0.3	.00227	.00521	.00538	.00537	→	
$\bar{K}_{Q_{y,z}}$	-0.3	.00197	.000324	.000326	→		
	0	.00197	.00200	→			
	0.3	.00197	.00423	.00429	.00428	→	
$\bar{C}_{F_R}$	-0.3	1.0125	1.0350	1.0320	→		
	0	.0258	.0257	.0256	→		
	0.3	1.0125	1.0344	1.0320	1.0318	→	
$\bar{C}_{M_R}$	-0.3	.06760	.06920	.06900	→		
	0	.00179	.00180	→			
	0.3	.06808	.06967	.06950	.06949	→	

NOTE: $K_F = \frac{F}{\rho n^2 D^4}$, $K_Q = \frac{Q}{\rho n^2 D^5}$, $C_{F_R} = \frac{F_R}{\frac{\rho}{2} A_R U^2}$, $C_{M_R} = \frac{M_R}{\frac{\rho}{2} A_R U^2 (2C_R)}$

Table II

Variations of Blade-Frequency Force and Moment Coefficients
With Iteration Number for a Range of Rudder Angles
(4-Blade Propeller and Rudder behind Mod V Hull)
$x_o = 0.8356\ r_o$

Amplitudes	Rudder Angle (rad)	Iteration Number 0	1	2	3	4	5
$\tilde{K}_{F_x}$	-0.3	.0121	.0120	→			
	0	.0121	.0120	→			
	0.3	.0121	.0120	→			
$\tilde{K}_{Q_x}$	-0.3	.00211	.00209	.00210	→		
	0	.00211	.00210	→			
	0.3	.00211	.00210	→			
$\tilde{K}_{F_y}$	-0.3	.00252	.00354	.00350	→		
	0	.00252	→				
	0.3	.00252	.00203	.00212	→		
$\tilde{K}_{Q_y}$	-0.3	.00201	.00249	.00246	→		
	0	.00201	.00200	→			
	0.3	.00201	.00194	.00200	→		
$\tilde{K}_{F_z}$	-0.3	.00279	.00302	.00299	→		
	0	.00279	→				
	0.3	.00279	.00279	.00284	.00285	→	
$\tilde{K}_{Q_z}$	-0.3	.00224	.00233	.00231	→		
	0	.00224	→				
	0.3	.00224	.00227	.00230	→		
$\tilde{C}_{F_R}$	-0.3	.0437	.0729	.0745	→		
	0	.0437	.0441	.0440	→		
	0.3	.0437	.0518	.0509	.0508	→	
$\tilde{C}_{M_R}$	-0.3	.0120	.0193	.0200	→		
	0	.0120	.0122	→			
	0.3	.0120	.0130	.0126	.0125	→	

Table III

Variation of Mean Force and Moment Coefficients
With Iteration Number for a Range of Rudder Angles
(4-Blade Propeller and Rudder behind Mod V Hull)
$x_o = 0.56\ r_o$

Amplitudes	Rudder Angle (rad)	Iteration Number 0	1	2	3	4	5
$\bar{K}_T$	-0.3	.3738	.3737	→	→	→	→
	-0.1	.3738	.3737	→	→	→	→
	0.3	.3738	.3737	→	→	→	→
$\bar{K}_Q$	-0.3	.06483	.06483	.06482	→	→	→
	-0.1	.06483	.06482	→	→	→	→
	0.3	.06483	.06483	.06482	→	→	→
$\bar{K}_{F_{y,z}}$	-0.3	.00227	.00825	.00842	.00801	.00795	.00796
	-0.1	.00227	.00290	.00260	.00245	→	→
	0.3	.00227	.00957	.01059	.01028	.01020	→
$\bar{K}_{Q_{y,z}}$	-0.3	.00197	.00224	.00254	.00239	.00235	.00236
	-0.1	.00197	.00057	.00054	.00061	→	→
	0.3	.00197	.00613	.00645	.00628	.00625	→
$\bar{C}_{F_R}$	-0.3	1.0128	1.0898	1.0531	1.0446	1.0457	1.0462
	-0.1	.3386	.3639	.3515	.3487	.3491	.3493
	0.3	1.0125	1.0909	1.0544	1.0459	1.0470	1.0475
$\bar{C}_{M_R}$	-0.3	.0675	.0715	.0689	.0684	.0685	→
	-0.1	.0224	.0237	.0228	.0226	.0227	→
	0.3	.0682	.0722	.0696	.0691	.0692	→

Table IV

Variations of Blade-Frequency Force and Moment Coefficients
With Iteration Number for a Range of Rudder Angles
(4-Blade Propeller and Rudder behind Mod V Hull)
$x_o = 0.56\ r_o$

Amplitudes	Rudder Angle (rad)	Iteration Number 0	1	2	3	4	5
$\tilde{K}_{F_x}$	-0.3	.0121	.0108	→			
	-0.1	.0121	.0111	→			
	0.3	.0121	.0119	.0117	→		
$\tilde{K}_{Q_x}$	-0.3	.00211	.00189	.00189	.00190	→	
	-0.1	.00211	.00195	.00194	→		
	0.3	.00211	.00207	.00205	→		
$\tilde{K}_{F_y}$	-0.3	.00252	.00963	.00951	.00913	.00909	.00911
	-0.1	.00252	.00438	.00414	.00401	→	
	0.3	.00252	.00736	.00816	.00789	.00782	→
$\tilde{K}_{Q_y}$	-0.3	.00201	.00562	.00545	.00525	.00524	→
	-0.1	.00201	.00279	.00260	.00254	→	
	0.3	.00201	.00462	.00515	.00502	.00498	→
$\tilde{K}_{F_z}$	-0.3	.00279	.00469	.00442	.00422	→	
	-0.1	.00279	.00312	.00290	.00286	→	
	0.3	.00279	.00343	.00418	.00414	.00409	→
$\tilde{K}_{Q_z}$	-0.3	.00224	.00292	.00271	.00263	→	
	-0.1	.00224	.00234	.00224	.00222	→	
	0.3	.00224	.00233	.00270	.00270	.00268	→
$\tilde{\tau}_{F_R}$	-0.3	.0539	.0963	.1056	.1048	→	
	-0.1	.0539	.0631	.0681	.0679	→	
	0.3	.0539	.0804	.0659	.0617	→	
$\tilde{\tau}_{M_R}$	-0.3	.0135	.0355	.0372	.0363	→	
	-0.1	.0135	.0195	.0204	.0201	→	
	0.3	.0135	.0234	.0218	.0204	→	

Table V

Variation of Mean Force and Moment Coefficients
With Iteration Number for a Range of Rudder Angles
(4-Blade Propeller and Rudder behind Mod V Hull)

$x_o = 0.72\ r_o$

Amplitudes	Rudder Angle (rad)	Iteration Number 0	1	2	3	4	5
$\bar{K}_T$	-0.3	.3738	→	→	→	→	→
	-0.1	.3738	→	→	→	→	→
	0.3	.3738	→	→	→	→	→
$\bar{K}_Q$	-0.3	.0648	→	→	→	→	→
	-0.1	.0648	→	→	→	→	→
	0.3	.0648	→	→	→	→	→
$\bar{K}_{F_{y,z}}$	-0.3	.00227	.00518	.00508	→	→	→
	-0.1	.00227	.00227	.00213	→	→	→
	0.3	.00227	.00661	.00688	→	→	→
$\bar{K}_{Q_{y,z}}$	-0.3	.00197	.00098	.00102	→	→	→
	-0.1	.00197	.00098				
	0.3	.00197	.00490	.00497	→	→	→
$\bar{C}_{F_R}$	-0.3	1.0128	1.0460	1.0392	1.0386	→	→
	-0.1	.3386	.3498	.3475	.3473	→	→
	0.3	1.0125	1.0455	1.0386	1.0347	→	→
$\bar{C}_{M_R}$	-0.3	.0675	.0699	.0692	→	→	→
	-0.1	.0224	.0232	.0230	→	→	→
	0.3	.0682	.0703	.0698	→	→	→

Table VI

Variations of Blade-Frequency Force and Moment Coefficients
With Iteration Number for a Range of Rudder Angles
(4-Blade Propeller and Rudder behind Mod V Hull)
$x_o = 0.72\ r_o$

Amplitudes	Rudder Angle (rad)	Iteration Number 0	1	2	3	4	5
$\tilde{K}_{F_x}$	-0.3	.0121	.0119	→			
	-0.1	.0121	.0119	→			
	0.3	.0121	.0119	→			
$\tilde{K}_{Q_x}$	-0.3	.00211	.00209	.00207	→		
	-0.1	.00211	.00207	→			
	0.3	.00211	.00210	.00208	→		
$\tilde{K}_{F_y}$	-0.3	.00252	.00462	→			
	-0.1	.00252	.00305	→			
	0.3	.00252	.00257	.00277	→		
$\tilde{K}_{Q_y}$	-0.3	.00201	.00303	→			
	-0.1	.00201	.00220	→			
	0.3	.00201	.00232	.00244	→		
$\tilde{K}_{F_z}$	-0.3	.00279	.00314	→			
	-0.1	.00279					
	0.3	.00279	.00306	→			
$\tilde{K}_{Q_z}$	-0.3	.00224	.00235	→			
	-0.1	.00224	.00222	→			
	0.3	.00224	.00239	→			
$\tilde{C}_{F_R}$	-0.3	.03446	.06031	.06390	→		
	-0.1	.03446	.04193	.04345	→		
	0.3	.03446	.04607	.04340	.0429	→	
$\tilde{C}_{M_R}$	-0.3	.01396	.02720	.02822	.02813	→	
	-0.1	.01396	.01798	.01834	→		
	0.3	.01396	.01625	.01573	.01560	→	

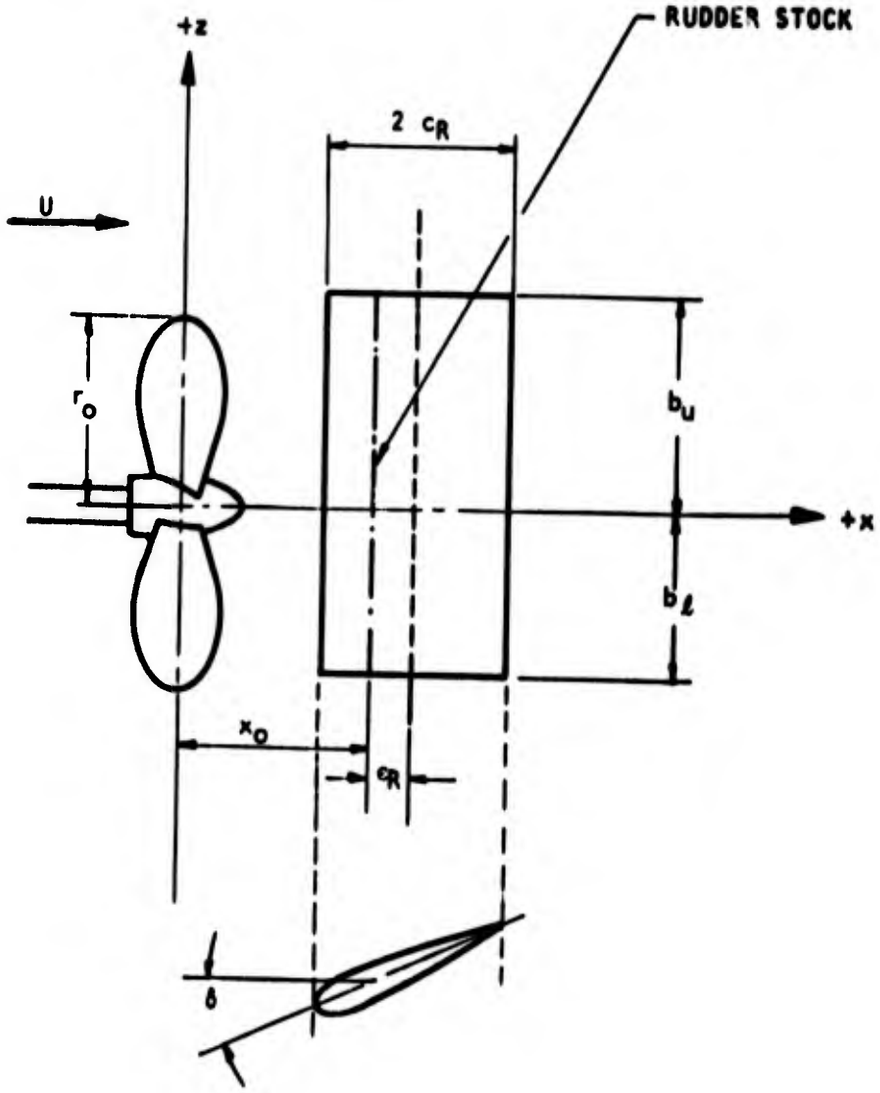

FIG. 1. PROPELLER-RUDDER ARRANGEMENT

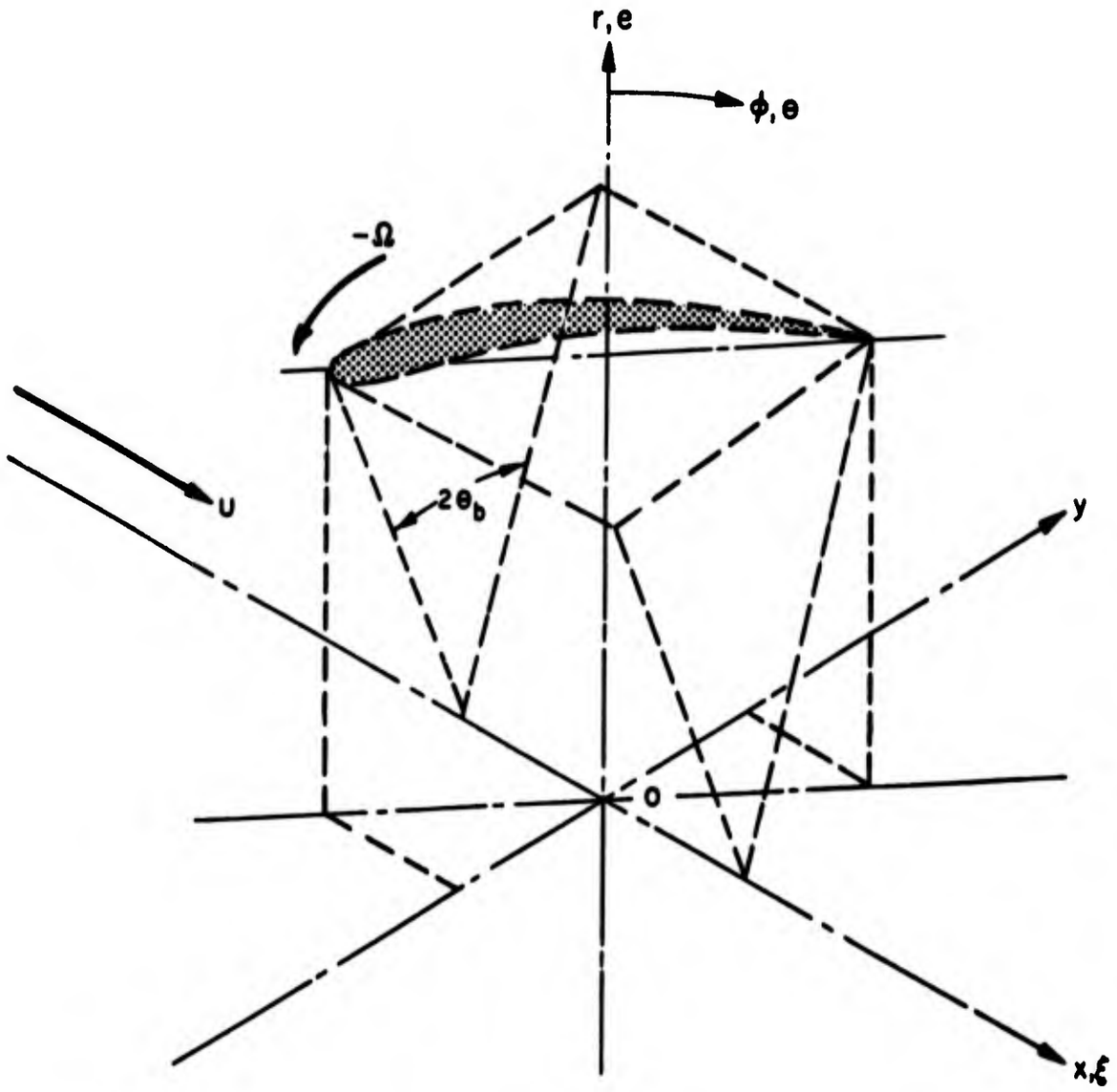

FIG. 2. COORDINATE SYSTEM OF PROPELLER

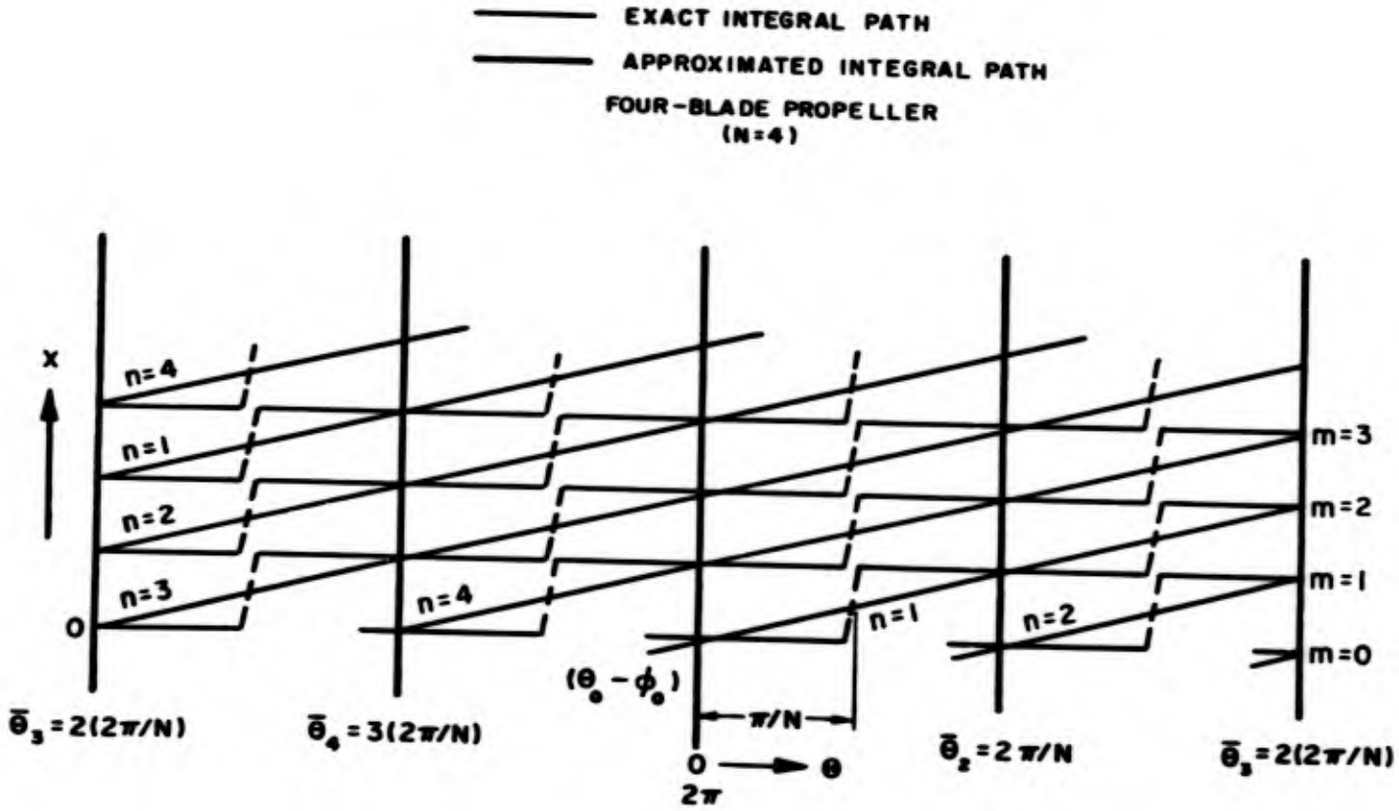

FIG. 3. APPROXIMATION OF INTEGRAL PATH

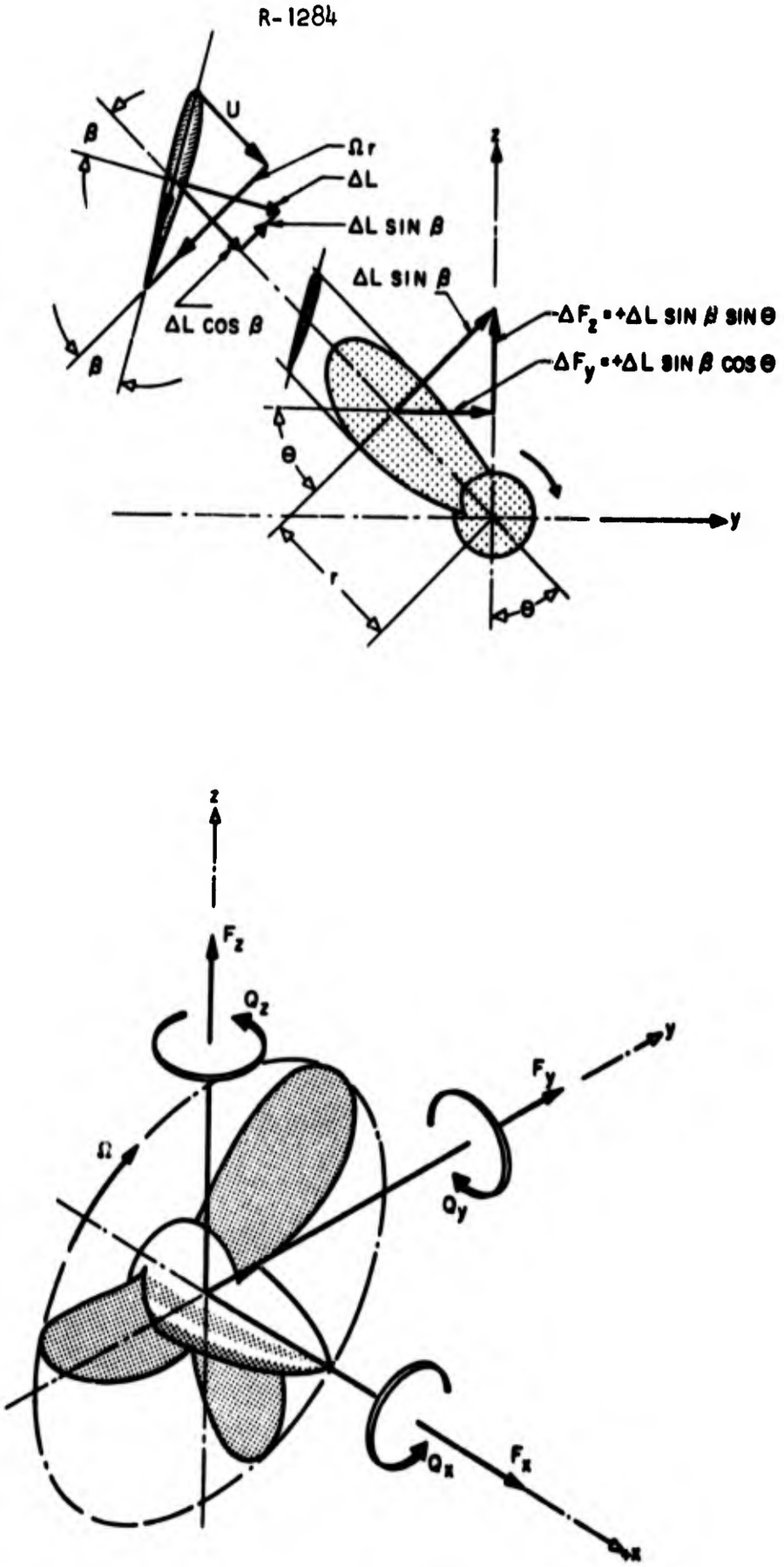

FIG. 4. RESOLUTION OF FORCES AND MOMENTS

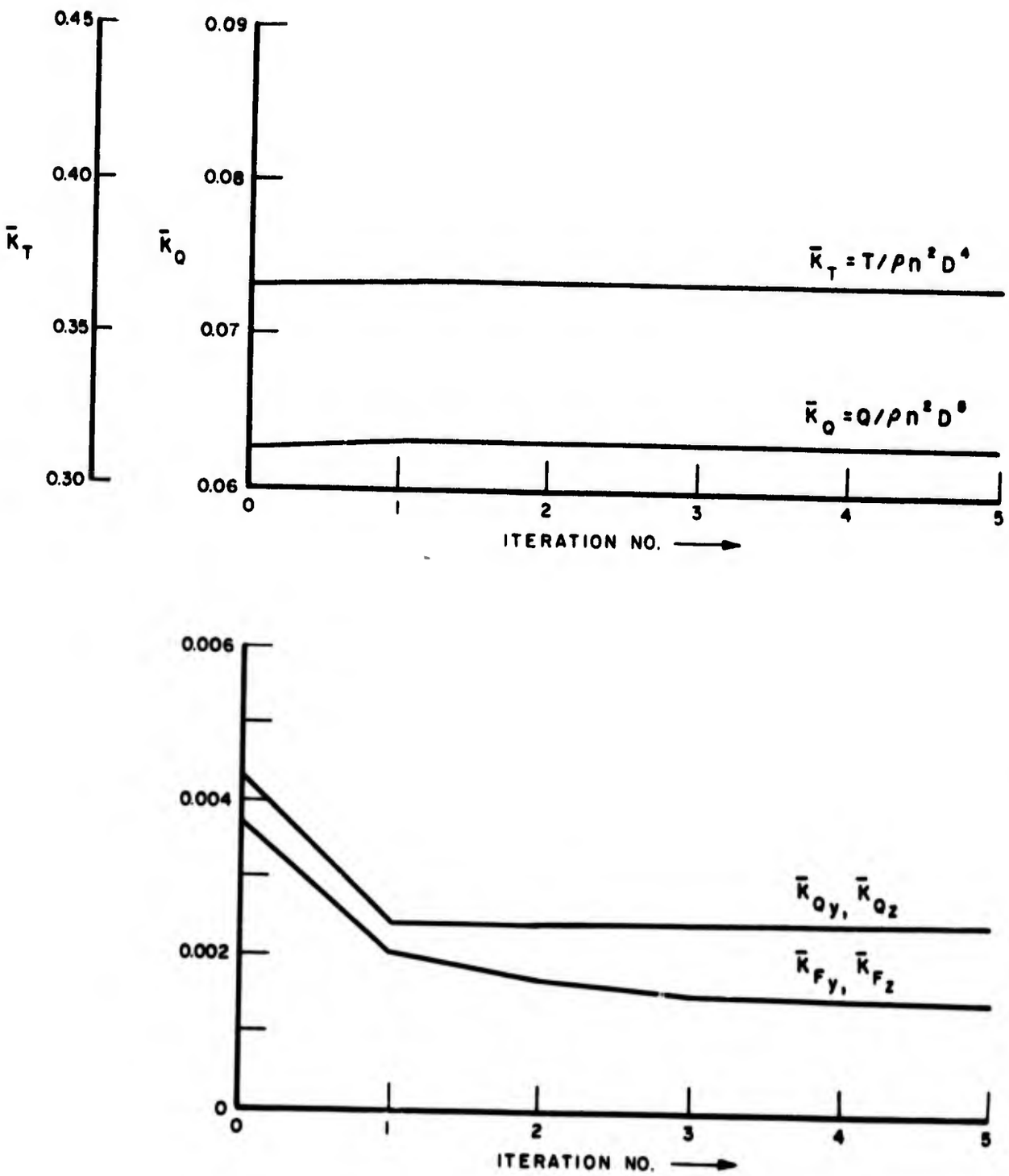

FIG. 5. AMPLITUDES OF PROPELLER MEAN FORCE AND MOMENT COEFFICIENTS (δ=-0.1 RAD, 3-BLADE PROPELLER)

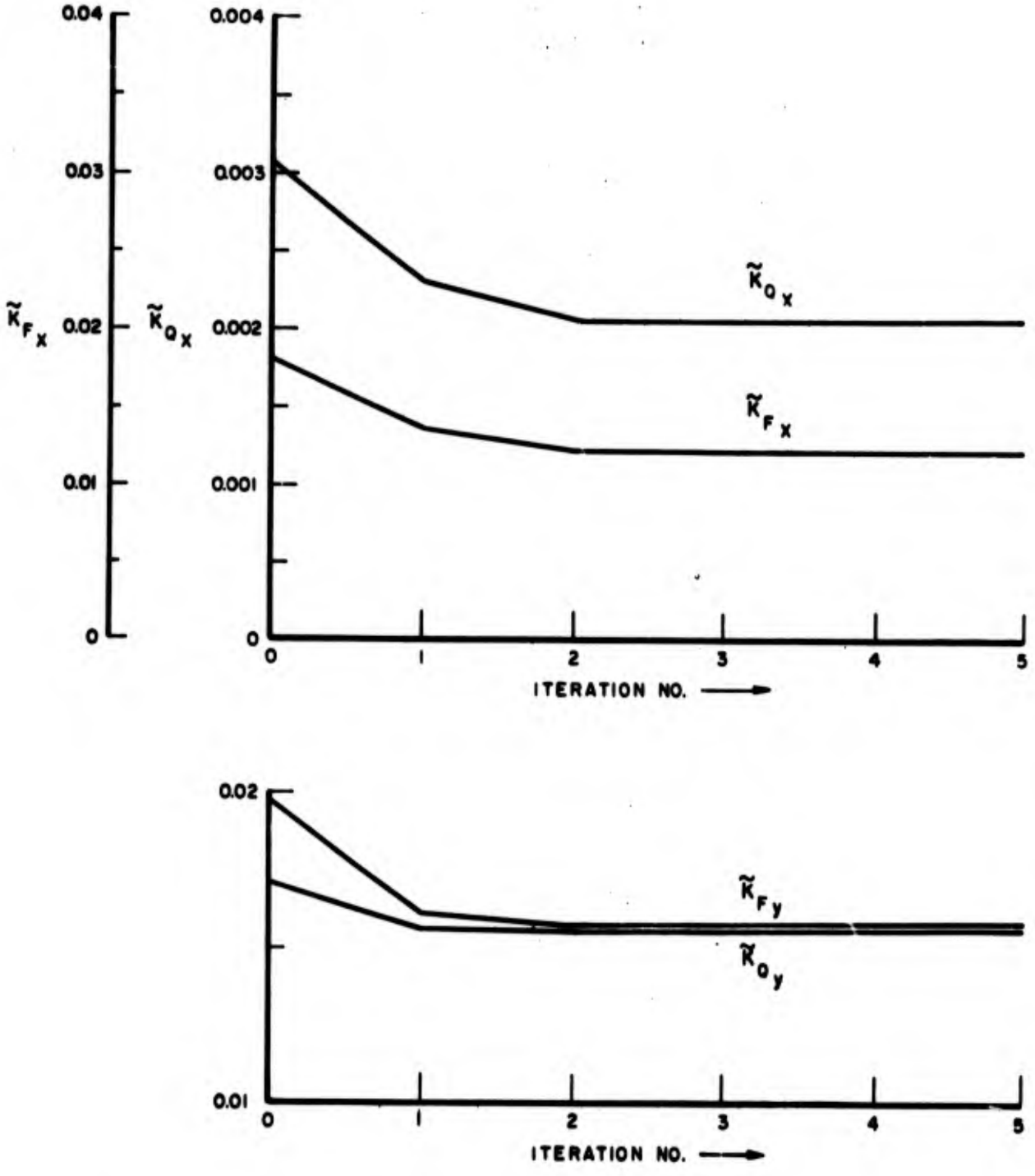

FIG. 6a. AMPLITUDES OF PROPELLER BLADE-FREQUENCY FORCE AND MOMENT COEFFICIENTS (δ = -0.1 RAD, 3-BLADE PROPELLER)

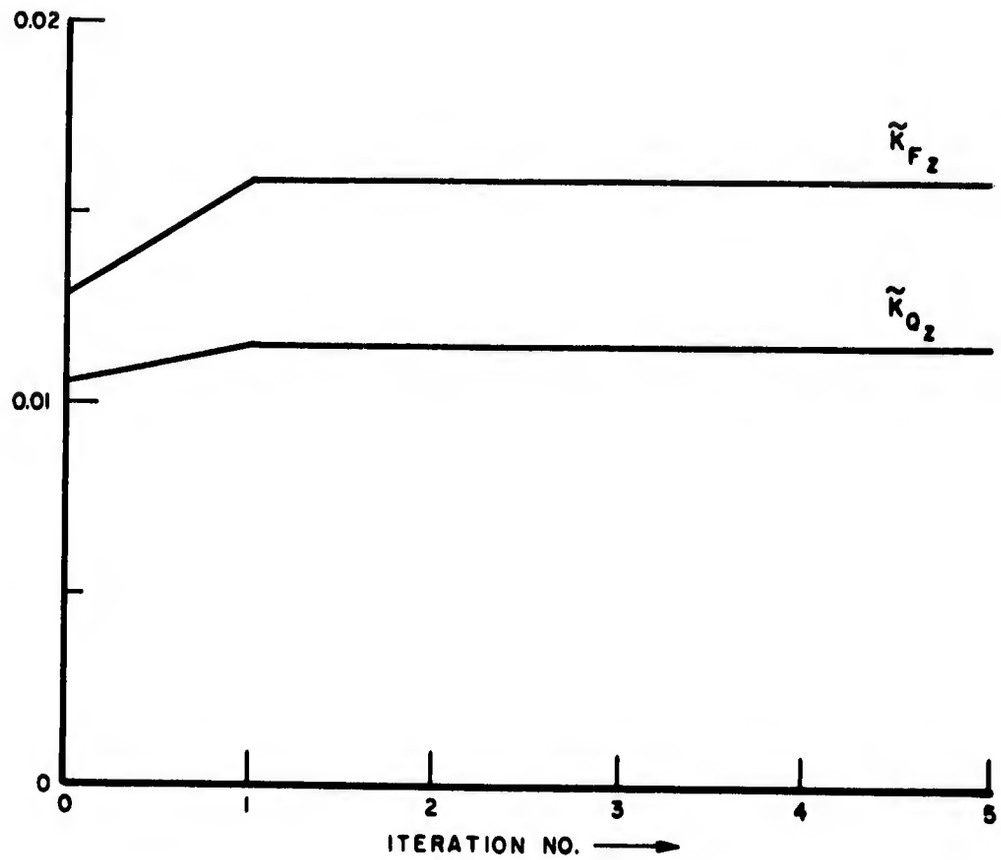

FIG. 6b. AMPLITUDES OF PROPELLER BLADE FREQUENCY FORCE AND MOMENT COEFFICIENTS (δ=-0.1 RAD, 3-BLADE PROPELLER)

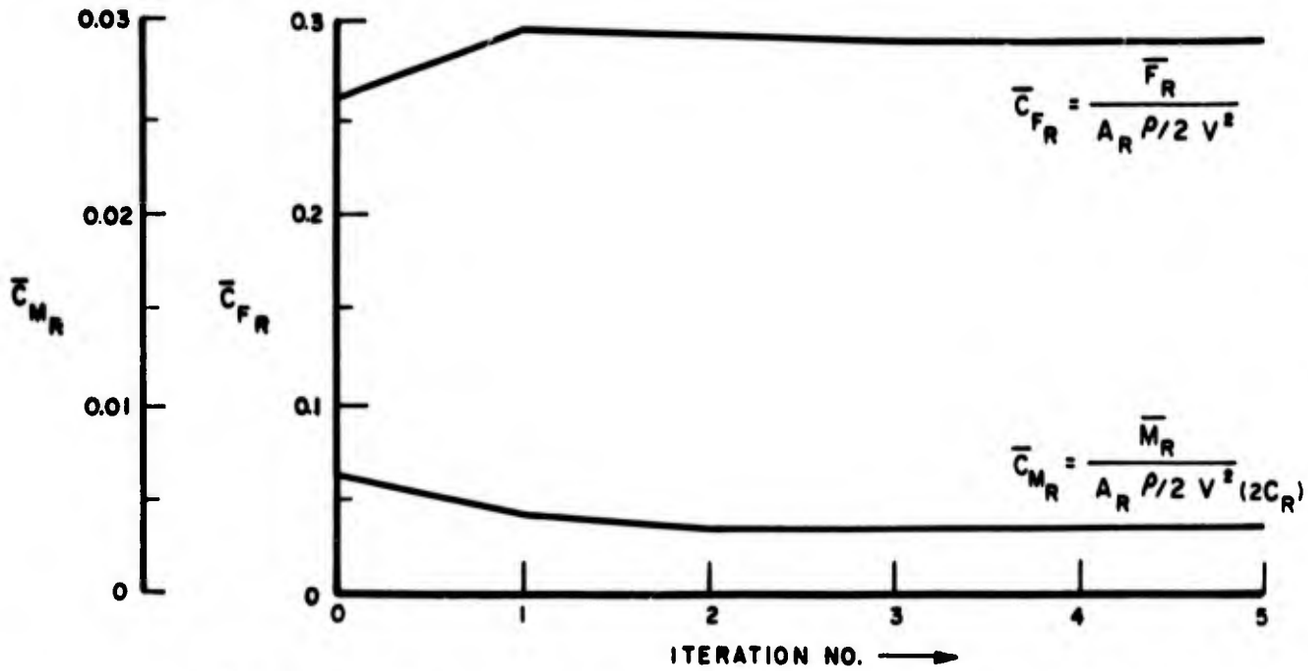

FIG. 7. AMPLITUDES OF MEAN RUDDER FORCE AND RUDDER STOCK MOMENT COEFFICIENTS (δ=-0.1 RAD, 3-BLADE PROPELLER)

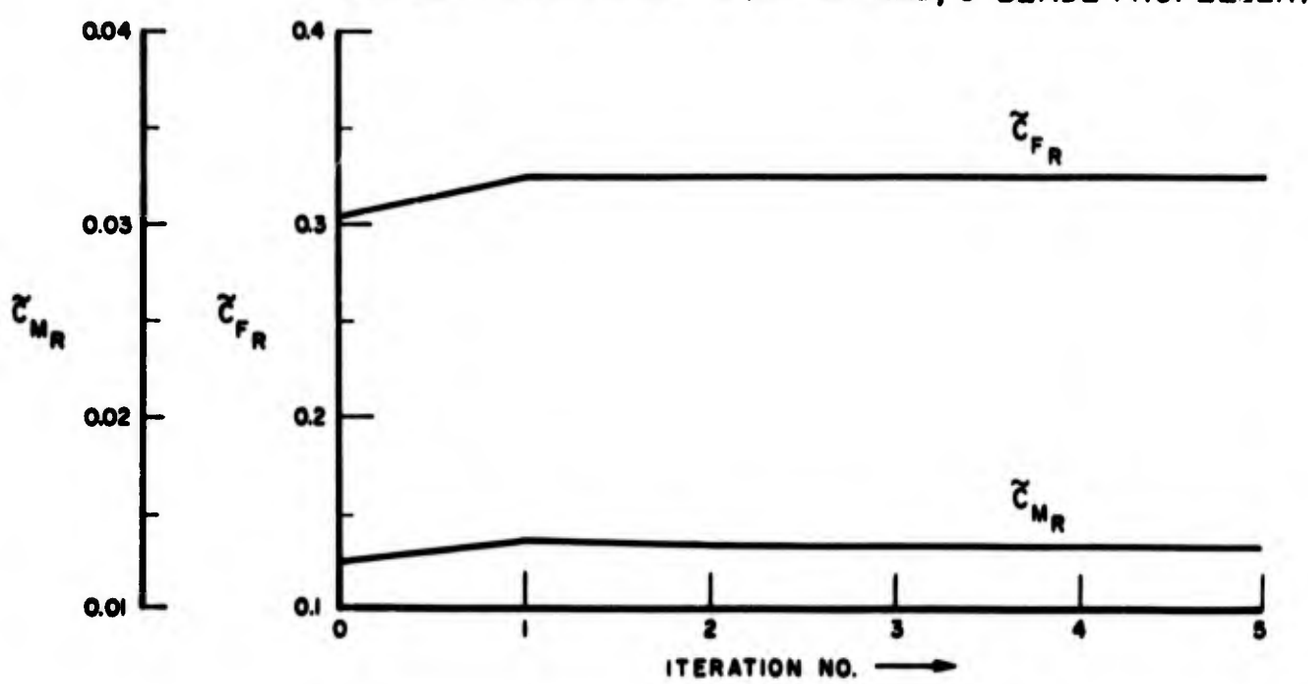

FIG. 7. AMPLITUDES OF BLADE FREQUENCY RUDDER FORCE AND RUDDER STOCK MOMENT COEFFICIENTS (δ=-0.1 RAD, 3-BLADE PROPELLER)

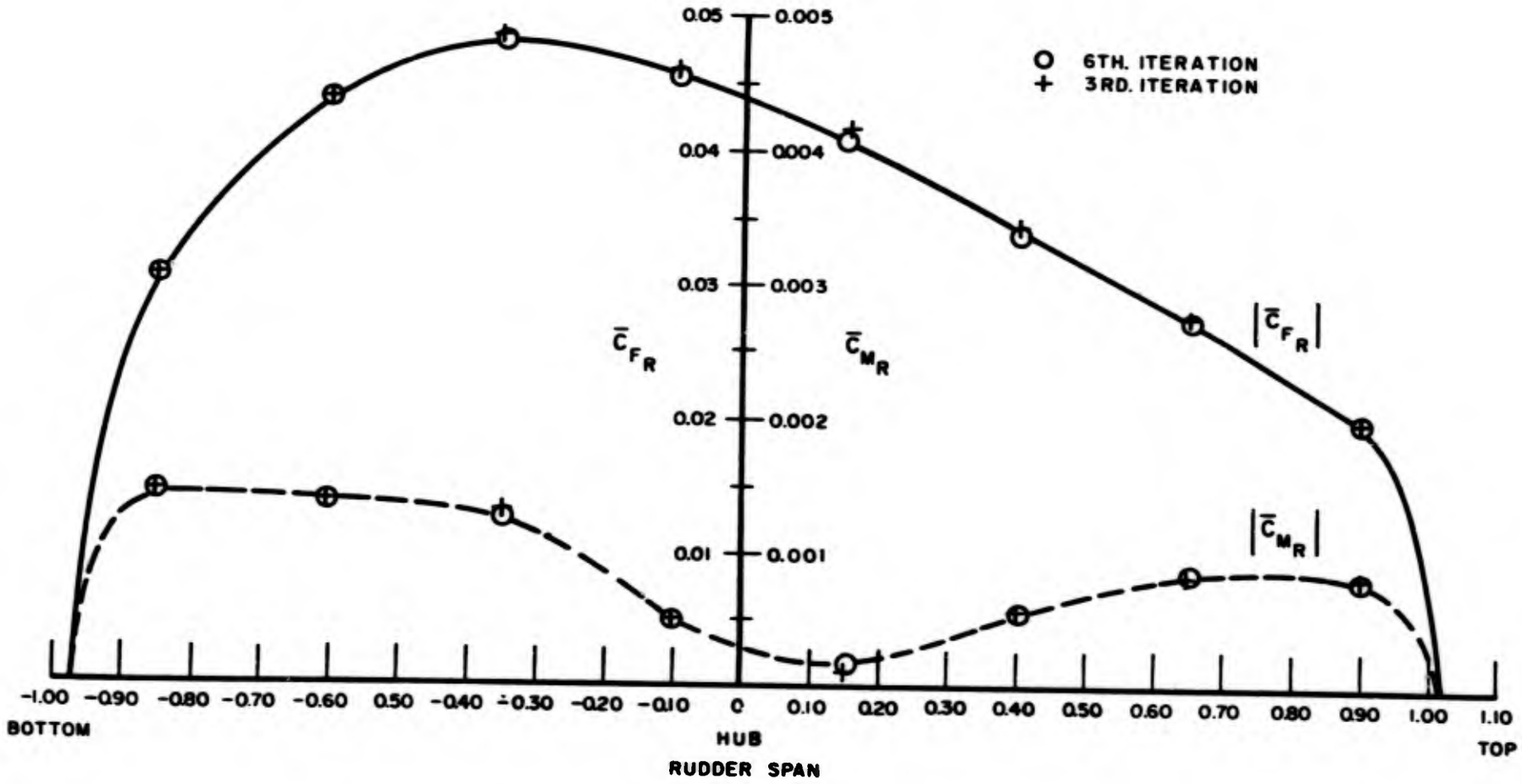

R-1284

FIG. 8. MEAN RUDDER FORCE AND MOMENT AMPLITUDES SPANWISE DISTRIBUTION
(δ = −0.1 RAD, 3-BLADE PROPELLER)

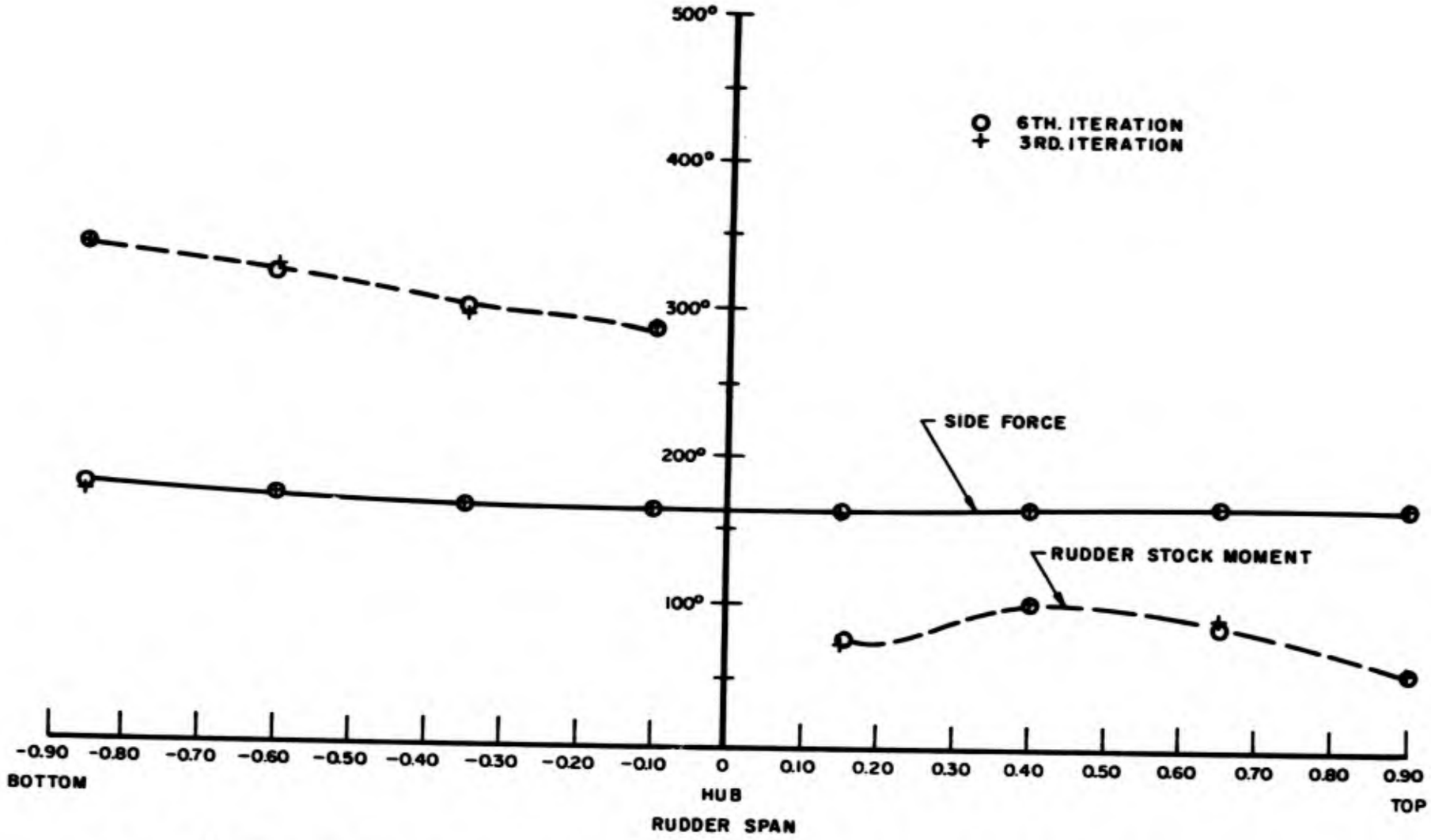

FIG. 9. MEAN RUDDER FORCE AND MOMENT PHASES SPANWISE DISTRIBUTION (δ =-0.1 RADIAN, 3-BLADE PROPELLER)

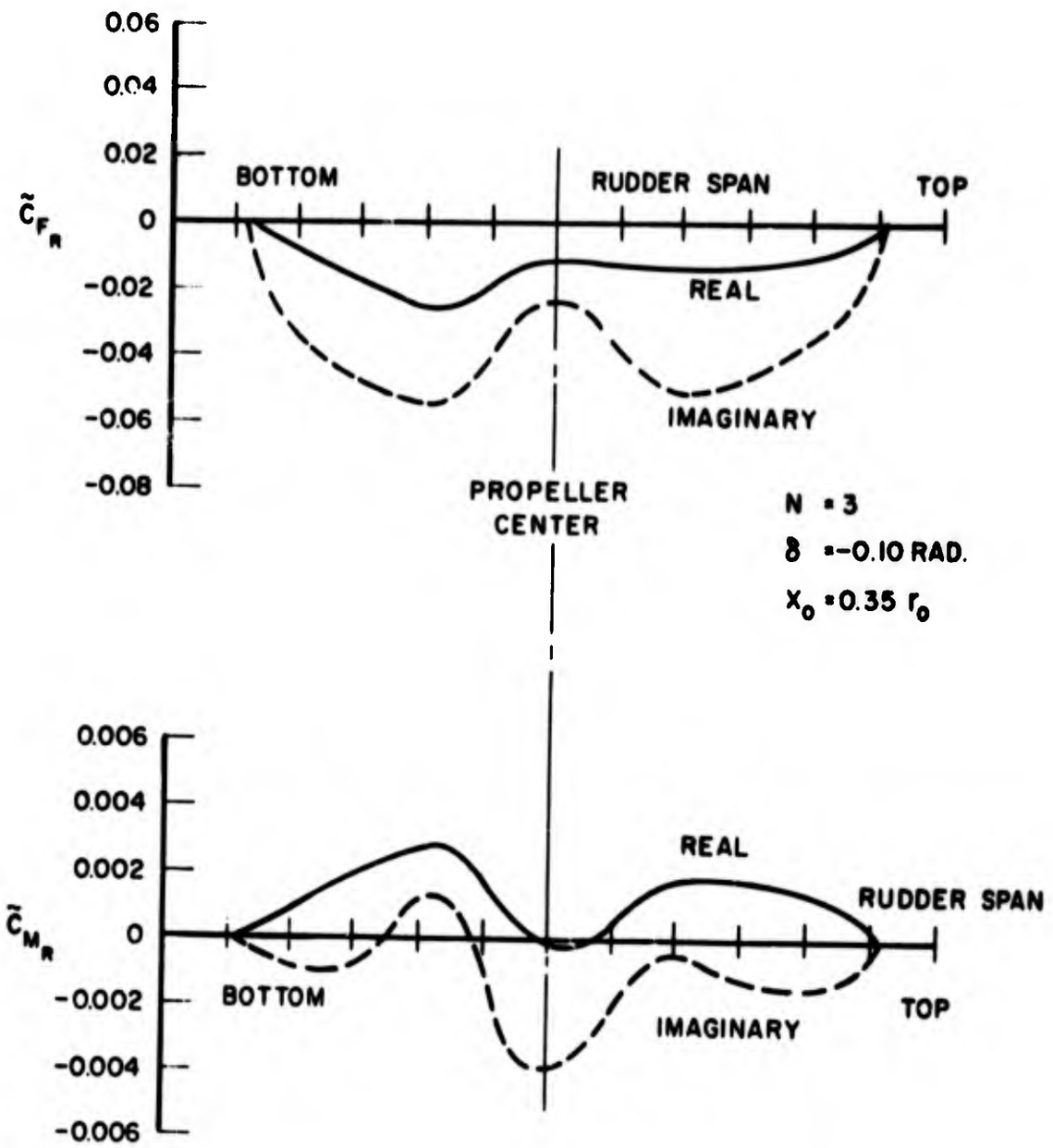

FIG. 10. SPANWISE DISTRIBUTION OF BLADE FREQUENCY $\tilde{C}_{F_R}$ AND $\tilde{C}_{M_R}$ FOR RUDDER ANGLE OF 0.1 RADIAN TO STARBOARD, AND RUDDER LOCATION $X_0 = 0.35\ r_0$ (3-BLADE PROPELLER AND RUDDER OF AR = 1.78 BEHIND MOD V HULL)

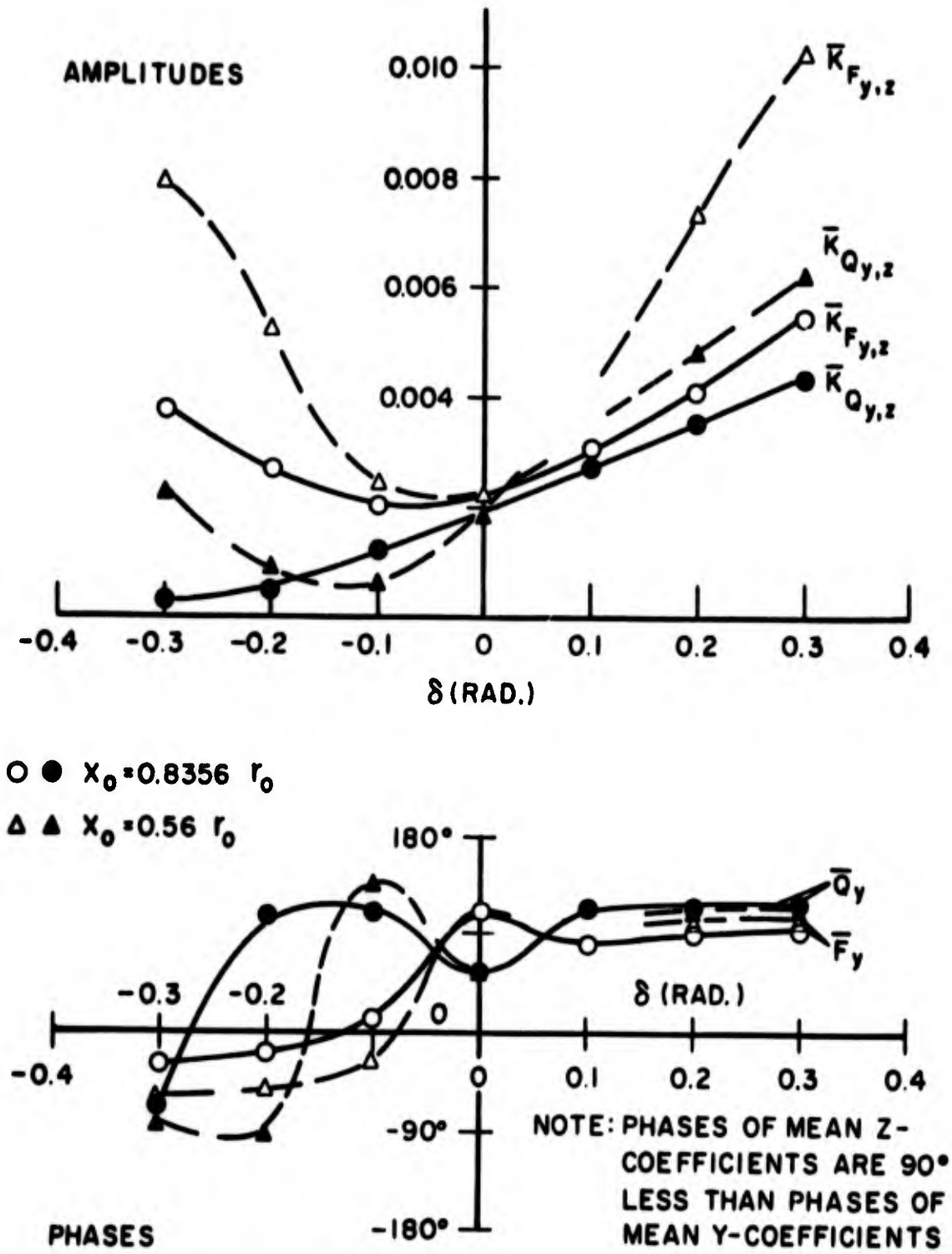

FIG. 11. MEAN BEARING FORCE AND BENDING MOMENT COEFFICIENTS VERSUS RUDDER ANGLE δ. (4-BLADE PROPELLER AND RUDDER BEHIND MOD V HULL)

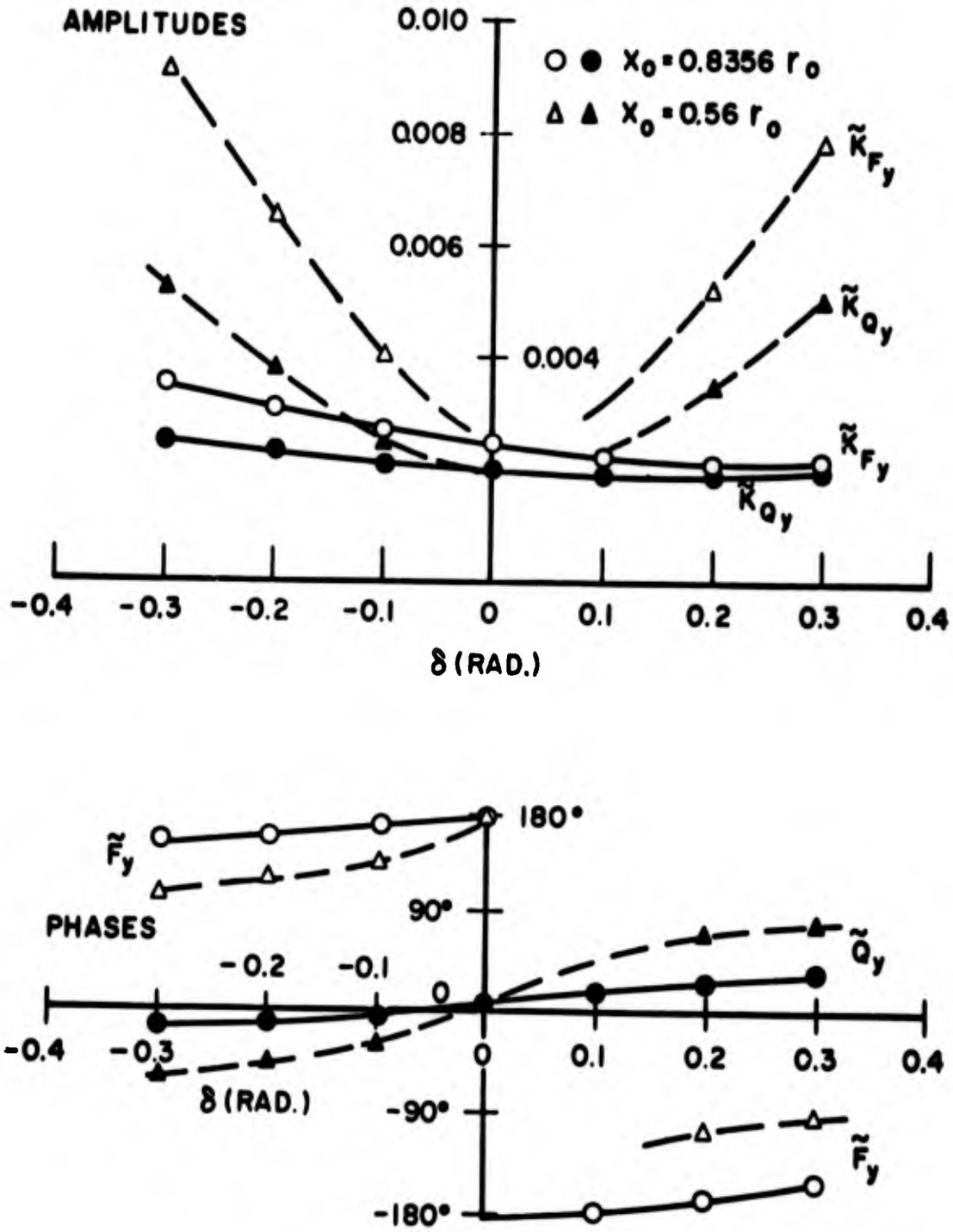

FIG. 12. BLADE-FREQUENCY COEFFICIENTS OF HORIZONTAL BEARING FORCE AND BENDING MOMENT ABOUT Y-AXIS VERSUS RUDDER ANGLE δ. (4-BLADE PROPELLER AND RUDDER BEHIND MOD V HULL)

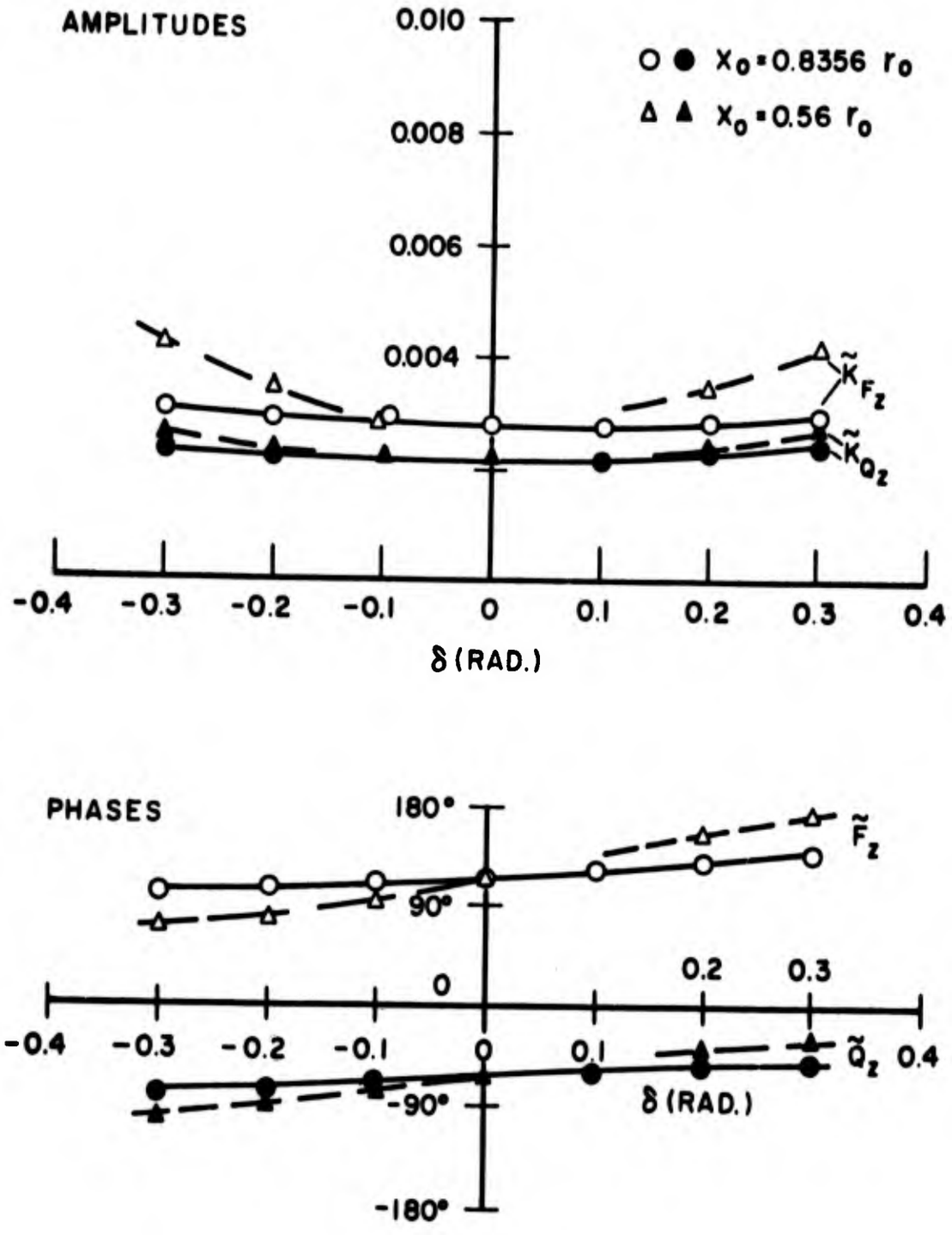

FIG. 13. BLADE-FREQUENCY COEFFICIENTS OF VERTICAL BEARING FORCE AND BENDING MOMENT ABOUT Z-AXIS VERSUS RUDDER ANGLE δ. (4-BLADE PROPELLER AND RUDDER BEHIND MOD V HULL)

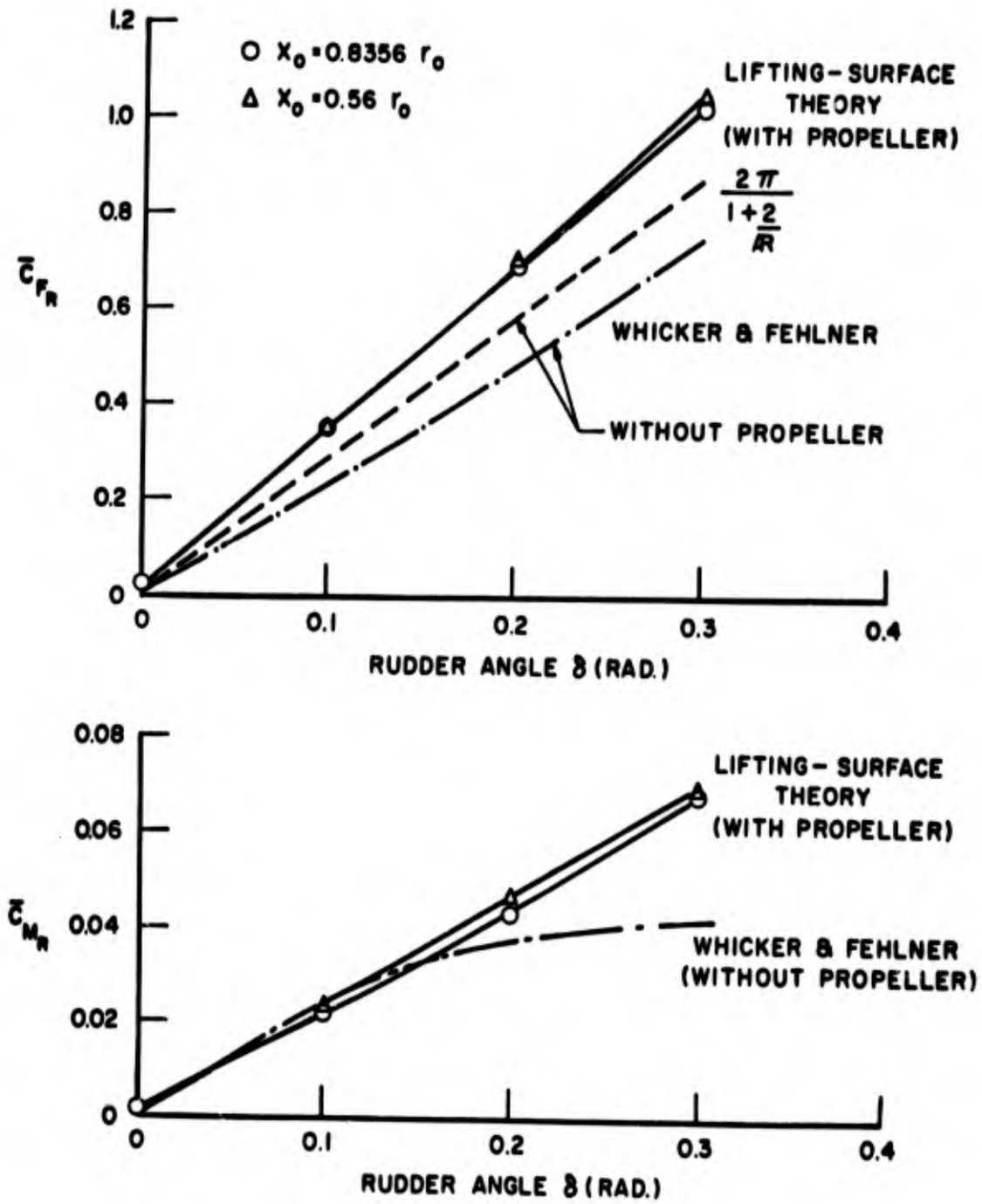

FIG. 14. MEAN RUDDER LATERAL FORCE AND RUDDER STOCK MOMENT COEFFICIENTS VERSUS RUDDER ANGLE (4-BLADE PROPELLER AND RUDDER BEHIND MOD V HULL)

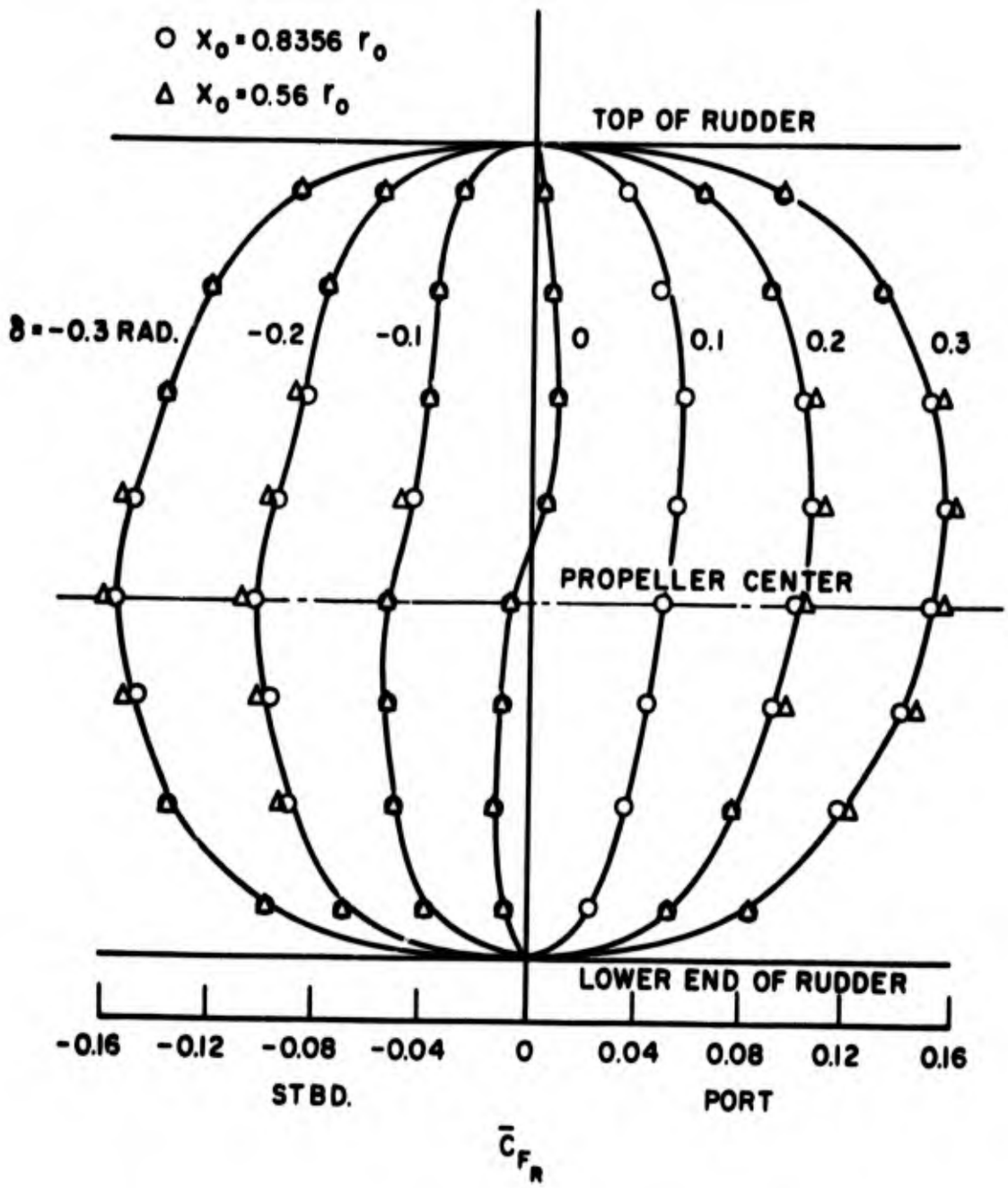

FIG. 15. SPANWISE DISTRIBUTION OF $\bar{C}_{F_R}$ FOR VARIOUS RUDDER ANGLES. (4-BLADE PROPELLER AND RUDDER BEHIND MOD V HULL)

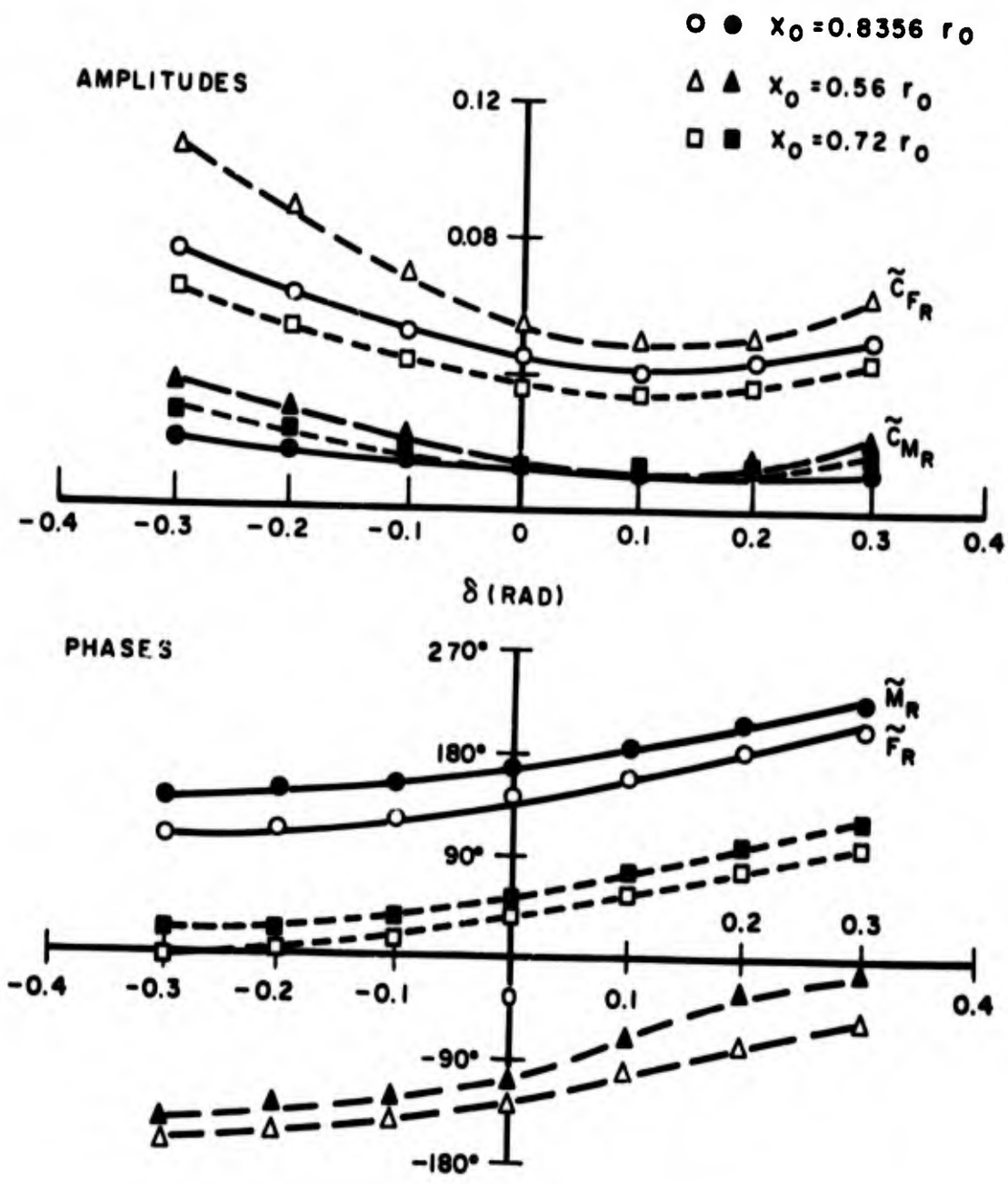

FIG. 16. BLADE-FREQUENCY RUDDER LATERAL FORCE AND RUDDER STOCK MOMENT COEFFICIENTS VERSUS RUDDER ANGLE (4-BLADE PROPELLER AND RUDDER BEHIND MOD V HULL)

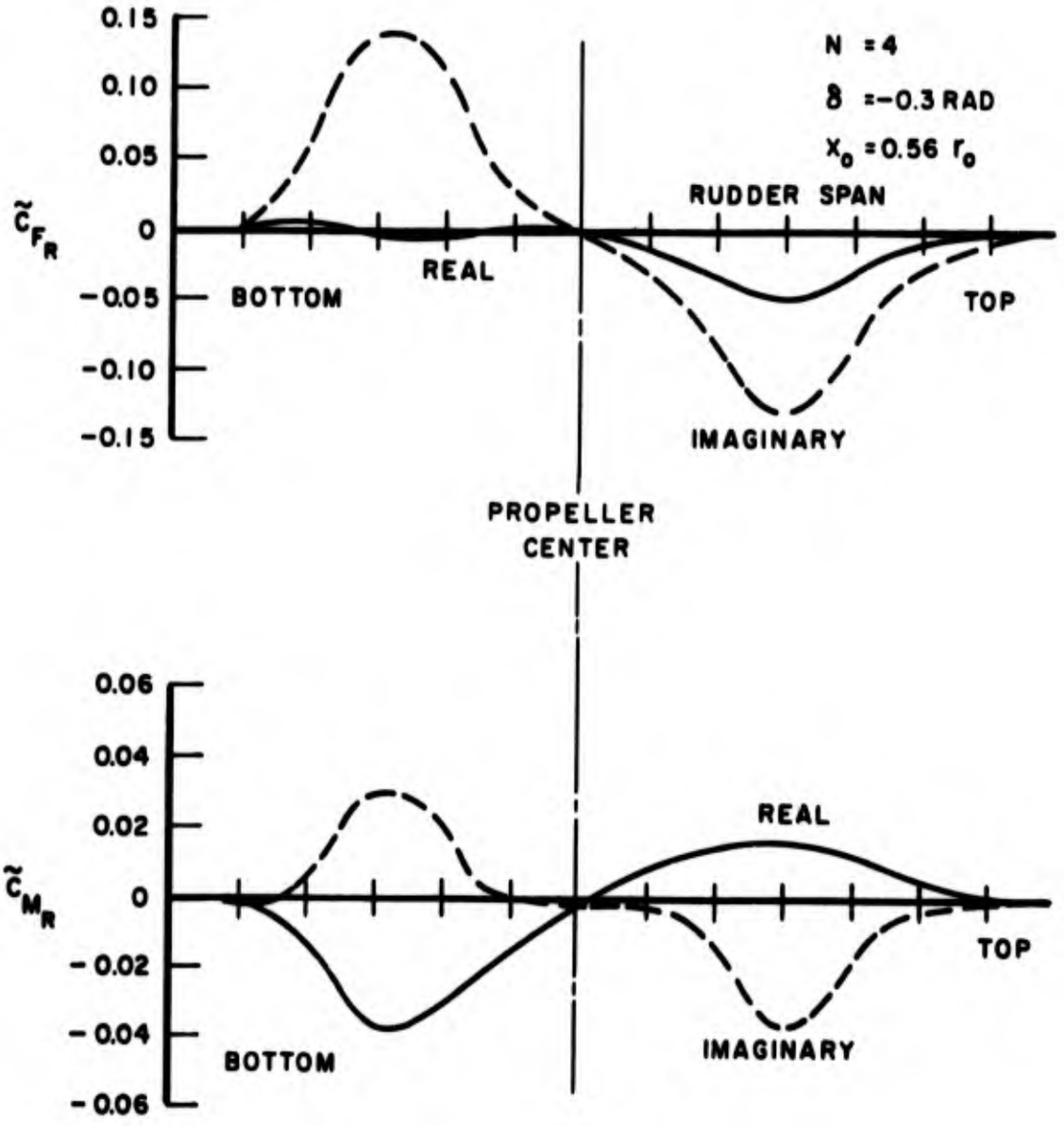

FIG. 17. SPANWISE DISTRIBUTION OF BLADE FREQUENCY $\tilde{C}_{F_R}$ AND $\tilde{C}_{M_R}$ FOR RUDDER ANGLE OF 0.3 RADIAN TO STARBOARD, AND RUDDER LOCATION $X_0 = 0.56 r_0$ (4-BLADE PROPELLER AND RUDDER OF AR = 1.72 BEHIND MOD V HULL)

APPENDIX A

EXAMINATION OF THE KERNEL K_{RP} FOR SINGULAR BEHAVIOR

Before the 1/R expansion, it is obvious that R cannot go to zero since τ is never zero. Therefore, K_{RP} as given by Eq. (59) is non-singular.

After introduction of expansion scheme (61), an integrable Cauchy-type singularity appears in the k-integration of Eq. (62). In order to detect whether or not higher-order singularities are hidden in the infinite m-series, the series will be analyzed for $|m| \geq |M|$ large.

The series can be rewritten for m large (or λ_2 large since $m = q - \lambda_2$) as

$$\sum_{m=M}^{\infty} \begin{pmatrix} +1 \\ (-1)^{m+1} \end{pmatrix} (A+B) \qquad (A-1)$$

where

$$A = m e^{-im\varphi_o} \left\{ \left[a^2\lambda_2 - \frac{m}{r^2} \right] \pi I_m(a\lambda_2\rho) K_m(a\lambda_2 r) e^{-ia\lambda_2(x-\xi)} \right.$$

$$+ ia \int_{-\infty}^{\infty} \frac{k I_m(|k|\rho) K_m(|k|r) e^{ik(x-\xi)}}{k+a\lambda_2} \, dk$$

$$\left. + i \frac{m}{r^2} \int_{-\infty}^{\infty} \frac{I_m(|k|\rho) K_m(|k|r) e^{ik(x-\xi)}}{k+a\lambda_2} \, dk \right\}$$

$$B = -m e^{im\varphi_o} \left\{ \left[a^2\lambda_2 + \frac{m}{r^2} \right] \pi I_m(a\lambda_2\rho) K_m(a\lambda_2 r) e^{-ia\lambda_2(x-\xi)} \right.$$

$$+ ia \int_{-\infty}^{\infty} \frac{k I_m(|k|\rho) K_m(|k|r) e^{ik(x-\xi)}}{k+a\lambda_2} dk$$

$$\left. - i \frac{m}{r^2} \int_{-\infty}^{\infty} \frac{I_m(|k|\rho) K_m(|k|r) e^{ik(x-\xi)}}{k+a\lambda_2} \, dk \right\}$$

(The subscripts P and R are dropped for convenience.)

When $m \geq M$ large, the following approximation can be used to analyze the infinite series for singularity

$$\int_{-\infty}^{\infty} f(k) \frac{e^{ik(x-\xi}}{k+a\lambda_2} dk \approx f(-a\lambda_2) \int_{-\infty}^{\infty} \frac{e^{ik(x-\xi)}}{k+a\lambda_2} dk \qquad (A-2)$$

By the residue theorem, since $(x-\xi) < 0$ in this case

$$\int_{-\infty}^{\infty} \frac{e^{ik(x-\xi)}}{k+a\lambda_2} dk = -i\pi e^{-ia\lambda_2 (x-\xi)} \qquad (A-3)$$

Making use of (A-2) and (A-3) with $f(k)$ in (A-2) alternately $k\, I_m(|k|\rho)K_m(|k|r)$ and $I_m(|k|\rho)K_m(|k|r)$,

$$A \approx m e^{-im\varphi_o}\Big\{ \left[a^2\lambda_2 - \frac{m}{r^2}\right]\pi\, I_m(a\lambda_2\rho)K_m(a\lambda_2 r)e^{-ia\lambda_2 (x-\xi)}$$

$$+ia\left[-i\pi e^{-ia\lambda_2 (x-\xi)}\right]\left[-a\lambda_2\, I_m(a\lambda_2\rho)K_m(a\lambda_2 r)\right]$$

$$+i\,\frac{m}{r^2}\left[-i\pi e^{-ia\lambda_2 (x-\xi)}\right]\left[I_m(a\lambda_2\rho)K_m(a\lambda_2 r)\right]\Big\}$$

$$\approx 0$$

Similarly, B can be shown to be approximately zero for large M. Therefore, the kernel K_{RP} has no singularity other than the Cauchy-type.

APPENDIX B

EVALUATION OF THE INTEGRAND OF $\bar{K}_{RP}$ AT $k = -a(q-m)$

With the substitution

$$\frac{k}{k+a(q-m)} = 1 - \frac{a(q-m)}{k+a(q-m)}$$

the k-integrals of Eq. (64) become

$$ia\int_{-\infty}^{\infty} f(k)dk - i\left[a^2(q-m) - \frac{m}{r^2}\right]\int_{-\infty}^{\infty} \frac{f(k)}{k+a(q-m)}\,dk$$

where

$$f(k) = I_m(|k|\rho)K_m(|k|r)e^{-ik(x_o+\epsilon_R-\sigma/a)}I^{(\bar{m})}\left((m-\frac{k}{a})\theta_b\right)\Lambda^{(\bar{n})}(-kC_R)$$

when $\rho < r$. When $\rho > r$, r and ρ are interchanged in $f(k)$. (Certain subscripts and superscripts have been omitted for simplicity in writing.)

The first integral is nonsingular; the second has a Cauchy-type singularity at $k = -a(q-m)$, where $(q-m) \geq 0$, i.e., it exists only in the sense of a Cauchy principal value. Then the second integral can be written as

$$\int_{-\infty}^{\infty} \frac{f(k)dk}{k+a(q-m)} = \int_0^{\infty} \frac{F(k)dk}{\left[k+a(q-m)\right]\left[k-a(q-m)\right]} = \int_0^{\infty} \frac{F(k)-F(a(q-m))}{\left[k^2-a^2(q-m)^2\right]}\,dk \qquad \text{(B-1)}$$

where

$$F(k) = f(k)\left[k-a(q-m)\right] - f(-k)\left[k+a(q-m)\right]$$

$$F(a(q-m)) = -2a(q-m)\cdot f(-a(q-m))$$

The value of the integrand of (B-1) at the singularity (i.e., the

finite contribution) is

$$\lim_{k\to a(q-m)} \left\{\text{integrand}\right\} = \left.\frac{\partial F(k)}{\partial k}\right|_{k=a(q-m)} /2a(q-m)$$

$$= \frac{f(a(q-m)-f(-a(q-m))}{2a(q-m)} - \left.\frac{\partial f(-k)}{\partial k}\right|_{k=a(q-m)} \qquad \text{(B-2)}$$

where

$$\frac{\partial f(-k)}{\partial k} = \frac{\partial}{\partial k}\left\{(IK)_m e^{ik(x_o+\epsilon_R-\sigma/a)}\, I^{(\bar{m})}((m+\tfrac{k}{a})\theta_b)\Lambda^{(\bar{n})}(kC_R)\right\}$$

$$= \left[\frac{\partial}{\partial k}(IK)_m\right] e^{ik(x_o+\epsilon_R-\sigma/a)}\, I^{(\bar{m})}((m+\tfrac{k}{a})\theta_b)\Lambda^{(\bar{n})}(kC_R)$$

$$+(IK)_m e^{ik(x_o+\epsilon_R-\sigma/a)}\Big[i(x_o+\epsilon_R-\sigma/a) I^{(\bar{m})}((m+\tfrac{k}{a})\theta_b)\Lambda^{(\bar{n})}(kC_R)$$

$$+\frac{\theta_b}{a}\frac{\partial I^{(\bar{m})}((m+\frac{k}{a})\theta_b}{\partial((m+\frac{k}{a})\theta_b)}\Lambda^{(\bar{n})}(kC_R)+C_R I^{(\bar{m})}((m+\tfrac{k}{a})\theta_b))\frac{\partial\Lambda^{(\bar{n})}(kC_R)}{\partial(kC_R)}\Big]$$

$$(IK)_m = \begin{cases} I_m(k\rho)K_m(kr) & \text{when } \rho < r \\ I_m(kr)K_m(k\rho) & \text{when } \rho > r \end{cases}$$

$$\frac{\partial(IK)_m}{\partial k} = \begin{cases} \rho I_{m-1}(k\rho)K_m(kr) - rI_m(k\rho)K_{m-1}(kr) - \frac{2m}{k}(IK)_m & \text{when } \rho < r \\ rI_{m-1}(kr)K_m(k\rho) - \rho I_m(kr)K_{m-1}(k\rho) - \frac{2m}{k}(IK)_m & \text{when } \rho > r \end{cases}$$

and

$$\frac{\partial I^{(\bar{m})}(x)}{\partial x} = iI_1^{(\bar{m})}(x) \qquad \text{(see Eq. 45)}$$

$$\frac{\partial\Lambda^{(\bar{n})}(x)}{\partial x} = -i\Lambda_1^{(\bar{n})}(x) \qquad \text{(see Eq. 44)} \qquad \text{(B-3)}$$

Equation (B-2) becomes

$$\lim_{k\to a(q-m)} \{\text{Integrand}\} =$$

$$\frac{1}{2a(q-m)} (IK)_m \Big|_{k=a(q-m)} \begin{cases} e^{-ia(q-m)(x_o+\epsilon_R-\sigma/a)} I^{(\bar{m})}((2m-q)\theta_b) \Lambda^{(\bar{n})}(-a(q-m)C_R) \\ -e^{ia(q-m)(x_o+\epsilon_R-\sigma/a)} I^{(\bar{m})}(q\theta_b) \Lambda^{(\bar{n})}(a(q-m)C_R) \end{cases}$$

$$- \frac{\partial (IK)_m}{\partial k} \Big|_{k=a(q-m)} \left\{ e^{ia(q-m)(x_o+\epsilon_R-\sigma/a)} I^{(\bar{m})}(q\theta_b) \Lambda^{(\bar{n})}(a(q-m)C_R) \right\}$$

$$-i(IK)_m \Big|_{k=a(q-m)} e^{ia(q-m)(x_o+\epsilon_R\sigma/a)} \Big\{ (x_o+\epsilon_R-\sigma/a) I^{(\bar{m})}(q\theta_b) \Lambda^{(\bar{n})}(a(q-m)C_R)$$

$$+ \frac{\theta_b}{a} I_1^{(\bar{m})}(q\theta_b) \Lambda^{(\bar{n})}(a(q-m)C_R)$$

$$- C_R I^{(\bar{m})}(q\theta_b) \Lambda_1^{(\bar{n})}(a(q-m)C_R) \Big\} \qquad \text{(B-4)}$$

Here for $\rho < r$

$$\frac{\partial (IK)_m}{\partial k} \Big|_{k=a(q-m)} = \rho I_{m-1}(a(q-m)\rho) K_m(a(q-m)r) - r I_m(a(q-m)\rho) K_{m-1}(a(q-m)r)$$

$$- \frac{2m}{a(q-m)} I_m(a(q-m)\rho) K_m(a(q-m)r) \qquad \text{(B-5)}$$

and for $\rho > r$, ρ and r are interchanged in (B-5).

BLANK PAGE

APPENDIX C

EXAMINATION OF THE KERNEL K_{PR} FOR SINGULAR BEHAVIOR

Before the 1/R Expansion

From Eq. (72) it is obvious that R can go to zero when $\rho_P = r_R$ and $\tau = 0$. Let the singular part of the kernel in the region $-\gamma \le \tau \le \gamma$, γ a small fixed number, be designated by K_o with

$$K_o = \lim_{\theta_o \to a\xi} \int_{-\gamma}^{\gamma} \left[\pm \frac{1}{r} \frac{\partial}{\partial \varphi}\right]_{\varphi=\pi}^{0} \frac{\rho}{\sqrt{1+a^2\rho^2}} \left(a \frac{\partial}{\partial \xi} - \frac{1}{\rho^2} \frac{\partial}{\partial \theta_o}\right) \frac{e^{-i\lambda a(\tau - x + \xi)}}{R} d\tau \quad \text{(C-1)}$$

where

$$R = \left[\tau^2 + r^2 + \rho^2 - 2r\rho\cos(\mu - \varphi)\right]^{\frac{1}{2}}$$

$$\mu = \theta_o - \Omega t + \bar{\theta}_n - a(\tau - x + \xi)$$

(The subscripts P and R have been omitted for convenience.) The derivative with respect to φ is

$$\left[\pm \frac{1}{r} \frac{\partial}{\partial \varphi}\right]_{\varphi=\pi}^{0} \left(\frac{1}{R}\right) = \frac{\rho \sin\mu}{\left[\tau^2 + r^2 + \rho^2 \mp 2r\rho\cos\mu\right]^{3/2}} \quad \text{(C-2)}$$

where the upper sign corresponds to $\varphi = 0$, $z_R > 0$ and the lower sign to $\varphi = \pi$, $z_R < 0$.

The derivative with respect to ξ is

$$a \frac{\partial}{\partial \xi} \left\{ e^{i\lambda a(\tau - x + \xi)} \frac{\rho \sin\mu}{\left[\tau^2 + r^2 + \rho^2 \mp 2r\rho\cos\mu\right]^{3/2}} \right\} =$$

$$a^2 \rho e^{i\lambda a(\tau - x + \xi)} \left\{ \frac{i\lambda \sin\mu - \cos\mu}{\left[\tau^2 + r^2 + \rho^2 \mp 2r\rho\cos\mu\right]^{3/2}} + \frac{(\pm) 3r\rho \sin^2\mu}{\left[\tau^2 + r^2 + \rho^2 \mp 2r\rho\cos\mu\right]^{5/2}} \right\} \quad \text{(C-3)}$$

and the derivative with respect to θ_o is

$$-\frac{1}{\rho^2}\frac{\partial}{\partial\theta_o}\left\{e^{i\lambda a(\tau-x+\xi)}\frac{\rho\sin\mu}{\left[\tau^2+r^2+\rho^2\mp 2r\rho\cos\mu\right]^{3/2}}\right\}=$$

$$-\frac{1}{\rho}e^{i\lambda a(\tau-x+\xi)}\left\{\frac{\cos\mu}{\left[\tau^2+r^2+\rho^2\mp 2r\rho\cos\mu\right]^{3/2}}+\frac{(\mp)3r\rho\sin^2\mu}{\left[\tau^2+r^2+\rho^2\mp 2r\rho\cos\mu\right]^{5/2}}\right\} \quad (C\text{-}4)$$

After taking the limits, K_o becomes

$$K_o=\frac{e^{-i\lambda a(x-\xi)}}{\sqrt{1+a^2\rho^2}}\int_{-\gamma}^{\gamma}e^{i\lambda a\tau}\left\{\frac{ia^2\rho^2\lambda\sin\mu-(a^2\rho^2+1)\cos\mu}{\left[\tau^2+r^2+\rho^2\mp 2r\rho\cos\mu\right]^{3/2}}\right.$$

$$\left.+\frac{(\pm)3r\rho(a^2\rho^2+1)\sin^2\mu}{\left[\tau^2+r^2+\rho^2\mp 2r\rho\cos\mu\right]^{5/2}}\right\}d\tau \quad (C\text{-}5)$$

where $\mu=\bar{\theta}_n-\Omega t-a(\tau-x)$. The condition for a singularity is that $\mu=-a\tau$ when $z_R>0$, or $\mu=-a\tau+\pi$ when $z_R<0$. Then (C-5) becomes

$$K_o=e^{-i\lambda a(x-\xi)}\int_{-\gamma}^{\gamma}\frac{e^{i\lambda a\tau}}{\sqrt{1+a^2\rho^2}}\left\{\frac{\mp ia^2\rho^2\lambda\sin a\tau\mp(a^2\rho^2+1)\cos a\tau}{\left[\tau^2+r^2+\rho^2-2r\rho\cos a\tau\right]^{3/2}}\right.$$

$$\left.\frac{\pm 3r\rho(a^2\rho^2+1)\sin^2 a\tau}{\left[\tau^2+r^2+\rho^2-2r\rho\cos a\tau\right]^{5/2}}\right\}d\tau \quad (C\text{-}6)$$

Let $\rho=r+\varepsilon$ where ε is very small, then the terms of K_o can be expanded in a series of ε and τ. Since the range of τ is also very small, the following approximations are used.

$$\tau^2 + r^2 + \rho^2 - 2r\rho \cos a\tau \approx \tau^2 + r^2 + (r+\epsilon)^2 - 2r(r+\epsilon)\left(1 - \frac{a^2\tau^2}{2}\right)$$

$$\approx \tau^2 (1 + r^2 a^2 + ra^2\epsilon) + \epsilon^2$$

$$\sin a\tau \approx a\tau$$

$$\cos a\tau \approx 1 - \frac{a^2\tau^2}{2}$$

$$e^{i\lambda a\tau} \approx 1 - \frac{\lambda^2 a^2 \tau^2}{2} + i\lambda a\tau$$

After these substitutions are made and the τ-integration is performed, the singular behavior of K_o is described by

$$\text{Singular Part of } K_o \approx \mp e^{-i\lambda a(x-\xi)} \left\{ \frac{2}{(1+a^2r^2)(\rho-r)^2} \right\} \text{ as } \rho \to r \qquad \text{(C-7)}$$

and is thus of the Hadamard type.

After the 1/R Expansion

The part of Eq. (75) corresponding to K_o of Eq. (C-1), after the τ-integration, can be written for large m as

$$K_o' = -\frac{1}{\pi} \frac{\rho}{r\sqrt{1+a^2\rho^2}} \sum_{m=M}^{\infty} \left\{ \begin{matrix} -e^{im\theta_o} & \text{for } z_R > 0 \\ e^{im(\theta_o \pm \pi)} & \text{for } z_R < 0 \end{matrix} \right\} m$$

$$\cdot \left\{ \pi\left(a^2 q - \frac{m}{\rho^2}\right) e^{-iaq(x-\xi)} \, I_m(aq\rho) K_m(aqr) \right.$$

$$+ ia \int_{-\infty}^{\infty} \frac{k I_m(|k|\rho) K_m(|k|r) e^{ik(x-\xi)}}{k+aq} \, dk$$

$$\left. + i \frac{m}{\rho^2} \int_{-\infty}^{\infty} \frac{I_m(|k|\rho) K_m(|k|r) e^{ik(x-\xi)}}{k+aq} \, dk \right\} \qquad \text{(C-8)}$$

The following approximations are made for large $m = M$ which are similar to those used in Appendix A with the exception that here $x - \xi > 0$.

$$\int_{-\infty}^{\infty} \frac{k I_m(|k|\rho) K_m(|k|r) e^{ik(x-\xi)}}{k+aq}\, dk \approx -i\pi a q I_m(aq\rho) K_m(aqr) e^{-iaq(x-\xi)}$$

$$\int_{-\infty}^{\infty} \frac{I_m(|k|\rho)\ K_m(|k|r) e^{ik(x-\xi)}}{k+aq} \approx i\pi I_m(aq\rho)\ K_m(aqr) e^{-iaq(x-\xi)}$$

Then for large m, the m-summation is

$$\sum_{m=M}^{\infty} \left\{ \begin{matrix} -e^{im\theta_o} \\ e^{im(\theta_o \pm \pi)} \end{matrix} \right\} m(2\pi)\left(a^2 q - \frac{m}{\rho^2}\right) e^{-iaq(x-\xi)}\ I_m(aq\rho) K_m(aqr)$$

The product of the modified Bessel functions can be approximated by*

$$I_m(aq\rho) K_m(aqr) \approx$$

$$\frac{1}{2\left[(m^2+a^2q^2\rho^2)(m^2+a^2q^2r^2)\right]^{\frac{1}{4}}} \left(\frac{\rho}{r}\right)^m \left(\frac{m+\sqrt{m^2+a^2q^2r^2}}{m+\sqrt{m^2+a^2q^2\rho^2}}\right)^m e^{-\left(\sqrt{m^2+a^2q^2r^2}-\sqrt{m^2+a^2q^2\rho^2}\right)}$$

For very large $m \gg q$

$$I_m(aq\rho) K_m(aqr) \approx \frac{1}{2m} \left(\frac{\rho}{r}\right)^m$$

Therefore for large m, K_o' is approximately

$$K_o' \approx -\frac{\rho e^{-iaq(x-\xi)}}{r\sqrt{1+a^2\rho^2}} \sum_{m=M}^{\infty} \left(\frac{\rho}{r}\right)^m \left(a^2 q - \frac{m}{\rho^2}\right)$$

$$\cdot \begin{pmatrix} -\cos m\theta_o - i \sin m\theta_o \\ \cos m(\theta_o \pm \pi) + i \sin m(\theta_o \pm \pi) \end{pmatrix} \qquad \text{(C-9)}$$

---

*NICHOLSON, J.W., "The Approximate Calculations of Bessel Functions of Imaginary Argument." Phil Mag.,Ser. 6,Vol.20,Dec. 1910, pp.938-943.

Let $X = \frac{\rho}{r} < 1$, then[**]

$$\sum_{m=1}^{\infty} X^m \sin m\alpha = \frac{X\sin\alpha}{1-2X\cos\alpha+X^2}$$

$$\sum_{m=0}^{\infty} X^m \cos m\alpha = \frac{1-X\cos\alpha}{1-2X\cos\alpha+X^2}$$

$$\sum_{m=1}^{\infty} mX^m \cos m\alpha = \frac{\partial}{\partial\alpha}\sum_{m=1}^{\infty} X^m \sin m\alpha = \frac{X\left[(1+X^2)\cos\alpha - 2X\right]}{\left[1-2X\cos\alpha+X^2\right]^2}$$

$$\sum_{m=1}^{\infty} mX^m \sin m\alpha = -\frac{\partial}{\partial\alpha}\sum_{m=0}^{\infty} X^m \cos m\alpha = \frac{X\sin\alpha(X^2-1)}{\left[1-2X\cos\alpha+X^2\right]^2} \qquad \text{(C-10)}$$

The singularity as $\rho \to r$ occurs when $\alpha = 0, 2\pi, 4\pi, \ldots$ in which case

$$\sum_{m=1}^{\infty} X^m \sin m\alpha = \sum_{m=1}^{\infty} mX^m \sin m\alpha = 0$$

$$\sum_{m=0}^{\infty} X^m \cos m\alpha = \frac{1}{1-X}$$

$$\sum_{m=1}^{\infty} mX^m \cos m\alpha = \frac{X}{(1-X)^2}$$

Since the summation from $m = 0$ to $m = M$ is obviously not singular, it can be shown that the singular part of K_o' reduces to

$$\mp \frac{e^{-iaq(x-\xi)}}{\sqrt{1+a^2\rho^2}}\left[\frac{1}{(\rho-r)^2} + a^2 q\,\frac{r}{\rho-r}\right] \text{ as } \rho \to r \qquad \text{(C-11)}$$

which has the same high-order Hadamard-type singularity as (C-7).

[**] JOLLEY, L.B.W., ed., Summation of Series, Dover Publications, Inc., New York 1961.

BLANK PAGE

APPENDIX D

EVALUATION OF THE INTEGRAND OF $\bar{K}_{PR}$ AT $k = -aq$

With the substitution

$$\frac{k}{k+aq} = 1 - \frac{aq}{k+aq}$$

the k-integrals of Eq. (75) become

$$ia \int_{-\infty}^{\infty} f(k)dk - i\left(a^2 q - \frac{m}{\rho^2}\right) \int_{-\infty}^{\infty} \frac{f(k)}{k+aq}\, dk$$

where

$$f(k) = I_m(|k|\rho)\, K_m(|k|r) e^{ik(x_o+\epsilon_R-\sigma/a)} I^{(\bar{m})}(-kC_R) \Lambda^{(\bar{n})}\left((m-\frac{k}{a})\theta_b\right)$$

when $\rho < r$, otherwise ρ and r are interchanged in $f(k)$.

The first integral is nonsingular; the second has a Cauchy-type singularity at $k = -aq$, similar to the singularity of $\bar{K}_{RP}$. For the reasons given in Appendix B, the present integral can be written as

$$\int_{-\infty}^{\infty} \frac{f(k)dk}{k+aq} = \int_{0}^{\infty} \frac{F(k)dk}{(k+aq)(k-aq)} = \int_{0}^{\infty} \frac{F(k)-F(aq)}{(k+aq)(k-aq)}\, dk \qquad (D\text{-}1)$$

where

$$F(k) = f(k)(k-aq) - f(-k)(k+aq)$$

$$F(aq) = -2aqf(-aq)$$

It can be shown (compare Appendix B), that at the singularity the integrand is finite and is equal to

$$\lim_{k\to aq}\{\text{integrand}\} =$$

$$\frac{1}{2aq}(IK)_m\Big|_{k=aq}\left\{e^{iaq(x_o+\epsilon_R-\sigma/a)}I^{(\bar{m})}(-aqC_R)\Lambda^{(\bar{n})}((m-q)\theta_b)\right.$$
$$\left.-e^{-iaq(x_o+\epsilon_R-\sigma/a)}I^{(\bar{m})}(aqC_R)\Lambda^{(\bar{n})}((m+q)\theta_b)\right\}$$

$$-\frac{\partial(IK)_m}{\partial k}\Big|_{k=aq}\left\{e^{-iaq(x_o+\epsilon_R-\sigma/a)}I^{(\bar{m})}(aqC_R)\Lambda^{(\bar{n})}((m+q)\theta_b)\right\}$$

$$+i(IK)_m\Big|_{k=aq}e^{-iaq(x_o+\epsilon_R-\sigma/a)}\left\{(x_o+\epsilon_R-\frac{\sigma}{a})I^{(\bar{m})}(aqC_R)\Lambda^{(\bar{n})}\right\}((m+q)\theta_b)$$
$$-C_R b_2^{(\bar{m})}(aqC_R)\Lambda^{(\bar{n})}((m+q)\theta_b)$$
$$+\frac{\theta_b}{a}I^{(\bar{m})}(aqC_R)\Lambda_1^{(\bar{n})}((m+q)\theta_b)\Big\} \qquad (D\text{-}2)$$

where for $\rho < r$

$$\frac{\partial(IK)_m}{\partial k}\Big|_{k=aq} = \rho I_{m-1}(aq\rho)K_m(aqr) - rI_m(aq\rho)K_{m-1}(aqr) - \frac{2m}{aq}I_m(aq\rho)K_m(aqr)$$

and for $\rho > r$

$$\frac{\partial(IK)_m}{\partial k}\Big|_{k=aq} = rI_{m-1}(aqr)K_m(aq\rho) - \rho I_m(aqr)K_{m-1}(aq\rho) - \frac{2m}{aq}I_m(aqr)K_m(aq\rho)$$

APPENDIX E

EVALUATION OF THE SINGULAR k-INTEGRAL OF $\bar{K}_{RR}$

The integral term of Eq. (88) can be written as

$$I = \int_{-\infty}^{\infty} \frac{F(k)\,dk}{k+qa} \tag{E-1}$$

where

$$F(k) = |k|z_o K_1(|k|z_o) I^{(\bar{m})}(-kC^r)\Lambda^{(\bar{n})}(-kC^\rho)e^{ik(\epsilon^r-\epsilon^\rho)}$$

As in Appendix B, it can be shown that

$$I = \int_{-\infty}^{\infty} \frac{F(k)-F(-qa)}{k+qa}\,dk + F(-qa)\int_{-\infty}^{\infty} \frac{dk}{k+qa} = \int_{-\infty}^{\infty} \frac{F(k)-F(-qa)}{k+qa}\,dk \tag{E-2}$$

For large $|k| \geq |M|$, $|M| > qa$, $F(k)$ is approximately zero, therefore

$$I \approx \int_{-M}^{M} \frac{F(k)-F(-qa)}{k+qa}\,dk - F(-qa)\left[\int_{-\infty}^{-M} + \int_{M}^{\infty}\right] \frac{dk}{k+qa} \tag{E-3}$$

But

$$\left[\int_{-\infty}^{-M} + \int_{M}^{\infty}\right] \frac{dk}{k+qa} = -2qa\int_{M}^{\infty} \frac{dk}{k^2-q^2a^2} = \log\left(\frac{k+qa}{k-qa}\right)\Bigg|_{M}^{\infty} = \log\frac{M-qa}{M+qa}$$

so that

$$I \approx \int_{-M}^{M} \frac{F(k)-F(-qa)}{k+qa}\,dk - F(-qa)\log\frac{M-qa}{M+qa}$$

and

$$\bar{K}_{RR}^{(\bar{m},\bar{n})} \approx -\frac{1}{4\pi\rho_f U r_o^2 z_o^2}\left\{qaz_o K_1(qaz_o) I^{(\bar{m})}(qaC^r)\Lambda^{(\bar{n})}(qaC^\rho)e^{-iqa(\epsilon^r-\epsilon^\rho)} \cdot \left[1 + \frac{i}{\pi}\log\frac{M-qa}{M+qa}\right] - \frac{i}{\pi}\int_{-M}^{M} \frac{F(k)-F(-qa)}{k+qa}\,dk\right\} \tag{E-4}$$

(M is chosen by trial.)

The k-integral of (E-4) can also be written as

$$+\frac{2I}{\pi}\int_0^M \frac{kz_oK_1(kz_o)f(k) - qaz_oK_1(qaz_o)f(qa)}{k^2 - q^2a^2}\,dk$$

where

$$f(k) = qa\ \mathrm{Re}\cdot\left[I^{(\bar{m})}(kC^r)\Lambda^{(\bar{n})}(kC^\rho)e^{-ik(\epsilon^r-\epsilon^\rho)}\right]$$

$$+ik\ \mathrm{Im}\left[I^{(\bar{m})}(kC^r)\Lambda^{(\bar{n})}(kC^\rho)e^{-ik(\epsilon^r-\epsilon^\rho)}\right]$$

and

$$f(qa) = qa\ I^{(\bar{m})}(qaC^r)\Lambda^{(\bar{n})}(qaC^\rho)e^{-iqa(\epsilon^r-\epsilon^\rho)} \qquad \text{(E-5)}$$

The finite contribution of the last integral at k = qa can be determined in a fashion similar to that of Appendix B.

APPENDIX F

THE ζ-INTEGRATION OF R_{RR} NEAR $z=\zeta$

In the rudder spanwise strip which includes the singularity, the ζ-integration will be performed before the k-integration. This strip will be divided into three parts so that the integral is of the form

$$I = \left[\int_{z-3\beta}^{z-\beta} + \int_{z-\beta}^{z+\beta} + \int_{z+\beta}^{z+3\beta}\right] R_{RR}^{(\bar{m},\bar{n})}\, d\zeta \qquad \text{(F-1)}$$

In the middle strip, where it can be assumed that $C^r = C^p$ and $\epsilon^r = \epsilon^p$, the ζ-integration involves (see Appendix E)

$$\int_{z-\beta}^{z+\beta} \left\{ \frac{qaz_o}{z_o^2} K_1(qaz_o) I^{(\bar{m})}(qaC) \Lambda^{(\bar{n})}(qaC) \left[1 + \frac{1}{\pi} \log \frac{M-qa}{M+qa}\right] \right.$$

$$\left. + \frac{2I}{\pi} \int_0^M \frac{kz_o K_1(kz_o) f(k) - qaz_o K_1(qaz_o) f(qa)}{z_o^2 (k^2 - q^2a^2)}\, dk \right\} d\zeta \qquad \text{(F-2)}$$

where

$$f(k) = qa\, \mathrm{Re}\cdot\left[I^{(\bar{m})}(kC)\Lambda^{(\bar{n})}(kC)\right] + Ik\, \mathrm{Im}\cdot\left[I^{(\bar{m})}(kC)\Lambda^{(\bar{n})}(kC)\right]$$

$$f(qa) = qa\, I^{(\bar{m})}(qaC)\Lambda^{(\bar{n})}(qaC)$$

In this region, $z-\beta < \zeta < z+\beta$, use can be made of a polynomial approximation* of the modified Bessel function for argument near zero, viz.,

$$xK_1(x) \approx x^2 \ln \frac{x}{2}(0.5 + .0625x^2) + 1 + .0386x^2 - .04205x^4 \qquad \text{(F-3)}$$

After substituting (F-3) into (F-2) and integrating with respect to ζ, noting that $z_o = |z-\zeta|$, the integral (F-2) becomes

*ABRAMOWITZ, M. and STEGUN, I.A., editors, Handbook of Mathematical Functions, National Bureau of Standards Applied Mathematics Series 55, Washington, D.C., June 1964, Chapter 9, Section 8.

$$\beta\Big\{g(qa)\,I^{(\bar{m})}\ (qaC)\Lambda^{(\bar{n})}\ (qaC)\Big[1+\frac{1}{\pi}\log\frac{M-qa}{M+qa}\Big]$$

$$+\frac{2I}{\pi}\int_0^M \frac{g(k)f(k)-g(qa)f(qa)}{k^2-q^2a^2}\,dk\Big\} \qquad \text{(F-4)}$$

where $g(k)=\frac{2}{3}\beta^2\ (.0625\log\frac{k}{2}-.06288)k^4$

$$+(-.9228+\log\frac{k}{2})k^2-\frac{2}{\beta^2}$$

$$+k^2\log\beta(1+.0417\,\beta^2k^2)$$

In the outer strips

$$\int_{z-3\beta}^{z-\beta}\bar{K}_{RR}^{(\bar{m},\bar{n})}d\zeta=\int_{z+\beta}^{z+3\beta}\bar{K}_{RR}^{(\bar{m},\bar{n})}d\zeta \qquad \text{(F-5)}$$

and for each strip a 3-point Gaussian quadrature is used. The integral is

$$\int_{z+\beta}^{z+3\beta}\bar{K}_{RR}^{(\bar{m},\bar{n})}d\zeta\approx-\frac{1}{4\pi\rho_f U}\beta\Big\{h(qa)\,I^{(\bar{m})}(qaC)\Lambda^{(\bar{n})}(qaC)\Big[1+\frac{1}{\pi}\log\frac{M-qa}{M+qa}\Big]$$

$$+\frac{2I}{\pi}\int_0^M\frac{h(k)f(k)-h(qa)f(qa)}{k^2-q^2a^2}\,dk\Big\}$$

where

$$h(k)=\sum_{l=1}^{3}\frac{z_{o_l}k\,K_1(z_{o_l}k)}{z_{o_l}^2}\,W_l$$

$$z_{o_1}=1.225403\,\beta \qquad W_1=5/9$$

$$z_{o_2}=2\,\beta \qquad W_2=8/9 \qquad \text{(F-6)}$$

$$z_{o_3}=2.774507\,\beta \qquad W_3=5/9$$

It is assumed here also that $C^r=C^p$ and $\epsilon^r=\epsilon^p$.

Hence,

$$\int_{z-3\beta}^{z+3\beta} \bar{K}_{RR}^{(\bar{m},\bar{n})} d\zeta \approx -\frac{\beta}{4\pi\rho_f U} \left\{ G(qa) I^{(\bar{m})}(qaC) \Lambda^{(\bar{n})}(qaC) \left[1 + \frac{1}{\pi} \log \frac{M-qa}{M+qa} \right] \right.$$

$$\left. + \frac{2I}{\pi} \int_0^M \frac{G(k)f(k) - G(qa)f(qa)}{k^2 - q^2a^2} \, dk \right\} \qquad (F\text{-}7)$$

where

$$G(k) = 2h(k) + g(k) \, .$$

APPENDIX G

EXPLICIT FORM OF EQUATION (91)

For convenience in writing, the ρ-integration and orders of the chordwise modes and lift operators, $\bar{n}$ and $\bar{m}$, will be omitted in the following.

Equation (74) of the text can then be expressed in the form

$$I_3 = \left[L_P^{(0)} + \sum_{\lambda_3=1}^{\infty} L_P^{(\lambda_3)} e^{i\lambda_3\Omega t}\right]\left[\bar{K}_{PR}^{(m_3=0)} + \sum_{m_3=1}^{\infty} \bar{K}_{PR}^{(m_3)} e^{-im_3\Omega t} + \sum_{m_3=1}^{\infty} \bar{K}_{PR}^{(-m_3)} e^{im_3\Omega t}\right] \qquad (G-1)$$

where

$$\lambda_3 - m_3 = \pm \ell N \ , \ \ell = 0,1,2 \ ...$$

Since in (G-1) λ_3 and m_3 are 0 or positive, it is easily shown that in the steady-state case when $\ell=0$

$$I_3 = L_P^{(0)} \bar{K}_{PR}^{(0)} + \sum_{\lambda_3=1}^{\infty} L_P^{(\lambda_3)} \bar{K}_{PR}^{(\lambda_3)} = \sum_{\lambda_3=0}^{\infty} L_P^{(\lambda_3)} \bar{K}_{PR}^{(\lambda_3)} \qquad (G-2)$$

and in the unsteady case ($\ell>0$)

$$I_3 = \sum_{\lambda_3=0}^{\infty} L_P^{(\lambda_3)} \bar{K}_{PR}^{(\lambda_3-\ell N)} e^{i\ell N\Omega t} + \sum_{\lambda_3=0}^{\infty} L_P^{(\lambda_3)} \bar{K}_{PR}^{(\lambda_3+\ell N)} e^{-i\ell N\Omega t} \qquad (G-3)$$

Equation (G-3) is equivalent to the first integral of Eq. (91) of the text. In a similar fashion, the second integral I_4 can be expressed as

$$I_4 = \sum_{\lambda_4=0}^{\infty} L_R^{(\lambda_4)} \bar{K}_{RR}^{(\lambda_4)} e^{i\lambda_4\Omega t} \qquad (G-4)$$

and since R.P.I_4 = -R.P.I_3 , Eq. (91) for $\ell > 0$ becomes

$$\text{R.P.}\left\{L_R^{(\ell N)}\ \bar{K}_{RR}(\ell N)\ e^{i\ell N\Omega t}\right\} = -\text{R.P.}\left\{\sum_{\lambda_3=0}^{\infty} L_P^{(\lambda_3)}\bar{K}_{PR}^{(\lambda_3-\ell N)} e^{i\ell N\Omega t} + \sum_{\lambda_3=0}^{\infty} L_P^{(\lambda_3)}\bar{K}^{(\lambda_3+\ell N)} e^{-i\ell N\Omega t}\right\} \quad \text{(G-5)}$$

Now $\text{R.P.}\left[(a+ib)e^{in\theta} + (c+id)e^{-in\theta}\right] = \text{R.P.}\left[(a+ib)e^{in\theta} + (c-id)e^{in\theta}\right]$

Therefore Eq. (G-5) is equivalent to

$$\text{R.P.}\left\{L_R^{(\ell N)}\ \bar{K}_{RR}(\ell N)\ e^{i\ell N\Omega t}\right\} = -\text{R.P.}\sum_{\lambda_3=0}^{\infty}\left\{L_P^{(\lambda_3)}\ \bar{K}_{PR}^{(\lambda_3-\ell N)} + \text{conj.}\left[L_P^{(\lambda_3)}\bar{K}_{PR}^{(\lambda_3+\ell N)}\right]\right\} e^{i\ell N\Omega t} \quad \text{(G-6)}$$

UNCLASSIFIED
Security Classification

DOCUMENT CONTROL DATA - R & D

Security classification of title, body of abstract and indexing annotation must be entered when the overall report is classified

1 ORIGINATING ACTIVITY (Corporate author) Davidson Laboratory, Stevens Institute of Technology	2a. REPORT SECURITY CLASSIFICATION Unclassified 2b. GROUP

3 REPORT TITLE

A THEORY FOR THE PROPELLER-RUDDER INTERACTION

4 DESCRIPTIVE NOTES (Type of report and, inclusive dates)
Final

5 AUTHOR(S) (First name, middle initial, last name)

S. Tsakonas, W.R. Jacobs, M.R. Ali

6 REPORT DATE August 1968	7a. TOTAL NO. OF PAGES 104	7b. NO. OF REFS 21
8a. CONTRACT OR GRANT NO. N600(167)61303XT06 and N00600-67-C-0725 b. PROJECT NO. c. d.	9a. ORIGINATOR'S REPORT NUMBER(S) R-1284 9b. OTHER REPORT NO(S) (Any other numbers that may be assigned this report)	

10. DISTRIBUTION STATEMENT

Distribution of this document is unlimited

11. SUPPLEMENTARY NOTES	12. SPONSORING MILITARY ACTIVITY Department of Hydromechanics Naval Ship Research & Development Center Washington, D. C.

13. ABSTRACT

The propeller-rudder interaction problem is studied by means of the unsteady lifting-surface theory. Both surfaces of arbitrary geometry are immersed in a nonuniform flowfield (i.e., hull wake) of an ideal incompressible fluid. The boundary-value problem yields a pair of surface integral equations, the inversion of which is achieved by the so-called "generalized lift operator" technique, a new approach developed by the authors, in conjunction with the presently used "mode-collocation" method. The analysis demonstrates the mechanism of the interaction phenomenon by exhibiting the filtering effects of the propeller on the harmonic constituents of the wake which allow the rudder to be exposed only to the blade harmonic and multiples thereof. A numerical procedure adaptable to the CDC 6600 computer has been developed which furnishes information about 1) the steady and time-dependent pressure distribution on both lifting surfaces, and 2) the resultant hydrodynamic force and moments. A limited number of calculations exhibits the importance of some parameters such as axial clearance, number of blades, and harmonic components of the hull wake.

14 KEY WORDS	LINK A		LINK B		LINK C	
	ROLE	WT	ROLE	WT	ROLE	WT
Hydrodynamics						
Unsteady Theory for Propeller-Rudder Interaction						